The completion of this thesis
was supported by the
Randy Seeling Award
given, in his memory, to another
outstanding graduate student
of the Geology Department,
University of Minnesota, Duluth.

PHYSICAL VOLCANOLOGY AND HYDROTHERMAL ALTERATION OF THE ARCHEAN VOLCANIC ROCKS AT THE EAGLES NEST VOLCANOGENIC MASSIVE SULPHIDE PROSPECT, NORTHERN MINNESOTA

A THESIS
SUBMITTED TO THE FACULTY OF THE GRADUATE SCHOOL
OF THE UNIVERSITY OF MINNESOTA
BY

STEVEN TERRY HOVIS

IN PARTIAL FULFILLMENT OF THE REQUIREMENTS FOR THE DEGREE OF
MASTER OF SCIENCE

MARCH, 2001

Abstract

The Eagles Nest Volcanogenic Massive Sulphide Prospect occurs within the Lower Ely Member of the 2.7 Ga Ely Greenstone Formation located within the Vermilion District of the Wawa Subprovince of the Superior Province of the Canadian Shield in Northeastern Minnesota. The object of this study is to characterize the physical volcanology and hydrothermal alteration of the rocks of the footwall to the massive sulphide mineralization. This was done by a combination of geological mapping, diamond drill core logging, thin section petrology, and major and trace element geochemistry. The entire sequence has been metamorphosed to greenschist facies. The mineralization is not exposed at the surface and was discovered by airborne Electromagnetic (EM) and Magnetism surveys, followed up by ground EM Loop and Magnetism surveys. This defined a target that was intersected by three diamond drill holes drilled by Newmont Exploration.

The footwall to the mineralization is composed of approximately 1300 meters of pillowed and massive andesite lava flows, with one lobe-hyaloclastite lava flow. The base of the footwall at Eagles Nest is intruded by the dioritic to tonalitic Purvis Lake Pluton. This contact is locally an intrusive breccia. The mineralized horizon consists of approximately 100-150 meters of oxide facies banded iron formation with thin lenses of massive pyrite +/- chalcopyrite +/- sphalerite, and is interlayered with thin, strongly altered andesite lava flows, and sedimentary rocks. The hanging wall is composed of pillowed and massive andesite, with one chemically distinctive basalt lava flow.

Hydrothermal alteration mineral assemblages throughout the stratigraphic package have been defined by thin section analysis. In the footwall, these assemblages are epidote +/- quartz, quartz +/- epidote, actinolite +/- epidote, and chlorite +/- quartz +/- sericite. The epidote +/- quartz and quartz +/- epidote assemblages are visible in outcrop as meter scale, locally intense, discontinuous, pale green alteration patches of pervasive alteration, and/or as fillings of amygdules and veinlets. Footwall alteration is semi-conformable, and widespread for many kilometers east and west along strike from the Eagles Nest map area (Peterson, in

prep). Mineralized horizon alteration mineral assemblages are chlorite + quartz, magnesium chlorite +/- sericite, and tremolite. Tremolite and magnesium chlorite alteration is interpreted to have occurred on, or immediately below the seafloor, and is syn- to post-mineralization in timing. Most rocks in the mineralized horizon have been intensely, to completely altered, and protolith is often impossible to distinguish. All alteration in the mineralized horizon is stratiform and no evidence of crosscutting alteration has been observed. Alteration mineral assemblages in the hanging wall consist of epidote +/- quartz, quartz +/- epidote, actinolite + epidote +/- quartz, chlorite +/- epidote +/- quartz. This alteration is younger than, but very similar in character to, that of the footwall.

Grant's isocon method (1986) was used to define changes in rock mass and the concentration of individual components as a result of hydrothermal alteration.

The Eagles Nest Prospect is interpreted to have been located on the flank of a subaqueous volcanic center during the time hydrothermal activity was precipitating the oxide and sulphide minerals. Water depth at Eagles Nest is estimated to have been 500 meters or less, based on observations of amygdule size and percentage within the andesite lava flows. The Purvis Lake Pluton was likely the synvolcanic intrusion driving volcanism at Eagles Nest and the surrounding area, but has intruded upwards in the stratigraphic sequence since the mineralizing event. Composition of oxide and sulphide minerals, alteration mineral assemblages, results from isocon analysis, and experimental work done by Seyfried and Janecky (1985) on hydrothermal fluids beneath mid-ocean ridges, all suggest that hydrothermal fluids in the Eagles Nest footwall never reached temperatures high enough to mobilize and concentrate significant amounts of Cu and Zn. At Eagles Nest the mineralized horizon does not contain significant Cu – Zn sulphides. Epidote +/- quartz alteration in the footwall is not a good exploration guide for VMS mineralization in the Lower Ely Greenstone.

Acknowledgements

I would like to thank my advisor, Dr. Ron Morton, for giving me the opportunity to learn from him. Without his patient guidance, this project would not have been as easily completed. Dr. Penny Morton and Dr. Nigel Wattrus provided valuable suggestions and advice while serving on my committee. Steve Hauck and the NRRI have provided financial support. Dean Peterson has given me an immense amount of assistance. I have greatly benefited from his expertise in field geology, map making, and computer software. Thank you to Dr. George Hudak for sharing his enthusiasm and knowledge. Thank you to the Faculty and Staff of the UMD Geological Sciences Department for the many things they have taught me, and for the help they have given during the time I spent with them. Most importantly, thank you to my parents for instilling in me the patience, persistence, and work ethic needed to accomplish this project. Their support is always behind me.

Table of Contents

List of Figures, Tables, and Plates

LIST OF FIGURES

LIST OF TABLES

LIST OF PLATES

CHAPTER 1
INTRODUCTION

Purpose

The purpose of this study is to characterize and interpret the physical volcanology and hydrothermal alteration of the footwall rocks at the Eagles Nest Prospect, a banded iron formation and volcanogenic massive sulphide (VMS) occurrence in Northern Minnesota. This thesis is part of a regional volcanological survey and study of volcanogenic massive sulphide showings in Northern Minnesota and will be included with findings from Five Mile Lake and Purvis Road VMS prospects. The study has been funded by the State of Minnesota Minerals Coordinating Committee through a grant to the University of Minnesota-Duluth and the Natural Resources Research Institute.

Location, Access, and Terrain

The mineralization at the Eagles Nest Prospect is located beneath the northern edge of Eagles Nest Lake No. 4 in north central St. Louis County, approximately one mile south of State Highway 169 along County Road 128 (T. 62N R. 14W S. 24, 25) (Figure 1). The field area lies within a combination of Bear Island State Forest and privately held land. The entire area is easily accessible with the exception of the immediate south shore of Eagles Nest Lake No. 4, where several private residences are located. The terrain consists of pine and birch forest interspersed with shallow swamp. Outcrop is most abundant in the southeastern part of the area, and is found along small knobs and ridges separated by swampy terrain. Outcrops are generally covered with lichen and moss making identification of mesoscopic textures challenging.

Methods of Study

Field Work

The first step in this study consisted of detailed geological outcrop mapping at 1" = 200' over an approximately 2.5 square mile area of footwall and the immediate hanging wall rocks to the mineralization. This was accomplished in six weeks during the summer

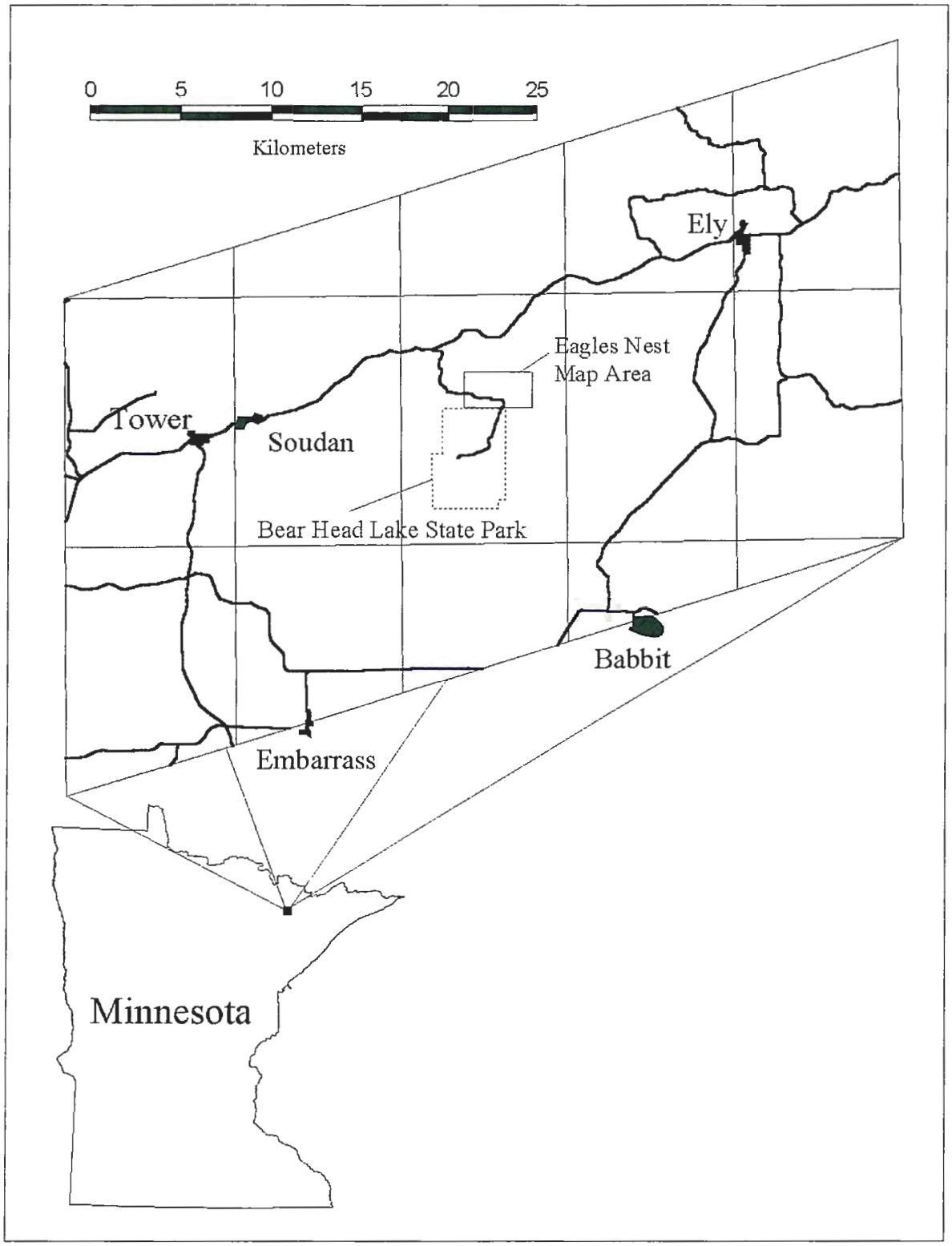

Figure 1: Location of the Eagles Nest Prospect, St. Louis County, Minnesota.

of 1999. This mapping served to spatially locate and identify rock units, structures, and alteration zones, and to describe primary volcanic textures. Samples of both relatively unaltered rocks and altered rocks were collected from outcrops, which were primarily mafic volcanic rocks and intrusive dikes of varying composition.

Newmont Exploration Limited drilled three diamond drill holes on the Eagles Nest property during the late 1980's. These were relogged at the Minnesota Department of Natural Resources Core Repository in Hibbing, Minnesota after field mapping was completed. Core samples were collected from the overlying mafic volcanics through the mineralized zone and into the footwall of the deposit.

Petrology

One hundred ten thin sections were made from rock samples collected from outcrop and diamond drill core. Thin sections enable the identification and classification of altered versus relatively unaltered rocks; alteration mineral assemblages; primary volcanic textures; and volcanic rock types.

Chemical Analysis

Fifty rock samples were selected for chemical analysis from outcrop and diamond drill core based on preliminary thin section study. These were sent to Activation Laboratories Ltd in Ontario, Canada for major and trace element analysis. These data were used to determine primary composition of the volcanic rocks, and to assist in defining hydrothermal alteration characteristics.

X-ray Diffraction Analysis (XRD)

The fine-grained nature of the volcanic rocks being studied made identification of some minerals in thin section difficult. Therefore, XRD techniques were used to further define mineral assemblages in selected thin sections. This was done using the University of Minnesota-Duluth Geological Sciences Department's XRD machine.

Previous Work

Newmont Exploration Limited conducted a gold exploration program over the Eagles Nest Prospect from 1986-1988. They performed magnetic and EM loop geophysical surveys, geochemical sampling, and diamond drilling at the site. Magnetic and EM surveys located a target conductor striking east-west at depth on the northern edge of Eagles Nest Lake No. 4. This was interpreted to be related to iron formation and possibly to gold mineralization associated with fluid movement along faults. Three diamond drill holes were drilled and a total depth of 1932 feet of core was collected. The drilling revealed thin units of banded oxide facies iron formation, small massive sulphide lenses, and anomalous gold values. Mineralization ranged from trace pyrite to 15-20% banded pyrite in 2-3 foot thick zones. The greatest occurrence of chalcopyrite was associated with the pyrite and ranged from 2-10%. Newmont did not deem the results of the drilling favorable for gold mineralization and the project was discontinued. Assays of rock, lake, stream, and seep samples collected by Newmont also show anomalous values of Au, Cu, and Zn (Peterson, pers com 2000). Dean Peterson compiled the geochemical data and drill hole logs from Eagles Nest while working on his Ph.D. thesis at the University of Minnesota-Duluth in the mid 1990's (Peterson, in prep). He produced a regional scale mineral potential geologic map that includes the Eagles Nest Prospect area. Finally, as part of an unpublished regional geologic study, George Hudak had whole rock geochemical analysis and thin sections made from eighteen core samples taken from hole EN-6. This data has been made available to the author for the purpose of this study.

Regional Geology

The Vermilion District of northern Minnesota lies within the Wawa Subprovince of the Superior Province of the Canadian Shield. The Superior Province is the core of the Canadian Shield and is composed of Precambrian rocks ranging in age from 3.1 Ga to 2.6 Ga that have remained geologically stable since the Late Archean (Card, 1990). Four distinct geological environments defined by lithology, structure, metamorphism, and geophysical characteristics are present in the Superior Province, and are used to divide it

into subprovinces (Card, 1990). These are the granite-greenstone, metasedimentary, plutonic, and high-grade gneissic terrains.

The Wawa Subprovince, which includes the Vermilion District of northeastern Minnesota, is a granite-greenstone terrain that consists of metamorphosed mafic lavas and minor felsic pyroclastic and lava flow units interspersed with small mafic to felsic plutons. Abundant volcanic derived siltstones occur interlayered with and adjacent to volcanic rocks (Card, 1990).

The Vermilion District encompasses the western portion of the Wawa Subprovince and is approximately 160 km long and 10-30 km wide. It is bounded on the south by the Giants Range Batholith, on the north by the Vermilion Granitic Complex, on the east by the Saginaw Batholith, and in the west it is covered by thick glacial deposits. Stratigraphically, it is composed of four units of metavolcanic and metasedimentary rocks that have been tilted to nearly vertical and trend east-west (Schultz, 1980). These four units are the Ely Greenstone Formation, the Knife Lake Group, the Lake Vermilion Formation, and the Newton Lake Formation (Figure 2).

The oldest rocks of the Vermilion District are the Ely Greenstone Formation, which is further subdivided into the Lower Ely, Soudan, and the Upper Ely members. The Lower Ely consists of mafic pillowed and massive lavas with local felsic volcanoclastic rocks. The Soudan Member is an oxide facies banded iron formation, whereas the Upper Ely consists of mafic massive and pillowed lavas. Both the Lower and Upper Ely have minor felsic pyroclastic deposits within the sequence. The Knife Lake Group and the Lake Vermilion Formation overlie the Upper Ely Greenstone and appear to be contemporaneous. The Knife Lake Group underlies the eastern part of the district and is intercalated with the Lake Vermilion Formation to the west. Both the Knife Lake Group and the Lake Vermilion Formation consist of graywackes, slates, and conglomerates of volcanic origin. The upper most strata of the Vermilion District are mafic lavas, intrusions, and clastic rocks of the Newton Lake Formation (Peterson and Jirsa, 1999).

Two areas with distinctly different structural characteristics are found in the Vermilion District. To the south is the Soudan Belt, a region of broad folds that plunge

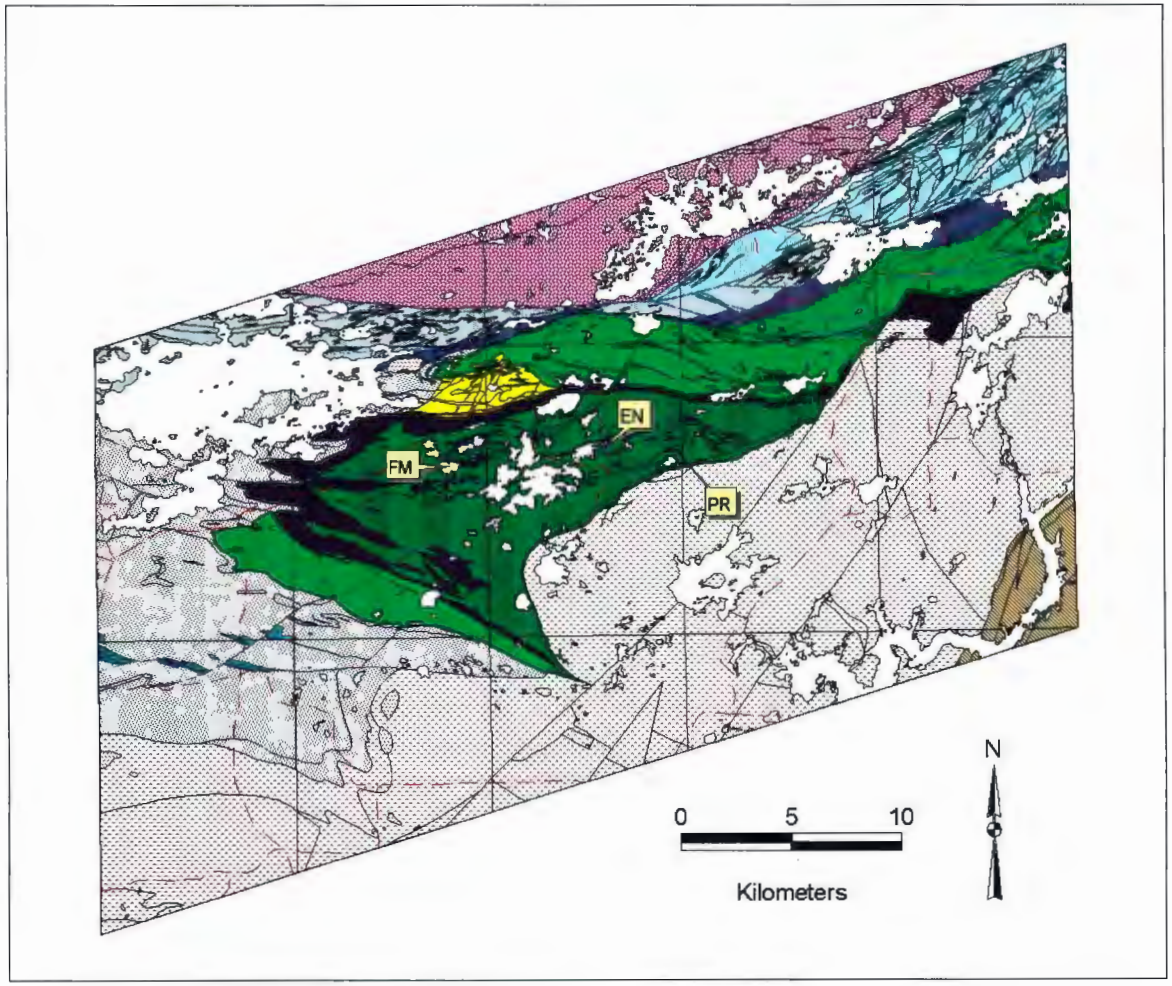

Figure 2: Geologic map of the western Vermilion District (Peterson and Jirsa, 1999a).

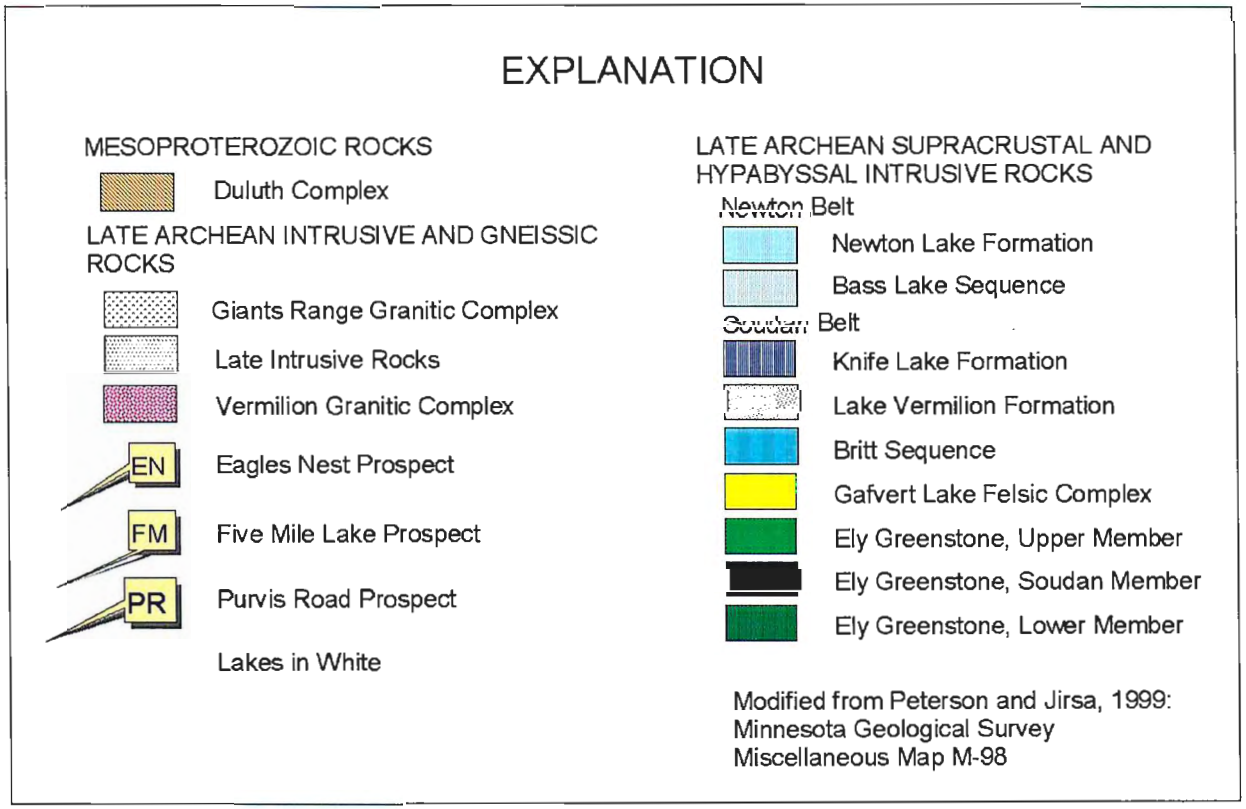

Figure 2a: Explanation to geologic map of the Vermilion District (Peterson and Jirsa, 1999a).

east or west and maintain stratigraphic continuity. Rock units in these fold limbs have dips near vertical. To the north the Newton Belt consists of north dipping fault panels. These belts are divided by the east-west trending Leech Lake structural disconformity (Southwick, *in* Peterson, 1999). Three deformation events have affected the Vermilion District as described by Jirsa et al (1992). The first, D_1, deformation produced broad, recumbent folds on a regional scale, as exemplified by the Tower-Soudan Anticline. Little or no evidence of D_1 deformation can be seen at outcrop scale due to a lack of developed cleavage. The second, D_2, deformation is dominant in the area and is recognized as outcrop scale folding, metamorphic fabric (well developed cleavage), and lineations. D_2 folds are upright with northeast trending axes and are readily observed in the metasediments. The D_2 folding is the result of northwest directed transpression that affected the entire area and was responsible for regional metamorphism to greenschist and/or amphibolite grades (Peterson, in prep). The age of the D_2 deformation is constrained by age dating of two intrusions of the Giants Range batholith that encompass the event. The pre-D_2 Brit granodiorite has an age of 2681 +/- 4 Ma and 2685 +/- 4 Ma and the post-D_2 Shannon Lake granite has a date of 2674 +/- 5 Ma (Boerboom et al. 1993). This makes the D_2 useful in determining age relationships of intrusive bodies. The last deformation, D_3, observed in the area produced northeast and northwest trending faults and a weak cleavage, and was probably related to the end of the D_2 deformation (Jirsa et al. 1992). These deformations are believed to be a result of island arcs accreting onto the margin of the craton (Card, 1990; Williams, 1990).

The Vermilion District has historically been important for its iron mineralization. The Soudan Member of the Ely Greenstone is composed of Algoma-type banded iron formation interspersed with thin lavas and tuffs (Morey et al. 1970). It has an average thickness of 700 meters and contains high-grade hematitic iron ore that was mined from the late 1800's until 1962 in the Soudan Mine (Peterson, in prep). At present, the Vermilion District is being recognized as having many characteristics favorable for volcanogenic massive sulphide and shear zone hosted gold mineralization. Several sites of interest are Five Mile Lake, Eagles Nest Lake No. 4 (the subject of this thesis), Gafvert

Lake, and the Purvis Road locales for VMS, and the Mud Creek and Murray Shear Zones for gold mineralization (Peterson and Jirsa, 1999).

CHAPTER 2

LITHOLOGY AND STRATIGRAPHY

Mafic volcanic rocks of the Lower Ely Greenstone are the dominant rock type within the Eagles Nest map area. Chemical analyses of samples taken from outcrops at Eagles Nest are used to assist in further classifying these rocks. Figures 3 & 4 has all samples from the footwall and hanging wall at Eagles Nest plotted on TAS and Jenson diagrams. From this group of analyses, several samples have been selected that represent the least altered rocks in the map area. These least altered samples show that the lava flows at Eagles Nest are dominantly andesites.

Total silica content is a commonly accepted basis for classifying igneous rocks. Total silica is also the most important chemical difference between a basalt and an andesite (Middlemost, 1980). The TAS diagram (LeMaitre, 1984) uses total weight percent SiO_2 plotted against weight percent $Na_2O + K_2O$ to distinguish among the range of volcanic rocks. The five least altered samples plot in the andesite field on this classification (Figure 5). Winchester and Floyd (1977) designed a plot of Zr/TiO_2 versus SiO_2 to define volcanic rock types. With this classification scheme the least altered samples plot well within the boundaries of the andesite field (Figure 6).

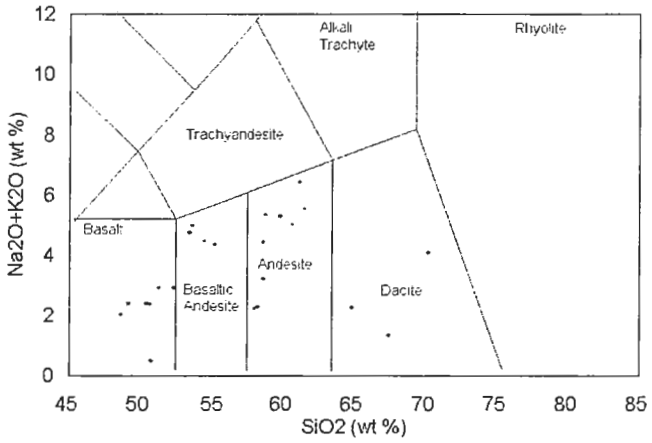

Figure 3: TAS (LeMaitre, 1986) diagram showing all chemical analyses from the footwall and hanging wall at Eagles Nest. Samples from the mineralized horizon are excluded due to extreme alteration.

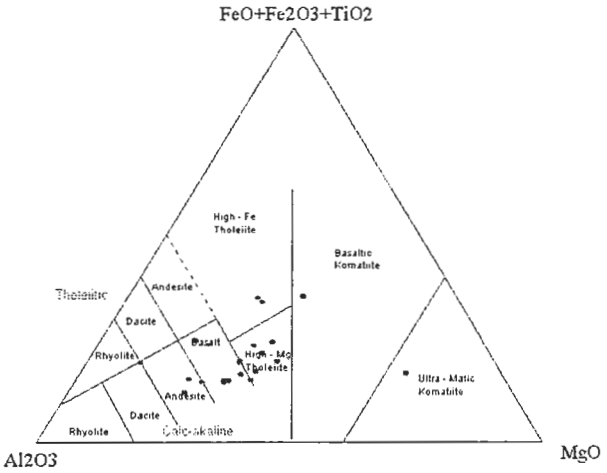

Figure 4: Jenson (1976) diagram showing all chemical analyses from the footwall and hanging wall at Eagles Nest. Samples from the mineralized horizon are excluded due to extreme alteration.

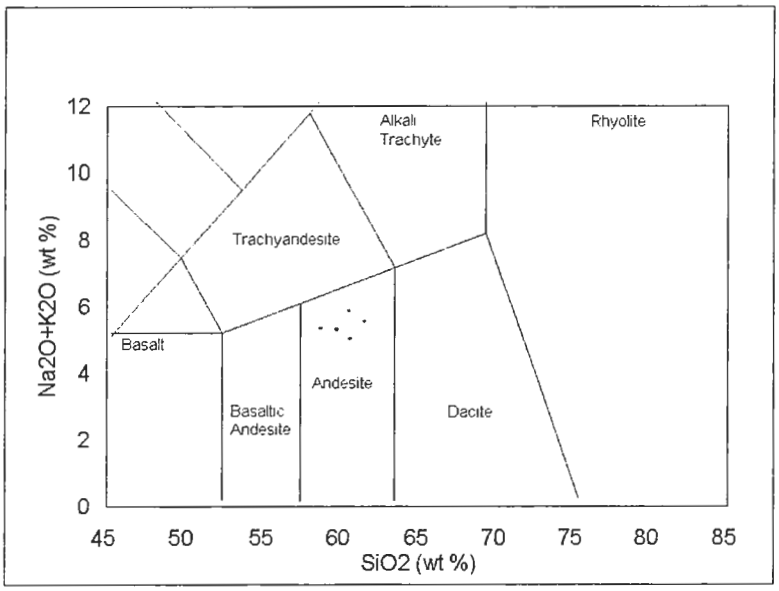

Figure 5: TAS diagram (LeMaitre, 1986) of least altered rocks from Eagles Nest

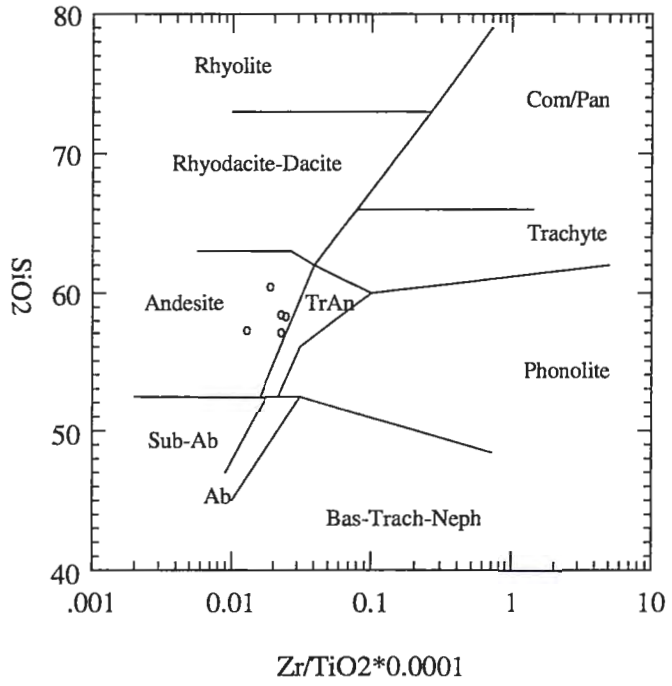

Figure 6: Winchester and Floyd diagram (1977) of least altered rocks from Eagles Nest. Com = Comendite, Pan = Pantellerite, Neph = Nephalinite, Bas = Basalt, AB = Alkaline Basalt, Trach = Trachyte.

Normalized values of Al_2O_3, MgO, and ($FeO + Fe_2O_3 + TiO_2$) in cation percent are plotted on a Jenson cation diagram. These values are not affected by slight variations in the weight percent of K, Na, Ca, and Si. This classification allows rock types of subalkalic volcanic rocks to be classified, and three different magma differentiation trends to be recognized (Jenson, 1976). The five least altered samples from Eagles Nest exhibit a distinct calc-alkaline differentiation trend. The calc-alkaline nature of these andesites suggests that these rocks are associated with island arc-style volcanism, which agrees with previous work done in the Lower Ely Greenstone (Southwick et al. 1998). Analyses of four of the five least altered samples plot within the compositional range of basalt, and one sample falls in the andesite field (Figure 7). The fact that these rock analyses plot as basalts on the Jenson diagram, but as andesites when silica and alkalis are considered, suggests that they are low K andesites. The chemical composition of

average calc-alkaline, low K andesite shows Al_2O_3 decreased by up to 2 weight percent over the higher K andesite (Gill, 1981) and this composition also plots as basalt on the Jenson diagram. The Al_2O_3 content of the Eagles Nest rocks most closely matches a low K andesite.

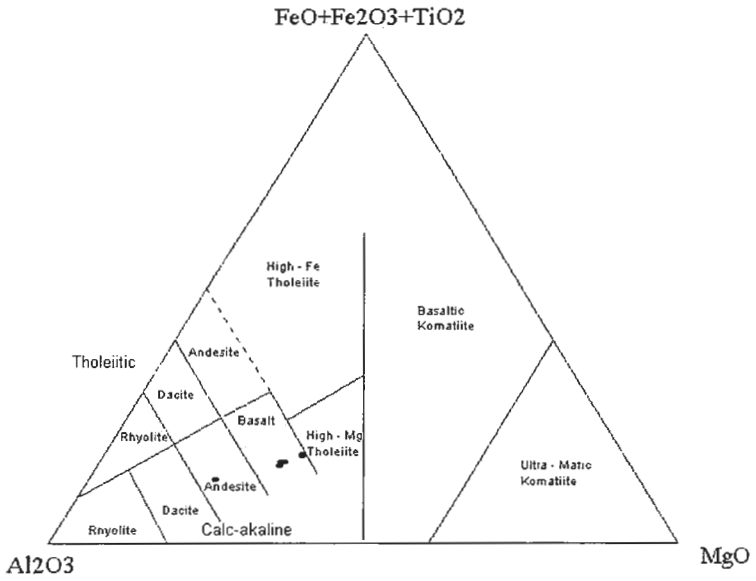

Figure 7: Jenson diagram (1976) of least altered rocks from Eagles Nest.

Lithological Description

The Eagles Nest map area (Plate 1) is located within the Lower Member of the Ely Greenstone, which is composed dominantly of pillowed and massive mafic lavas with local felsic fragmental horizons and small plutons. The entire sequence has been metamorphosed to greenschist grade (Peterson, in prep). Approximately 1575 meters of vertical strata were mapped at Eagles Nest. All rock units in the map area strike approximately east-west and dip 70°-80° to the north. The Purvis Lake Pluton lies at the southern margin of the map area and stratigraphically at the bottom of the sequence. The Purvis Lake Pluton is overlain by approximately 1300 meters of massive, amygdaloidal, and pillowed andesitic lava flows that make up the footwall to the mineralized horizon. The mineralized package is not exposed at the surface and is only observed in three

diamond drill cores. It consists of approximately100-150 meters of alternating, thinly bedded, strongly altered mafic lavas, one thin felsic unit, epiclastic rocks, and banded iron formation. The hanging wall is composed of pillowed, massive, and amygdaloidal andesite with one chemically distinctive basalt lava flow. X-ray Diffraction analysis was used in conjunction with thin section study to identify the fine grained minerals of the lava flows.

For purposes of description, the stratigraphy has been divided into four separate groups, in stratigraphic order these groups are: the Purvis Lake Pluton, the Footwall Lavas, the Mineralized Package, and the Hanging Wall Lavas. The geologic map of the Eagles Nest Prospect is presented in Plate 1.

Purvis Lake Pluton

The Purvis Lake Pluton occurs in the southeast portion of the Eagles Nest map area and was first mapped and described by Dean Peterson and Mark Jirsa (1999a). In size, it is approximately six kilometers long and has a maximum thickness of one kilometer (Peterson and Jirsa, 1999a). The D_2 deformation cleavage cuts the pluton and significant contact metamorphism has not been observed (Peterson, 1999). The bulk of the pluton lies east of the Eagles Nest Prospect. In the thesis area the stratigraphically thin, western most portion of the Purvis Lake Pluton is a light grey, fine-grained, granular diorite that has undergone low grade metamorphism. Thin section study shows that it is composed of 50% 1-2 mm plagioclase and 40% actinolite/hornblende with 5% quartz and 3% epidote. The plagioclase is moderately altered to sericite. Minor quartz is interstitial to the coarse plagioclase and amphibole, and minor epidote alteration is present in 1 mm patches. A second sample of the Purvis Lake Pluton was made available for this study by Peterson, who collected it several miles east of Eagles Nest (Peterson, in prep). In hand sample it is described as a white, medium grained tonalite. The mafic minerals are partly replaced by epidote and chlorite and minor veinlets of pyrite and quartz with chalcopyrite are present (Peterson, in prep).

Whole rock chemical analysis was performed on the two samples described above. The first sample, from the southeast corner of the Eagles Nest map area, has a

normative classification of diorite (Appendix 2). This sample lies in the basaltic andesite compostion field of the TAS diagram (Figure 8), similar to the andesite lavas that sit stratigraphically above it. The second sample, taken to the east, is considerably more felsic than the sample from Eagles Nest and has a normative composition of granodiorite (Appendix 2), and plots in the dacite field on the TAS diagram (Figure 8). Further study would be required to better define the compositional variations within the Purvis Lake Pluton.

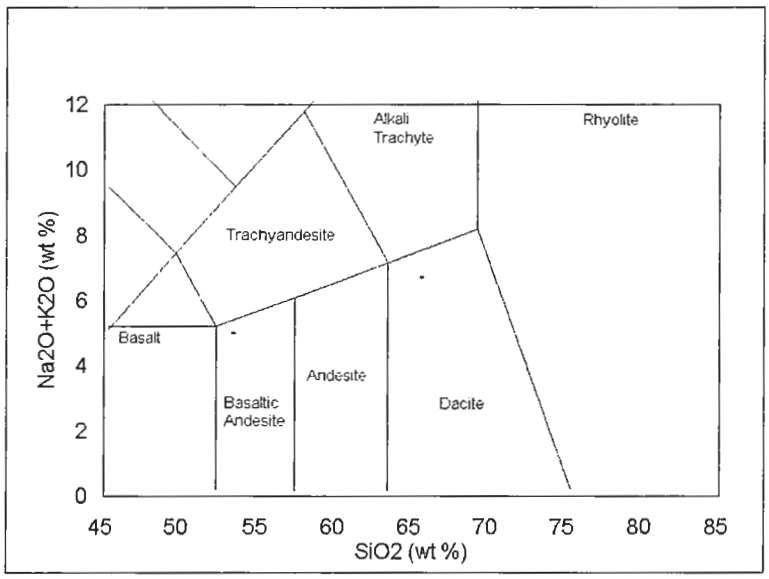

Figure 8: TAS diagram (LeMaitre, 1986) of two samples from the Purvis Lake Pluton.

The top of the Purvis Lake Pluton at Eagles Nest is an intrusive breccia that clearly crosscuts the overlying volcanic rocks. The pluton has intruded into the lavas, carrying with it a mixture of angular xenoliths. Outcrops at the margin of the intrusion contain approximately 20% 5 to 40 centimeter diameter xenoliths of epidote altered andesite, aplite, hornblendite, diorite, and granodiorite set in a matrix of dioritic, to locally granodioritic composition (Figure 9). Another magmatic breccia is located approximately 400 meters higher in the section. It is at least 60 meters wide and varies in composition from light grey tonalite to white granodiorite. The clasts in the breccia are angular, 8 to 30 centimeter diameter fragments of andesite and mafic and intermediate

Figure 9: Outcrop of magmatic breccia near the top of the Pruvis Lake Pluton containing xenoliths of epidote altered andesite, diorite, and granodiorite in a dioritic and granodiortic groundmass.

Figure 10: Intermediate composition dike crosscutting pillowed andesite. Widest part is approximately 10 centimeters thick.

intrusions making up 10% of the outcrop. Immediately adjacent to, and surrounded by this intrusion, is a strongly amygdaloidal andesite of the same character as the andesites observed lower in the stratigraphy. It is possible that this may be a large, meter scale xenolith brought up by the intruding magma. However, lack of exposure hinders confirmation. Finally, similar magmatic breccia outcrops, containing clasts of banded iron formation up to 0.5 meters and smaller clasts of quartz-epidote altered andesites, have been found further to the east of Eagles Nest by Peterson (1999, in prep). The evidence above indicates that the Purvis Lake Pluton had multiple intrusive phases.

Contact metamorphism is not obvious along the contacts of the intrusion. The low temperature albite-epidote facies of contact metamorphism of a mafic rock is defined by a mineral assemblage of albite, epidote, actinolite, and chlorite (Blatt and Tracy, 1996). Many of these minerals are ubiquitous in the andesites that have been intruded by the Purvis Lake Pluton, making recognition of a contact metamorphic aureole difficult. However, one outcrop near the upper intrusion has 0.5-1 centimeter round blebs of actinolite-chlorite, a texture not observed elsewhere, that is interpreted to be the result of contact metamorphism. This, combined with the presence of the magmatic breccia, suggests that the Purvis Lake Pluton is not in the same stratigraphic position that it occupied when the Eagles Nest area was volcanically active.

Dikes

Throughout the stratigraphy, many small dikes crosscut the Eagles Nest lavas. They range in size from < 0.05 to approximately 2 meters wide, trend generally northward, and vary from dark grey and fine grained to cream colored and medium grained (Figure 10). From hand sample and thin section study these dikes are dioritic to tonalitic in composition, and are predominately composed of plagioclase feldspar and amphibole. Quartz percentages range from 0-30% and biotite occurs in several samples. Other minor minerals observed are epidote, sericite, chlorite, calcite, and pyrite.

One strongly altered outcrop sample appears to be an ultramafic dike from its chemical analysis. This is based on high MgO and low SiO_2 content of the rock. Other dikes observed in the field, but which have no chemical analysis or thin section, are dark

colored and mafic; some contain biotite and appear lamprophyric. Epidote and chlorite in the dikes are likely a result of the regional greenschist metamorphism. One outcrop has 10 – 18 centimeter magnetite veins that contain angular epidotized clasts of the immediate wall rock (Figure 11).

Footwall Lavas

Approximately 1300 meters of andesitic lavas occur between the mineralized horizon and the Purvis Lake Pluton. All of the lavas have been metamorphosed to greenschist facies. Several primary volcanic textures can be seen in outcrops of these flows including lava lobes, hyaloclastite, flow breccias, pillows, and amygdaloidal flows. Pillows are the most common feature observed.

One large andesitic outcrop in the southern portion of the field area has characteristics similar to what has been described as lobe hyaloclastite flow morphology (Gibson et al. 1999). This outcrop is approximately 10 meters long and 1.5 meters high and has 15 to 40 centimeter diameter irregular, massive lava clasts with glassy rims that are encased in a matrix of fine grained hyaloclastite (Figures 12 & 13). According to Gibson et al (1999), lobe hyaloclastites are typical of subaqueous rhyolitic lava domes and form when felsic lava intrudes a water-saturated mixture of hyaloclastite and breccia on the outer margin of a dome and is quenched. Though this morphology has been described dominantly in rhyolite complexes, it could be developed in a viscous andesite (Morton, pers com 2000).

Massive andesite lavas are medium to dark grey-green and very fine grained in hand sample, some are porphyritic in thin section. The andesites have a local, weak east-west foliation. Joints and fractures are iron oxide stained. One percent disseminated, fine grained, euhedral pyrite is common. Patches of epidote +/- quartz alteration occur on a centimeter to meter scale and cause the rock to take on a pale grey to strong apple green color depending on the local ratio of epidote to quartz. Actinolite-chlorite alteration is locally pervasive and gives the rock a dark green color. Nowhere in the sequence were significant phenocrysts visible in hand sample.

Figure 11: Dark grey magnetite vein crosscutting epidotized andesite in the footwall.

Figure 12: Outcrop of andesitic lobe hyaloclatite showing white lava pods within a dark grey hyaloclastite matrix.

Figure 13: Close up of a coarse grained hyaloclastite matrix from lobe hyaloclastite andesite lava flow.

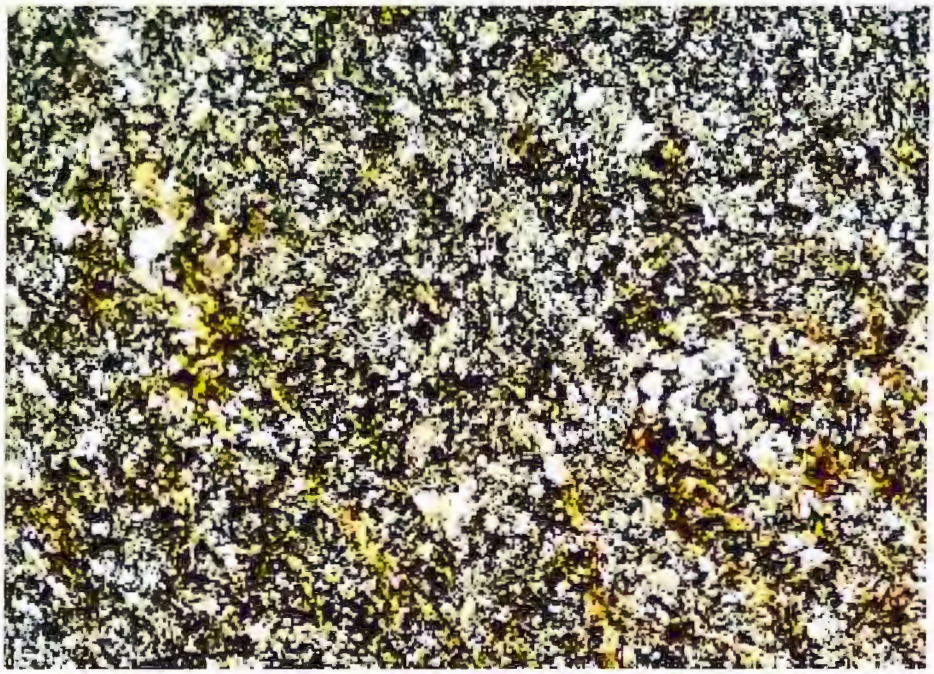

Figure 14: Photomicrograph of a least altered sample of andesite lava. Mineral assemblage is very fine grained quartz/feldspar groundmass with chlorite + quartz + calcite. Crossed polars, field of view = 2.5 mm.

In thin section the least altered massive flows are composed of 10-60% plagioclase that occurs in two forms (Figure 14). The feldspar occurs as either ≤ 1 mm, euhedral, zoned phenocrysts that may be partially altered to sericite, or as part of a very fine grained groundmass where it is intergrown with quartz and only identifiable by x-ray diffraction analysis. One thin section clearly shows quench texture plagioclase phenocrysts (Figures 15 & 16). More commonly the flows are composed primarily of 20-60 percent fine grained, dark green, elongate actinolite with variable amounts of quartz, chlorite, and epidote and 1% opaque grains, usually pyrite. Carbonate alteration becomes more common near the mineralized horizon.

Pillowed lavas are common throughout the sequence. Pillow size ranges from approximately 20 to 70 centimeters in diameter. Pillow rims are dark green, 2 to 4 centimeters thick, and are typically altered to actinolite + chlorite with disseminated pyrite (Figure 17). Fine-grained hyaloclastite is common along pillow rims and as matrix between pillows, and is easily identified in thin section as angular clasts cemented by quartz (Figures 18 & 19). One to 10 mm diameter, round to elongate amygdules of quartz, epidote, or carbonate occur along pillow margins; pillow interiors are locally epidote +/- quartz altered and pale apple green in color (Figure 20).

Amygdules are common in both massive and pillowed flow types. They range in size from <1 mm to approximately 10 mm with the majority being 2-4 mm. Amygdule percentages range from 1% to >50%, with the greatest concentration found along pillow rims and in zones of massive lavas that probably represent flow tops. The most intense vesiculation occurs deep in the footwall rocks where some of the largest vesicles are approximately 8-12 mm. Pillows in this area show a concentration of up to 60% vesicles within 8 centimeters of pillow rims. One sample taken from outcrop higher in the section (approximately 500 meters below the mineralized horizon) appears scoriaceous, having 30% stretched and flattened amygdules that are in contact with one another. The composition of the amygdules is most commonly quartz, quartz + epidote, or epidote with actinolite and carbonate. In thin section many amygdules are zoned with quartz rims and epidote interiors (Figure 21). Carbonate amygdules become more common

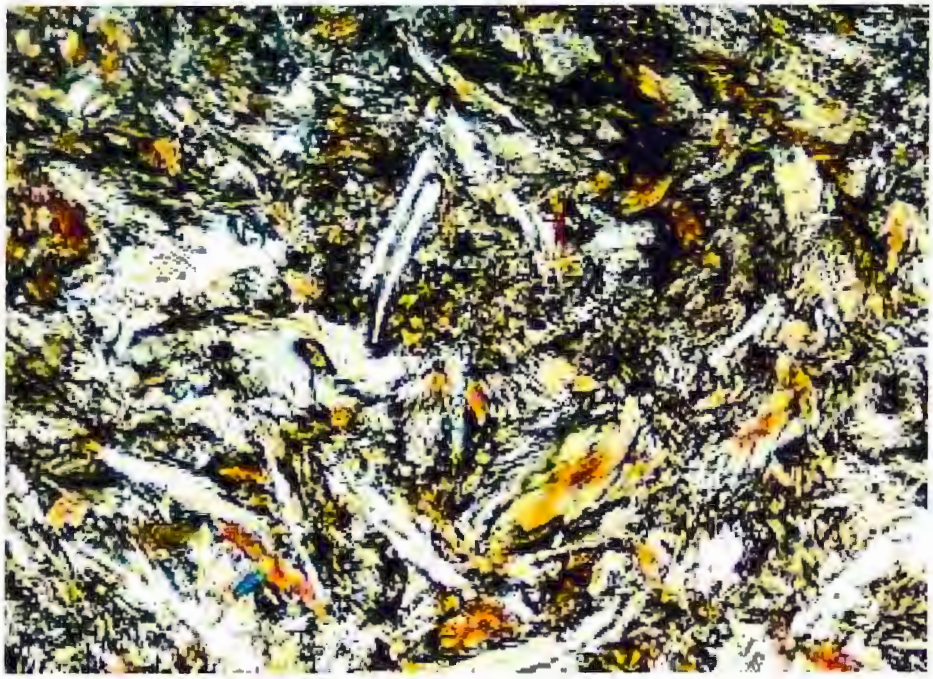

Figure 15: Photomicrograph of least altered andesite lava with quenched plagioclase feldspar. Mineral assemblage is plagioclase + actinolite + chlorite + epidote + quartz w/ minor calcite. Crossed polars, field of view = 1 mm.

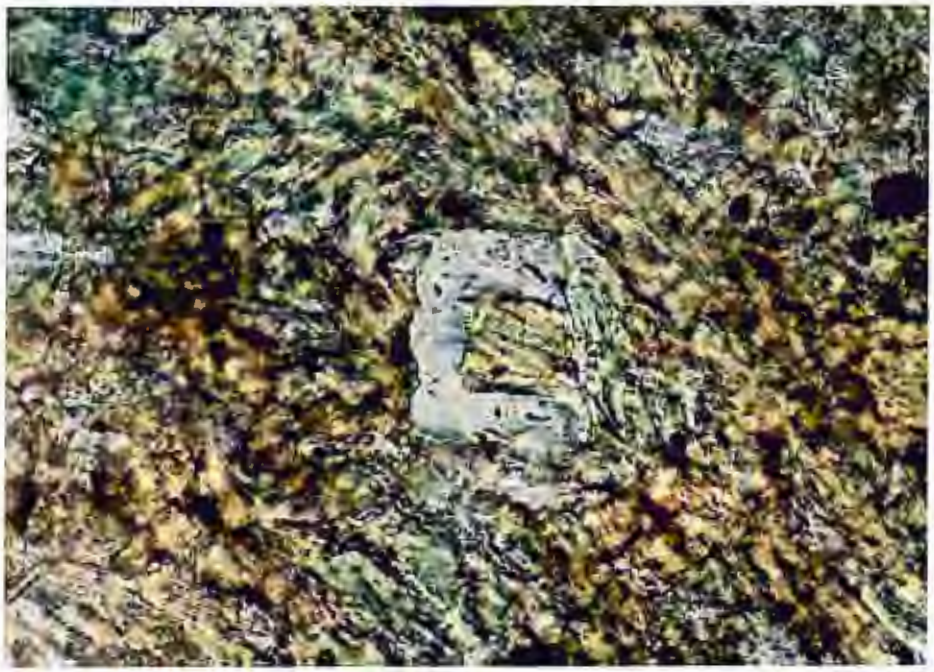

Figure 16: Photomicrograph of least altered andesite lava with quenched feldspar showing interior glass replaced by actinolite. Crossed polars, field of view = 0.25 mm.

Figure 17: Epidote altered pillowed andesite lava from the footwall. Pencil for scale.

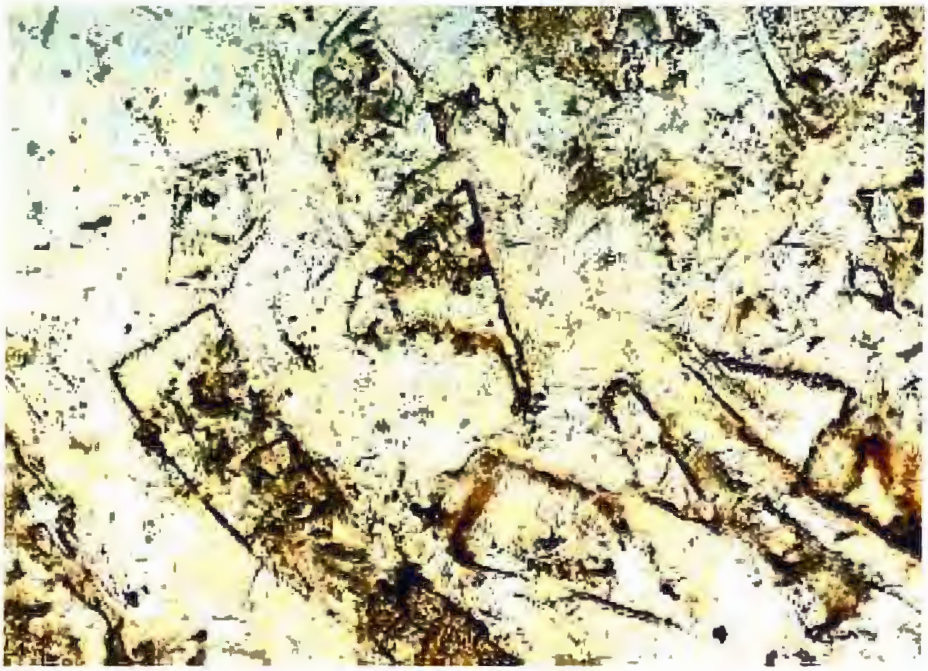

Figure 18: Photomicrograph showing fine grained hyaloclastite. Plane polarized light, field of view = 2.5 mm.

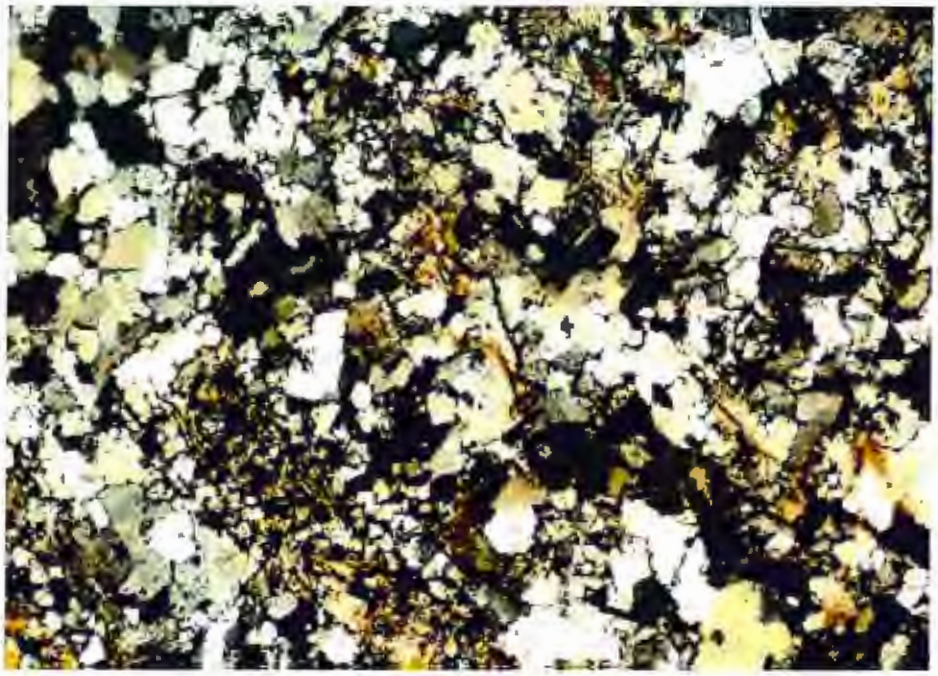

Figure 19: Photomicrograh showing quartz alteration of fine grained hyaloclastite. Same view as Figure 15. Crossed polars, field of view = 2.5 mm.

Figure 20: Epidote altered pillow interior from the footwall andesite. Three centimeter thick dikes at top of photograph.

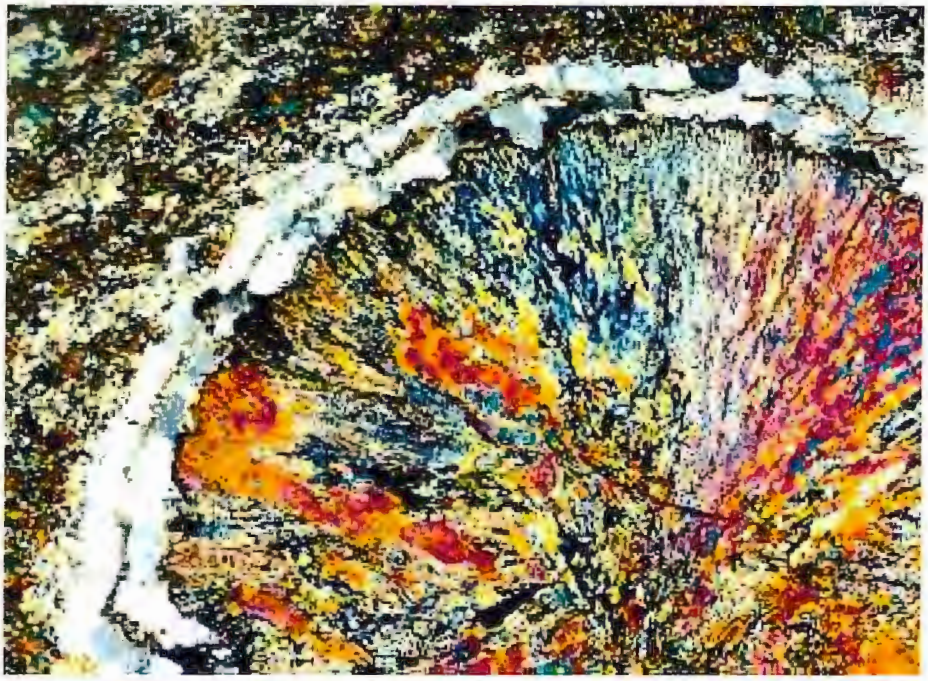

Figure 21: Photomicrograph showing amygdule with a quartz rim and epidote interior. Crossed polars, field of view = 2.5 mm

higher in the section. Amygdule shapes are round, elongate, and elongate with angular corners indicating lava movement as the vesicle formed.

Mineralized Horizon

The following description of the mineralized horizon is based upon core descriptions from three diamond drill holes that intersect mineralization. Rocks of the mineralized horizon are not exposed at the surface. Drill holes are arranged in an east-west trending line approximately 100-150 meters north of the margin of Eagles Nest Lake No. 4, are oriented at 160°, and dip at 45°. The mineralization lies within an approximately 100-150 meter thick package of strongly altered banded iron formation, thin lava flows, and epiclastic rocks. Thin massive sulphide lenses are found within the banded iron formation. The transition from footwall lavas to the mineralized package is well defined and is marked by the first appearance of epiclastic sediments and a change of alteration mineralogy and intensity. Individual units within the mineralized horizon may be only 0.5 to 1 meter thick and are frequently discontinuous between the three drill holes (Figure 22). Each unit is describe below.

In core, rocks interpreted to represent epiclastic sediments appear to be very fine grained, tan to grey, chlorite and/or sericite rich siltstones. Microscopic study shows them to be composed of ≤ 0.05 mm mineral grains of 30-45% chlorite, 20-40% carbonate, 2-5% sericite, 2-5% quartz, and 5-50% quartz/plagioclase groundmass and contain what appear to be fine-grained rock fragments. These rocks have been interpreted to have been sedimentary due to the presence of broken quartz and plagioclase grains and fine-grained rock fragments (Figure 23).

The banded iron formations are predominately oxide facies, but may contain variable amounts of pyrite. The iron formations range in thickness from 1.5 to 21 meters and may be interlayered with epiclastic rocks, mafic lava flows, and massive sulphide horizons. The primary constituents of the iron formations are fine-grained to very fine-grained magnetite interlayered with quartz, or with fine-grained fibrous tremolite. Minor talc, calcite, sericite, chlorite, and tremolite locally occur. Bed thicknesses are <1 mm to 3-4 mm and typically alternate layers of euhedral to subhedral magnetite + quartz and

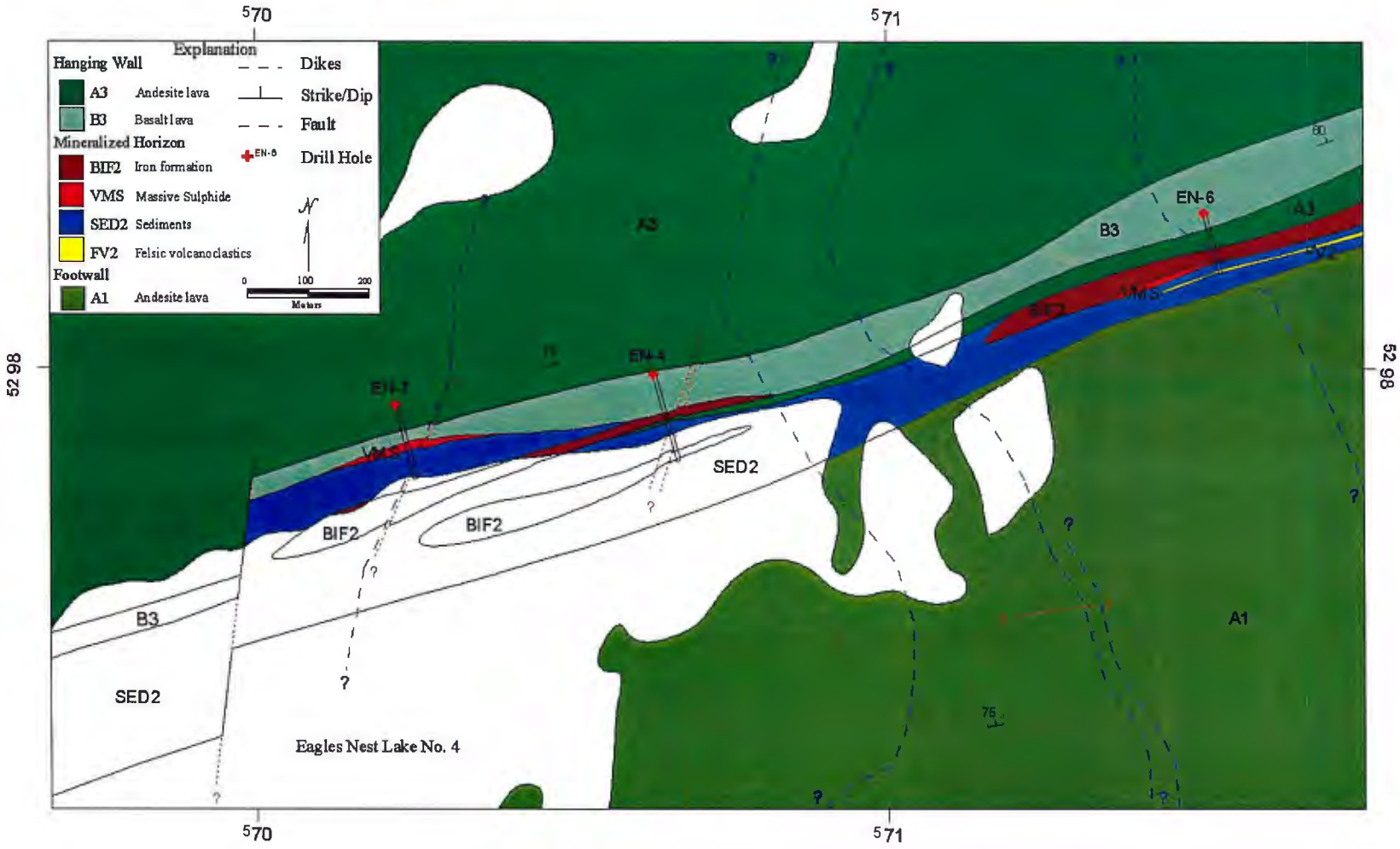

Figure 22: Geology of the Mineralized Horizon at the Eagles Nest Prospect.

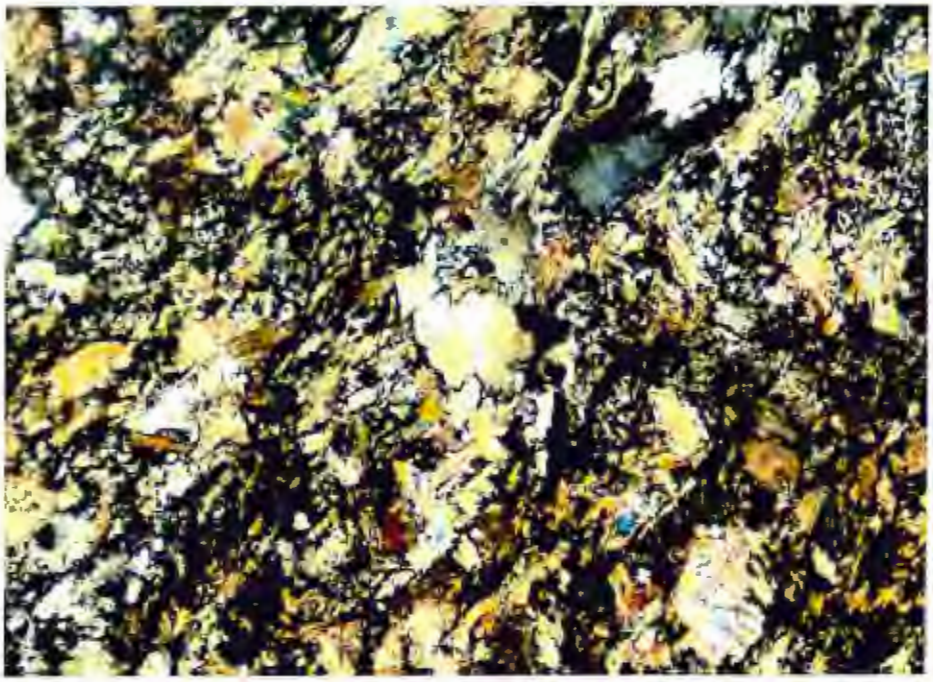

Figure 23: Photomicrograph of very fine grained, altered sedimentary rock with irregular quartz grain at center. Chlorite, carbonate, and sericite are the alteration minerals. Crossed polars, field of view = 1 mm.

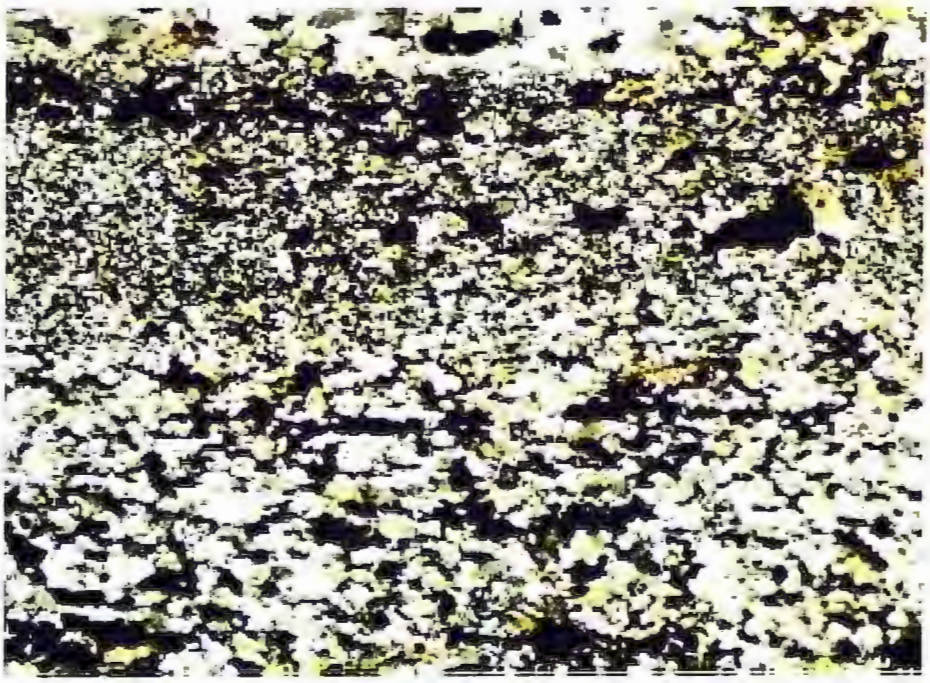

Figure 24: Photomicrograph of banded iron formation with quartz, magnetite, minor pyrite, and minor calcite. Crossed polars, field view = 2.5 mm.

chert (Figure 24). Pyrite, when present, is euhedral. In some cases calcite has replaced the pre-existing mineralogy, and is interlayered with chert, minor pyrite, and chlorite. Calcite grains range from < 1 mm to 2 mm and may be euhedral to anhedral. Some iron formation units are brecciated.

Thin massive sulphide lenses are present in all three drill holes. Hole EN-7 has 3.6 meters of banded and brecciated massive to semi-massive pyrite (10-80%) +/- minor sphalerite with varying amounts of quartz, chlorite, carbonate, and sericite overlain by 1.8 meters of cherty exhalite. Hole EN-4 has thin stringers of semi-massive and massive sulphide interlayered with oxide facies iron formation. The massive sulphide consists of up to 90% pyrite with 1-2% chalcopyrite and sphalerite. This is immediately overlain by a thin lava flow. Hole EN-6 has 1.2 meters of semi-massive sulphide consisting of 40-50% pyrite interlayered with chert and chlorite. This unit is interlayered with oxide facies iron formation.

One thin section, from hole EN-6, appears to represent a felsic sedimentary rock, because of the presence of < 0.5 mm quartz crystals. This unit was not recognized in core. It has a very fine grained quartz/feldspar + chlorite groundmass with 2-3% quartz crystals and patches and blebs of calcite.

Banded iron formation units shown on the map represent several thin units that have been combined so that they can be displayed at map scale. In actuality, the top portion of the banded iron formations in all three drill holes are not homogenous sequences and are separated by several thin (2-3 meter) lava flows. The flows have been strongly altered and are sometimes only identifiable as such by the presence of plagioclase phenocrysts that have not been completely replaced by various alteration minerals.

Hanging Wall Lava

Massive, amygdaloidal, and pillowed andesitic lava flows make up the majority of the hanging wall to the Eagles Nest mineralization. However, based on the chemistry of samples from the hanging wall, a thin sequence of basaltic lava flows has been identified (Figure 25 & 26). The basalt occurs a few meters above the last iron formation

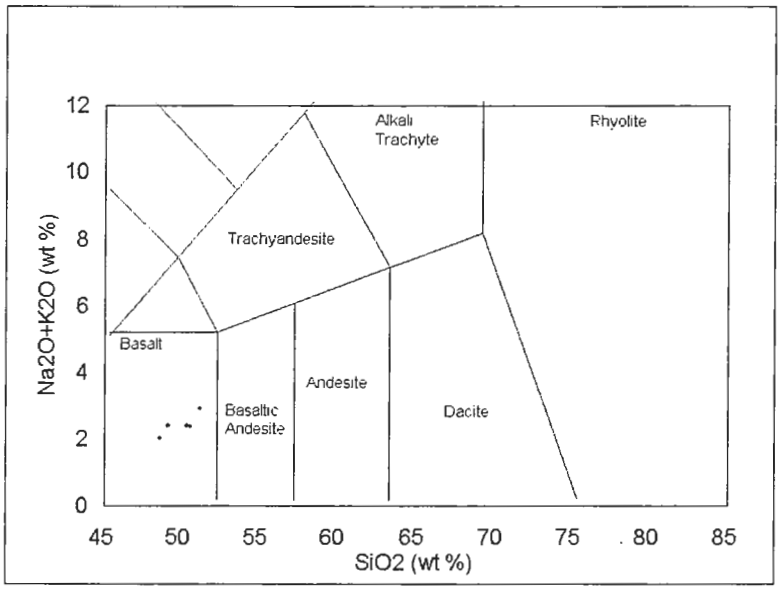

Figure 25: TAS diagram (LeMaitre, 1986) of hanging wall basalts at Eagles Nest.

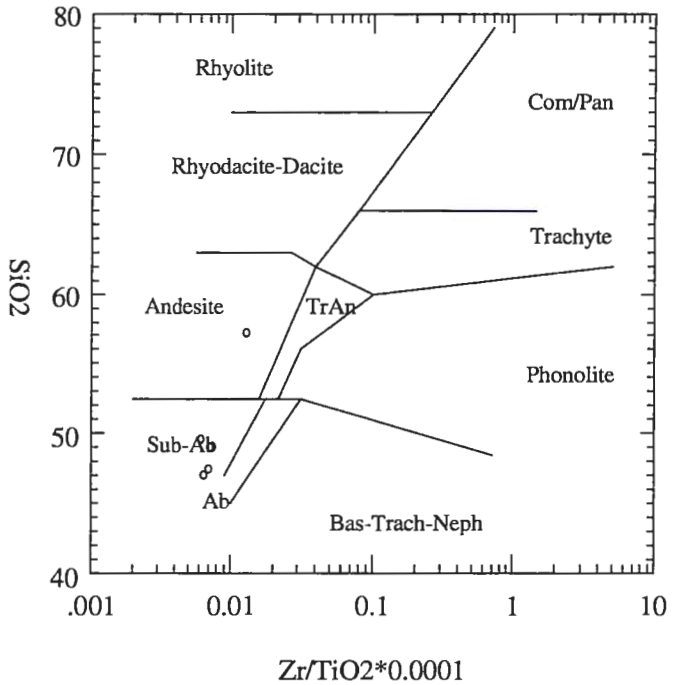

Figure 26: Winchester and Floyd diagram (1977) of hanging wall rocks at Eagles Nest. Com = Comendite, Pan = Pantellerite, Neph = Nephalinite, Bas = Basalt, AB = Alkaline Basalt, Trach = Trachyte.

unit in hole EN-6, with an andesite lava flow in between. In the two western most drill holes the basalt flow appears to be the first lava above the iron formation (Figure 22). This basaltic flow has twice the Ti content, low Si, and increased Fe and Mg contents compared to the andesites above and below them. They are not distinguishable from andesites in the field, except possibly by pillow shape

Pillowed flows within the basalts have a slightly more fluid morphology than those seen within any of the andesites, probably due to lower viscosity of the lava. Pillows have flattened and elongated shapes and occur as small, approximately 20 centimeter diameter pillows that increase in size to larger, > 50 centimeter pillows (Figure 27). Pillow rims are 5-7 centimeters thick, composed of soft actinolite + chlorite, and may be strongly iron stained. The interiors of the pillows are variably quartz-epidote altered, and may have 5-10%, 2-3 mm amygdules distributed toward the upper surface of the pillow. Minor pyrite grains along with quartz and epidote blebs are common.

The hanging wall lavas are metamorphosed to greenschist facies, moderately to strongly altered, and are generally fine-grained with 20-80% fibrous actinolite, 5-40% euhedral to subhedral epidote grains and clots, 5-30% elongate chlorite of varying composition, 5-30% quartz grains or very fine-grained quartz/plagioclase groundmass, 5-45% euhedral to subhedral, twinned, sericite altered plagioclase, and minor subhedral pyrite and magnetite. Calcite is locally abundant, making up as much as 60% of the rock.

Dikes in the hanging wall are common. Light grey, quartz-feldspar porphyry dikes are found in both the drill core of the mineralized horizon and in outcrop in the hanging wall. They are physically very similar to dikes seen at the Five Mile Lake Prospect that are thought to be intrusions into shear zones associated with the Murray Shear Zone (Hudak, pers com 2000). Dikes of diabase and intermediate compositions have also been observed.

Trace Elements

Comparison of major element oxides referred to above suggest that the Purvis Lake Pluton is similar in composition to the footwall lavas immediately above it. This would suggest that the Purvis Lake Pluton is the synvolcanic intrusion to the Eagles Nest

Figure 27: Epidote altered pillows in the hanging wall basalt lava flow.

only one sample from the Purvis Lake Pluton has trace element data that can be used in this comparison, and the pluton is variable in composition over short distances.

The rare earth elements (REE) have been shown to be mostly immobile during low grade metamorphism, weathering, and hydrothermal alteration (Michard, 1989), and so can be used to look for relationships between two rocks. Spider diagrams are constructed from normalized trace elements that are incompatible with the mantle, and are used to compare mafic volcanic rocks (Rollinson, 1993). Pearce's (1983) MORB-normalized diagram has been used here. Plotting trace element data on these two diagrams allows similarities or dissimilarities between the Purvis Lake Pluton and the footwall andesites to be easily seen. The data used for these plots is the same group of samples used for the iscon analysis in Chapter 4 (Table 2).

Plotting samples of the Purvis Lake Pluton and least altered footwall andesite on the REE diagram shows that they have a similar trend (Figure 28), which also closely matches the trend of the remaining altered footwall andesite samples (Figure 29). Samples of hanging wall basalts and andesites plotted on the same diagram show much

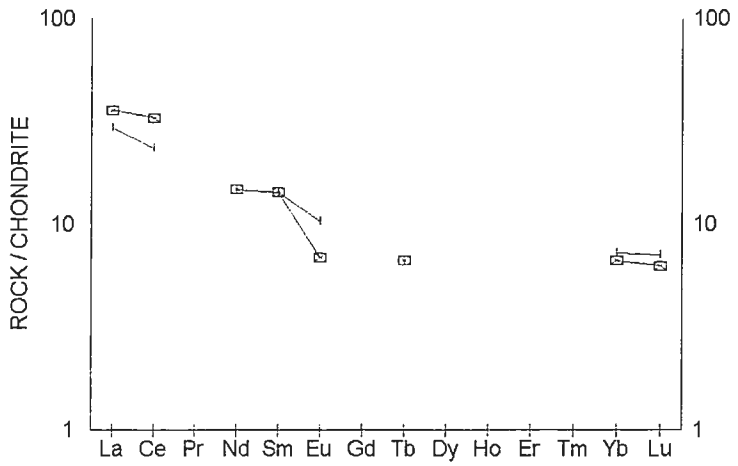

Figure 28: Rare earth element (REE) diagram of samples from the Purvis Lake Pluton and the least altered footwall andesite at Eagles Nest.

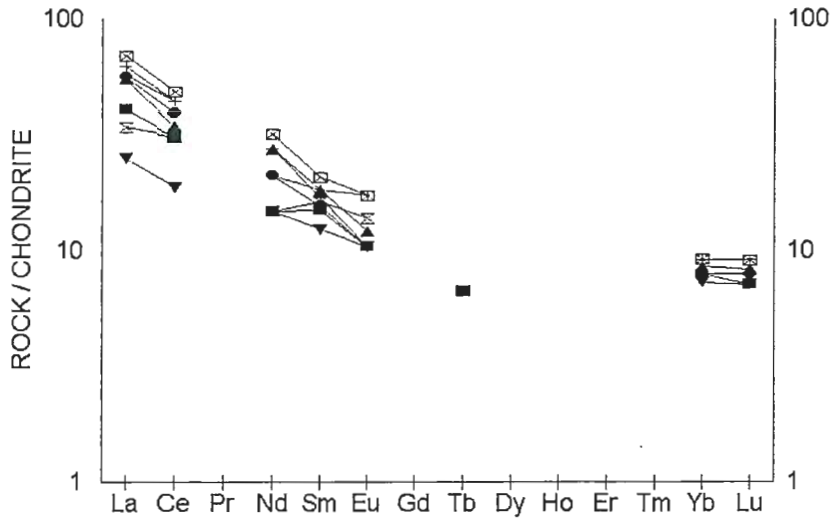

Figure 29: Rare earth element (REE) diagram of samples from altered andesites of the footwall at Eagles Nest.

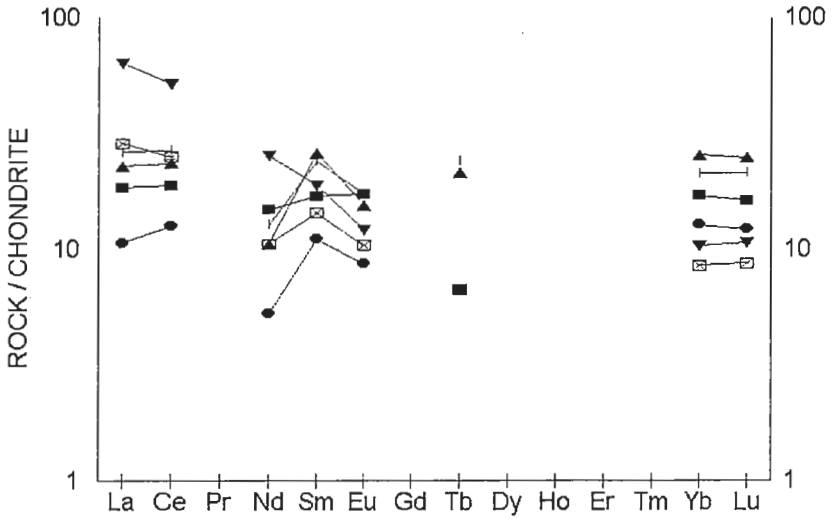

Figure 30: Rare earth element (REE) diagram of samples from andesites and basalts of the hanging wall at Eagles Nest.

variation from sample to sample within the group (Figure 30). Finally, the overall slope of hanging wall samples is flatter than that seen in the footwall.

The same sample set has been plotted on spider diagrams. The Purvis Lake Pluton and least altered andesite have a nearly identical trend on this diagram (Figure 31). Plotting the rest of the footwall samples on the diagram gives a pattern that closely matches the pattern of the Purvis Lake Pluton sample (Figure 32). The andesites and basalts of the hanging wall do not have the same pattern as the rocks of the footwall, and have more variability within the group than do the footwall rocks (Figure 33).

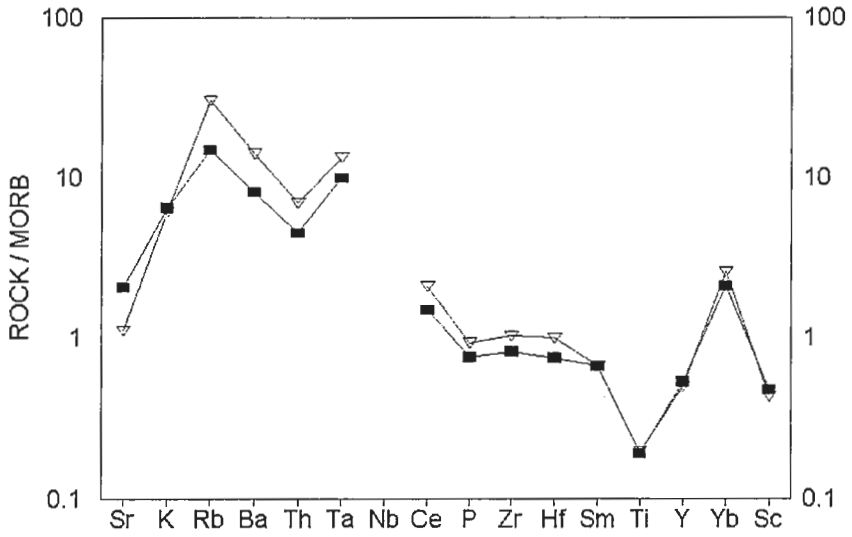

Figure 31: Spider diagram (Pearce, 1983) of samples from the Purvis Lake Pluton and least altered footwall andesite at Eagles Nest.

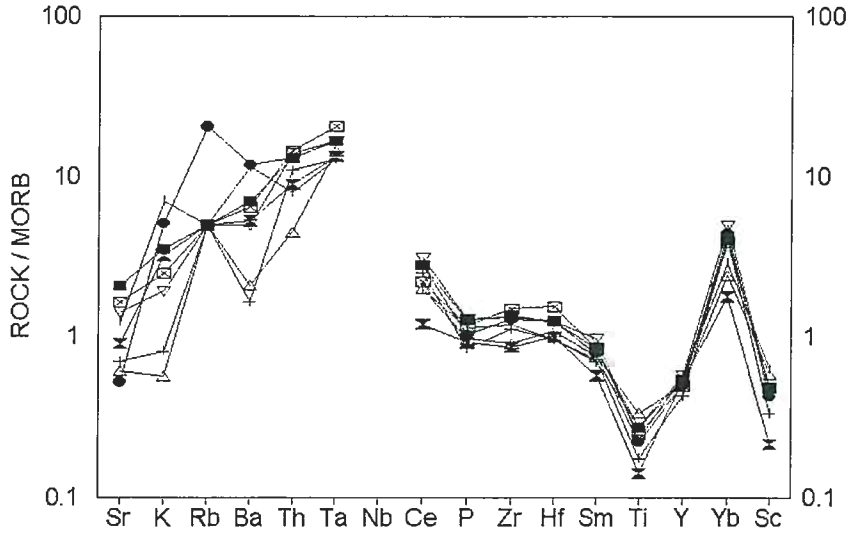

Figure 32: Spider diagram (Pearce, 1983) of samples from altered footwall andesites at Eagles Nest.

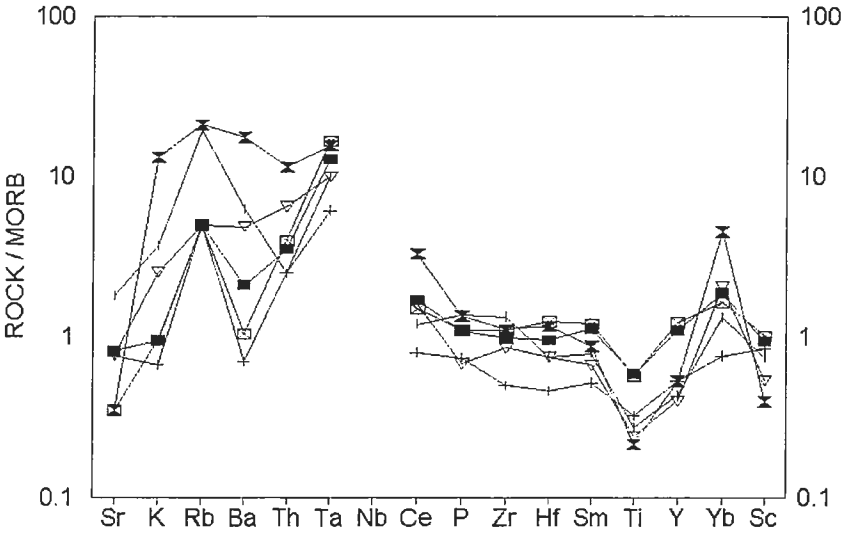

Figure 33: Spider diagram (Pearce, 1983) of samples from the hanging wall basalts and andesites at Eagles Nest.

The trace and major element data suggest a common origin for both the footwall rocks and the Purvis Lake Pluton. This relationship lends evidence to the hypothesis that the Purvis Lake Pluton could easily have been the synvolcanic intrusion feeding volcanism at Eagles Nest during the time that the footwall rocks were emplaced.

Geophysics at Eagles Nest

Ground based Electromagnetic Loop (EM) and Total Field Magnetism geophysical surveys were completed on the Eagles Nest property by Newmont Exploration during 1986-87 to define a geophysical anomaly that was originally detected by a regional airborne magnetic survey. The conductor was further constrained based on these data and three diamond drill holes were completed.

The Total Field Magnetism data have been contoured and overlain on the map of the Eagles Nest area (Figure 34). This survey was used to extend the mineralized horizon beyond the limits of the drill hole data on the geologic map of Eagles Nest. The magnetic anomaly that corresponds to the mineralization extends for a total strike length of approximately 2 kilometers and trends off the map to both the east and west. Based on an offset in the magnetic anomaly, a fault was placed on the geologic map to the west of hole EN-7. Several more offsets occur further to the west beyond the map area (Peterson et al. 1999a). The Total Field Magnetism survey did not extend over the surface of Eagles Nest Lake No. 4 and consequently, a large band of irregular contours is seen on the Total Field Magnetism map that result from the computer extrapolating to fill an area where no data exist.

The ground EM survey extended over Eagles Nest Lake No. 4. It shows an anomaly that lies along the north shore of the lake and closely corresponds to the magnetic anomaly (Figure 35). The anomaly is broken and offset in several places. This may be a reflection of the discontinuous nature of iron formation units or a result of faulting. It does not precisely correspond with iron formation units observed in drill core.

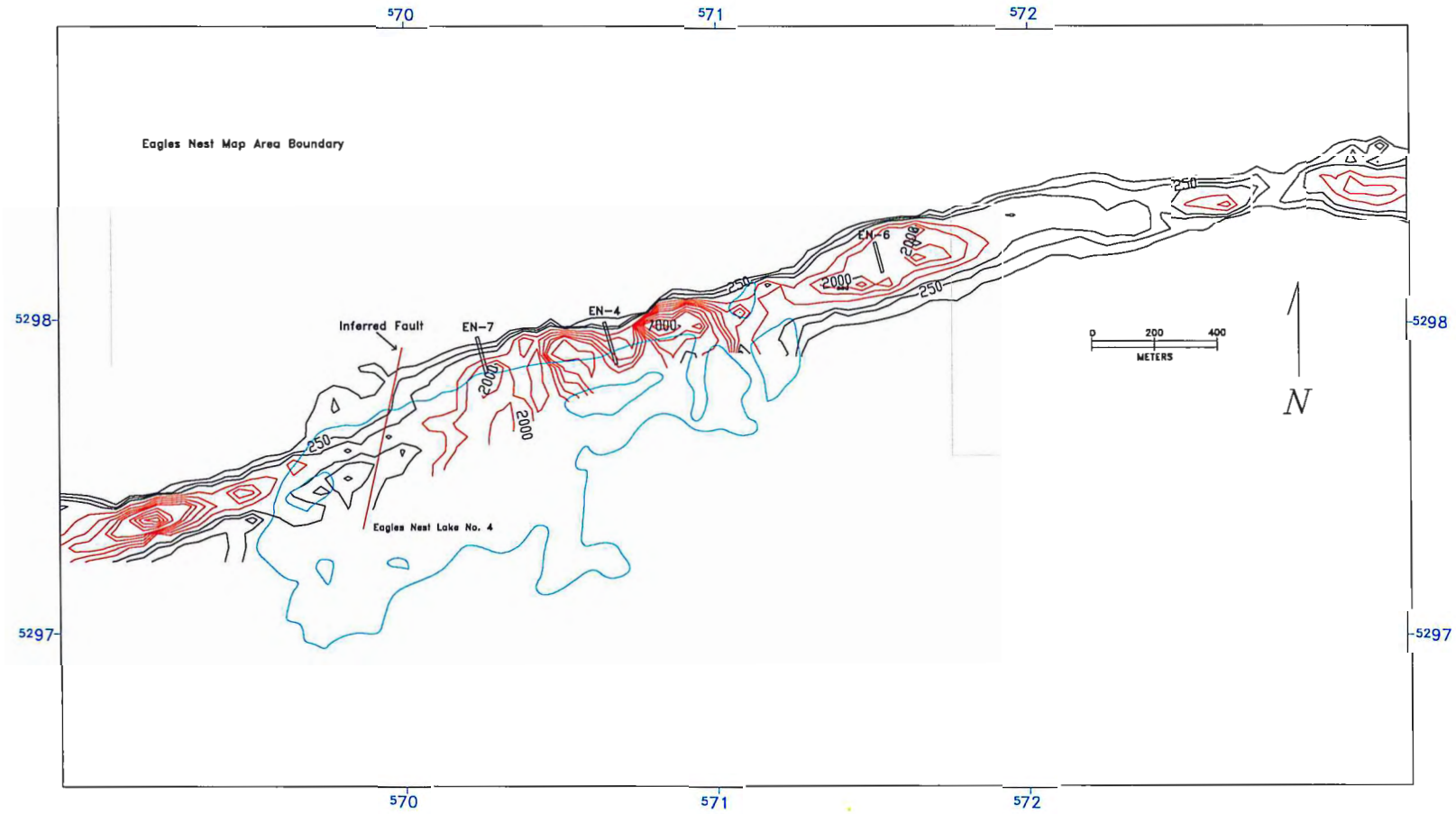

Figure 34: Contour map of the Total Field Magnetism anomaly at the Eagles Nest Prospect. Red contours indicate the most intense region of the anomaly. Ground based survey grid did not extend over Eagles Nest Lake No. 4. Surface projection of diamond drill holes shown.

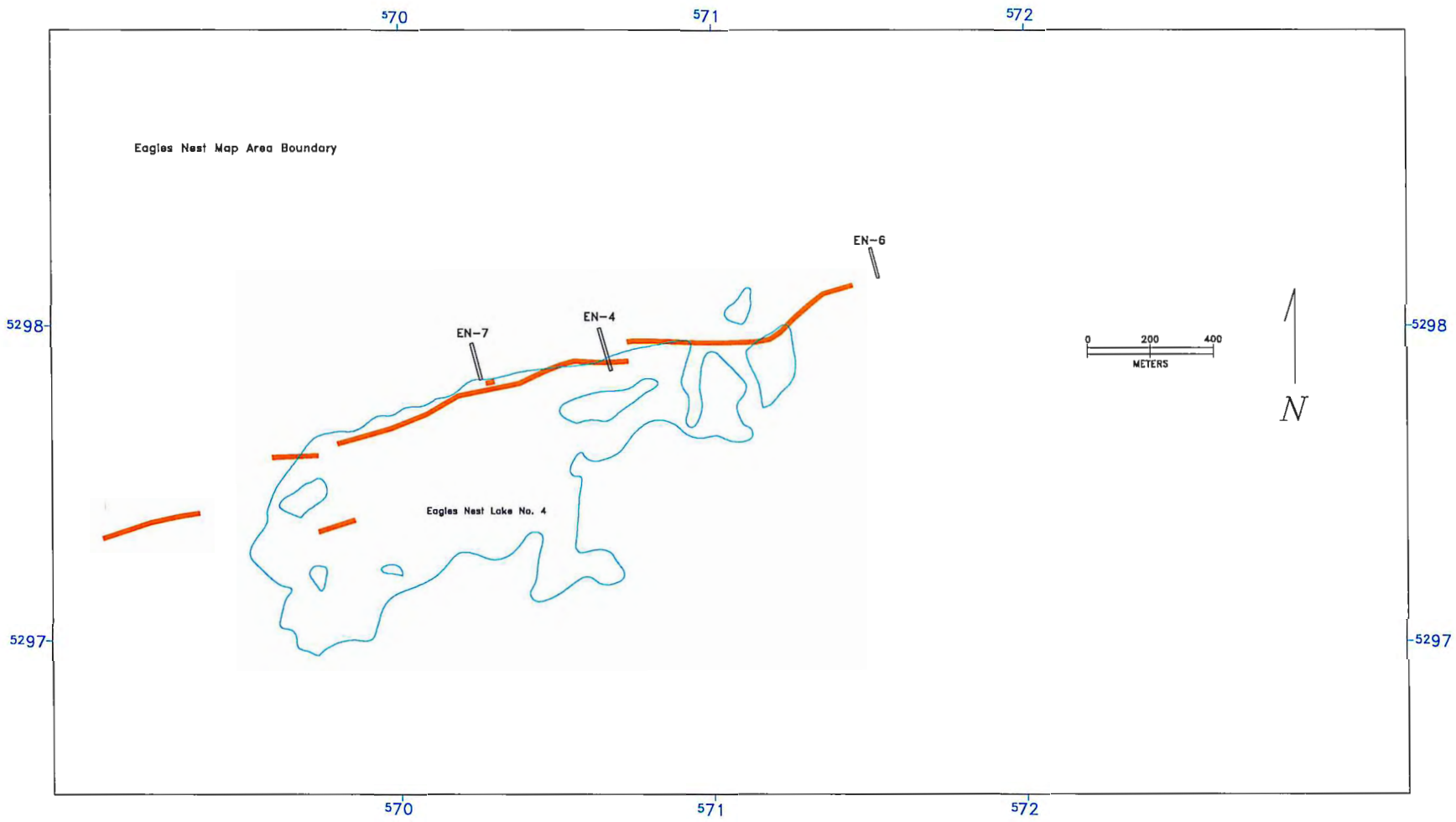

Figure 35: Electromagnetic anomaly at Eagles Nest shown in orange.

Lithologic Interpretation

Reconstruction of volcanic facies morphologies is an important tool for assessing the potential of a given volcanic stratigraphic sequence to contain volcanic associated massive sulphide deposits (Gibson et al. 1999). This is accomplished by recognizing synvolcanic plutons, synvolcanic dikes, synvolcanic faults, lava flow characteristics, and pyroclastic deposits in the field and determining their relationship to one another (Gibson, et al, 1999). At Eagles Nest the limited outcrop exposure and limited drill hole footage has hindered the application of this method. However, several conclusions can be drawn from the data available. Figure 36 is a cross section showing where Eagles Nest is interpreted to have been located with respect to an eruptive center.

Synvolcanic intrusions are emplaced at shallow depths beneath an eruptive center where they feed volcanic activity at the surface through a system of dikes and sills (Gibson et al. 1999). The D_2 cleavage and lack of a contact metamorphic aureole is cited as evidence that the Purvis Lake Pluton is synvolcanic and not associated with the Giants Range Batholith found immediately to the south (Peterson, 1999). The pluton is also mineralized with chalcopyrite and pyrite further to the east (Peterson, 1999). Major and trace element analysis, age, and location tend to indicate that the Purvis Lake Pluton was the source of volcanism at Eagles Nest. However, when volcanism was active at the stratigraphic level that is now Eagles Nest, the pluton mostly likely was not in its present position. The fragments in the top of the pluton, and minor contact metamorphism, suggest that the rocks being intruded were relatively cool and brittle. This would not be the case if the magma was making its way into the base of a wet, warm volcanic pile. It may be that this part of the Purvis Lake Pluton intruded to its present position when the mafic lavas above it had cooled to ambient temperatures, possibly due to renewed volcanism at a later time.

The main bulk of the pluton is further to the east of Eagles Nest. If the central portion of a synvolcanic pluton sits beneath the center of volcanic activity (Gibson et al, 1999), then, in conjunction with previous mapping in the area (Peterson, in prep), it seems plausible that Eagles Nest is in a distal position to the center of most intense volcanism. No synvolcanic faults have been positively identified. Many of the dikes at

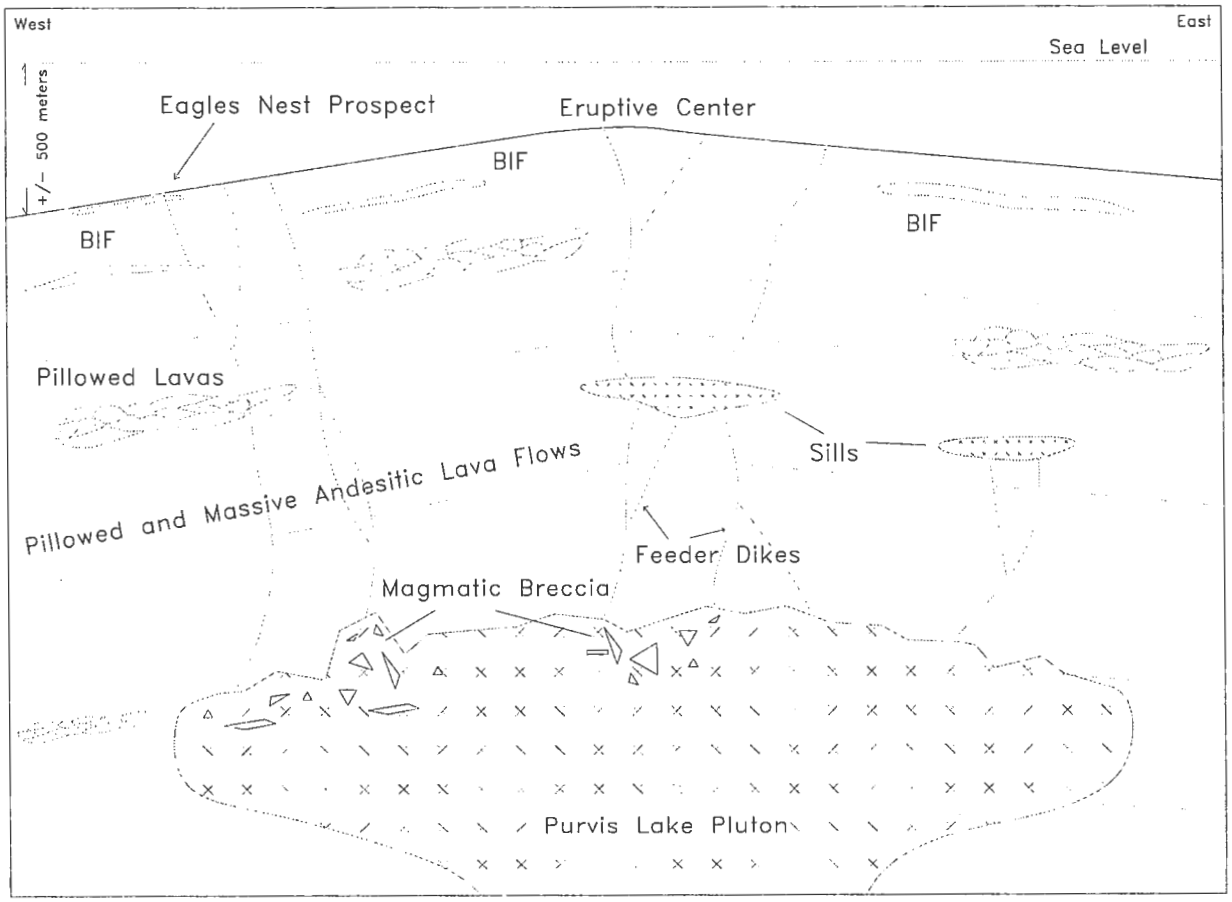

Figure 36: Generalized cross section of the proposed volcanic setting at Eagles Nest Prospect. BIF = banded iron formation. Not to scale.

Eagles Nest appear to have similar compositions to the lavas lying higher in the sequence (based on outcrop samples) and may represent volcanic feeders. However, whether these dikes are coming directly from the Purvis Lake Pluton has not been determined.

All volcanic rocks mapped at Eagles Nest with the exception of a portion of the drill core, are pillowed or massive andesite and basalt lava flows extruded subaqueously. Water depth may be generally constrained by presence, size, and abundance of vesicles within a lava, and by the presence of explosive eruptive deposits (Gibson et al. 1999; Macpherson, 1984). As hydrostatic pressure increases with increasing water depth, vesicle growth is inhibited. Therefore, as water depth increases, vesicles become smaller and fewer in number (Macpherson, 1984; Moore, 1973; Jones, 1969). Amygdules in the flows at Eagles Nest occur along pillow rims in pillowed lavas and within localized areas of massive flows. They range in size from < 1 mm to a maximum of approximately 8-12 mm. Estimated average size of vesicles is 2-4 mm. Amygdules seen in pillow interiors are evenly distributed around the radius of the pillow and amygdule percentages may be as great as 60% within 8 centimeters of the pillow rim. Amygdule content is most intense in the lower portions of the footwall. The hanging wall lavas have less amygdules than the rocks found in the footwall, and the amygdules are concentrated toward the upper pillow surface. This change in amygdule content may indicate that water depth increased during the time lava flows were building up to the stratigraphic level of the mineralized horizon.

It is possible to qualify water depth into the broad category of shallow or deep from the data collected during this study. With the exception of one thin unit in the mineralized horizon, no pyroclastic material has been found in the Eagles Nest sequence of lava flows. Two possible reasons for the absence of explosive volcanic deposits are: 1) that volcanism never became subaerial, nor was water depth ever shallow enough to allow an explosive type volcanic eruption to occur, or 2) that the style of volcanism was passive-effusive, and the absence of pyroclastic material is not related to water depth at all. To have an explosive eruption in mafic magmas, water depth would need to be less than 500 meters, below this depth, explosive eruptions are thought to be unlikely due to high hydrostatic pressure (Kokelaar, 1986). In this instance, the lack of pyroclastic

deposits could be interpreted to mean that water depth at this site was greater than 500 meters. However, the best interpretation, as suggested by the abundance, size, and distribution of amygdules in the lava flows throughout the stratigraphic sequence, is that water depth was probably less than 500 meters (Morton and Franklin, 1987, Gibson et al. 1999; Macpherson, 1984) and explosive eruptions were not occurring at this time.

A clear stratigraphic break occurs at the base of the mineralized package. It is marked by an abrupt transition from the footwall lavas, to sedimentary rocks and banded iron formation. This stratigraphic break marks the beginning of a period of quiescence in volcanic activity within the immediate area. The lack of extruding lava allowed hydrothermal venting at the seafloor to continue uninterrupted for an extending time period. The sediments that occur here have probably been eroded from the upper slopes of the volcanic edifice, while the banded iron formation was precipitated directly onto the ocean floor when the hydrothermal fluid exited the vent and mixed with sea water. During this time, small volcanic eruptions occurred in the area and may have temporarily disrupted the sea floor hot springs when andesitic lavas flowed over active hydrothermal vents and sealed them. At some point after approximately 100-150 meters of precipitates, sediments, and lavas had accumulated, large scale volcanism resumed and began depositing the rocks of the hanging wall. Whether this renewal of volcanism was responsible for ending hydrothermal venting can not be determined.

CHAPTER 3

ALTERATION

The andesitic lava flows of the Eagles Nest Prospect have experienced both regional metamorphism and hydrothermal alteration. It is therefore necessary to distinguish between metamorphic mineral assemblages and true hydrothermal alteration mineral assemblages. Because many of the alteration minerals and metamorphic minerals are the same, the alteration assemblages have been delineated by physical and chemical comparison to the overprinting metamorphic mineral assemblage. Texture is the primary means used to distinguish alteration minerals from metamorphic minerals in hand sample and thin section. Minerals related to hydrothermal alteration have precipitated in veinlets and amygdules, or have pervasively replaced the original rock in irregular patches of intense alteration that may be centimeters to meters in diameter. Samples that have experienced only greenschist grade metamorphism are referred to as least altered.

Greenschist facies metamorphism of mafic rocks produces a mineral assemblage of chlorite + albite + calcite + actinolite + ilmenite +/- epidote +/- biotite (Blatt and Tracy, 1996). This is consistent with the least altered mineral assemblage observed in the andesite lavas throughout the map area; in thin section they are composed of actinolite + chlorite + epidote + plagioclase +/- quartz. Actinolite is fine-grained, fibrous, randomly oriented and pervasive, composing 0-60% of the rock. Plagioclase occurs as < 1 mm euhedral grains and/or as very fine-grained groundmass combined with quartz. Chlorite is present as stringers and uniform disseminations making up 5-30% of the rock and is sometimes hard to distinguish from chlorite related to alteration. Epidote occurs as 0-10% discrete blebs (Figure 14).

Due to the fine grained nature of the rocks, optical study of thin sections was not always sufficient to identify all minerals present. When this was the case, X-ray diffraction (XRD) was used to analyze selected rock samples. Mineral assemblage descriptions that refer to fine-grained minerals in groundmass are typically based on these XRD analyses.

The following alteration assemblages are grouped and described according to stratigraphic position and presented in temporal order from oldest to youngest. Timing of

alteration events has been determined by observation of mineral textures in thin section. However, the fine-grained nature of these rocks frequently makes cross cutting relationships between the mineral grains indistinct. The map showing alteration assemblages and their distribution is presented in Plate 2.

Footwall Alteration

Alteration in the footwall rocks at Eagles Nest is semiconformable in attitude and can be found for many kilometers along strike (Peterson and Jirsa, 1999). This semiconformable alteration may be characterized as patchy and discontinuous over the entire map area owing, most probably, to the variable permeability of the lava flows (Morton and Franklin, 1987). Alteration most commonly occurs along and within pillow rims, as fillings in amygdules, as veinlets, and as pervasive replacements, or as a combination of the four. Quenched and shattered pillow rims (hyaloclastite) and the open space of vesicles and fractures provided space for fluid to move through the lavas. As a result, alteration commonly occurs as several square meters of intense, pervasively altered rock, enclosed by least altered material. Locally, it may be restricted primarily to veinlets, amygdules, and pillow rims in otherwise mildly altered outcrops.

The temporal order of alteration in the footwall, beginning with the oldest alteration observed is epidote +/- quartz, quartz +/- epidote, actinolite +/- epidote, and chlorite +/- quartz +/- sericite.

Epidote +/- quartz

The epidote +/- quartz mineral assemblage is the most common alteration type found at the Eagles Nest Prospect. When most intense, epidote +/- quartz alteration occurs as irregular, pale apple green patches and/or veinlets and vesicle fillings in the rock. It typically has a sharp, but irregular contact with unaltered rock, and is most common in pillowed lavas where it occurs primarily in pillow interiors. This mineral assemblage is composed of 30-70% epidote and 5-20% quartz. Actinolite, chlorite, and sericite typically make up the remainder of the rock (Figure 37). The prevalent patchy

epidote-quartz alteration seen within the map area has been traced laterally to the east and west for many miles in the Lower Ely Greenstone Formation (Peterson and Jirsa, 1999).

Quartz +/- epidote

Pervasive silicification occurs in only three samples. It is not particularly intense and may represent instances where quartz is the most abundant mineral in epidote +/- quartz-type alteration. It appears as a pale grey discoloration in outcrop, and makes the rock very hard. Mineralogically, it is composed of 30-50% quartz, 20-35% actinolite, and 5-15% epidote. The alteration is also discontinuous and patchy. More common is a second style of quartz alteration which forms veinlets, amygdules, or occurs as open space fillings in hyaloclastite (Figure 19). Quartz commonly forms an outer rim around the wall of an amygdule which is then filled with epidote. In this case, the percentage of quartz in the rock may be only 5-10%.

Actinolite +/- epidote

Actinolite is one of the most common minerals observed in the footwall andesites and its abundance is attributed to both hydrothermal alteration and regional metamorphism. The majority of actinolite that occurs in the groundmass of the rock is thought to be from metamorphism because it is common in most rocks throughout the map area and has no clear pattern associated with it. However, experimental studies of hydrothermal alteration of seafloor basalts by seawater derived fluids conducted by Seyfried and Janecky (1985) showed that fibrous masses of actinolite formed in glassy basalts, but did not develop in more crystalline basalts. Assuming that similar alteration characteristics would hold true for the andesites in question, some of the groundmass actinolite could be from alteration of particularly vitreous original groundmass. Pillow rims have been intensely altered to actinolite, and it follows that the glassy nature of the rim would produce the fibrous texture described above (Figure 38). Actinolite alteration also takes the form of discrete 2-3 mm patches composed of 1 mm fibrous mineral grains, and as < 1 mm wide crosscutting veinlets in a groundmass that has little or no actinolite (Figure 39).

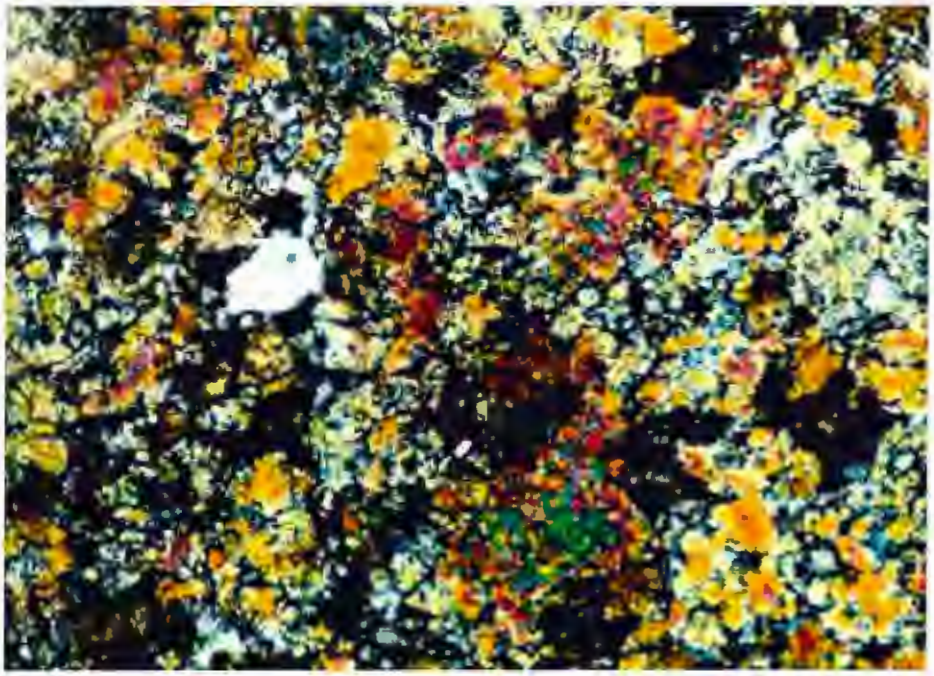

Figure 37: Photomicrograph showing intense epidote +/- quartz alteration. Crossed polars, field of view = 2.5 mm.

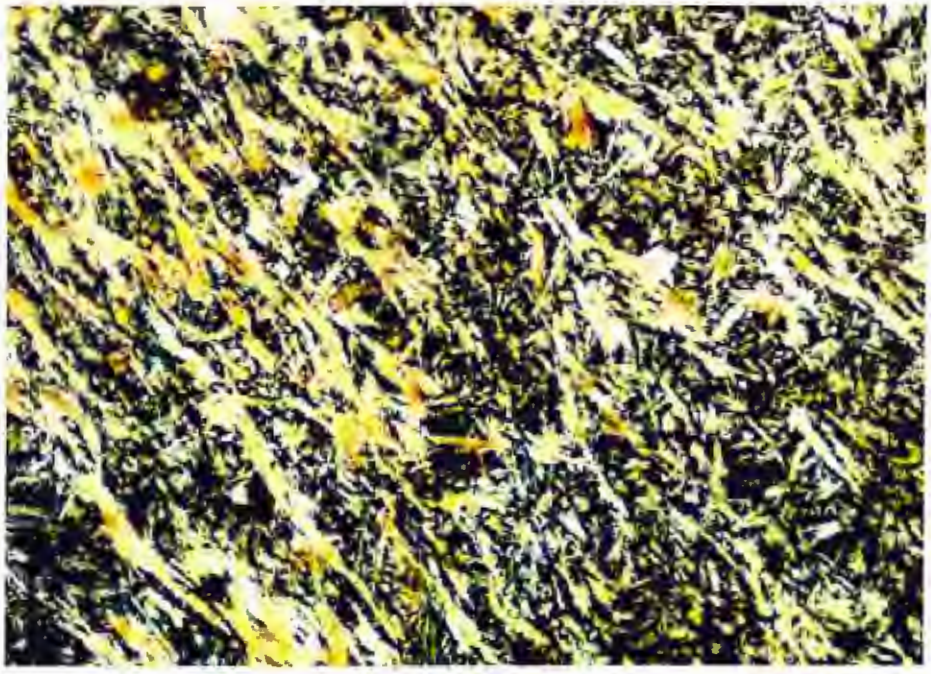

Figure 38: Photomicrograph showing strong actinolite alteration. Crossed polars, field of view = 1 mm.

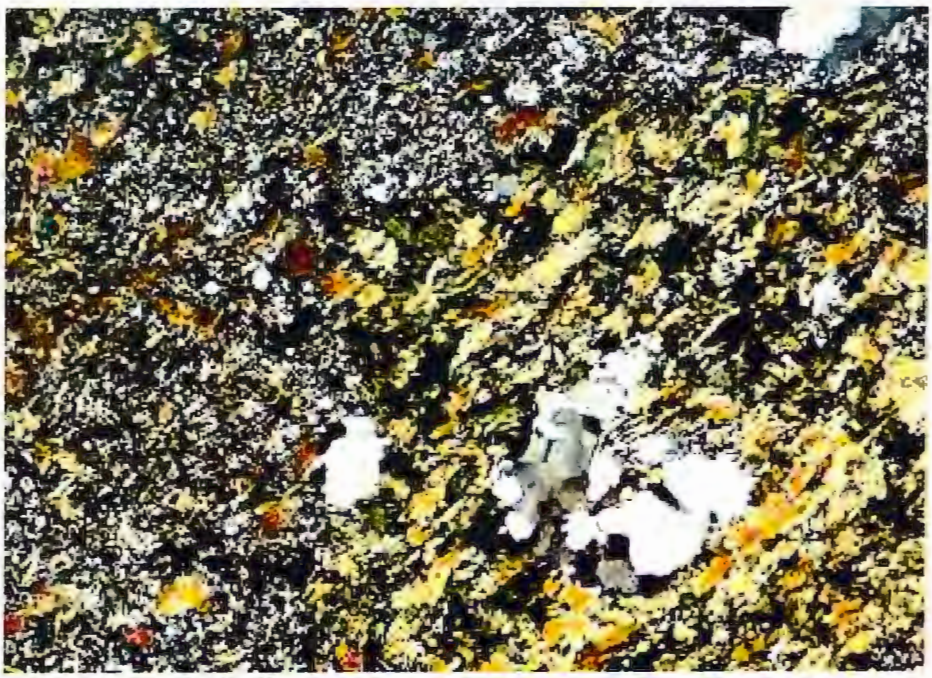

Figure 39: Photomicrograph of patchy actinolite alteration surrounding an irregular quartz amydule. Crossed polars, field of view 2.5 mm.

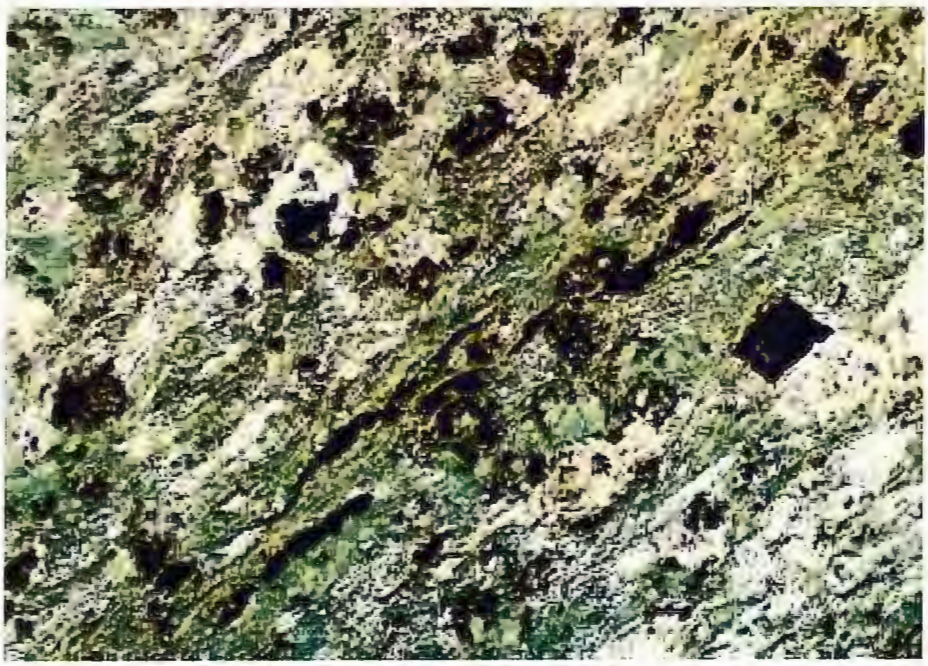

Figure 40: Photomicrograph showing chlorite alteration. With actinolite, calcite, and minor pyrite also shown. Plane polarized light, field of view = 2.5 mm.

Chlorite +/- quartz +/- sericite

Chlorite is a common product of hydrothermal alteration of mafic seafloor lavas by seawater related fluids (Seyfried and Janecky, 1985). This alteration type is not dominant at Eagles Nest, possibly due to the intermediate composition of the lavas or low fluid temperatures. It is found as pervasive replacement, 1-3 mm patches, veinlets, and/or amygdule fillings. Based on thin section study only, the composition of the chlorite appears to be intermediate between Fe-rich and Mg-rich end members. X-ray diffraction techniques are not suitable for distinguishing Fe:Mg ratios in a chlorite. The chlorite appears dark brown to medium green in polarized light. Quartz may or may not be associated with the chlorite alteration. When present, sericite partially replaces plagioclase. Typically, rocks with this alteration assemblage contain 25-35% chlorite, 5-15% quartz, 20-70% actinolite, and 5-10% sericite (Figure 40).

Mineralized Horizon Alteration

Hydrothermal alteration within the mineralized horizon represents the most intense alteration seen at Eagles Nest. The alteration is semiconformable with the stratigraphy, and no evidence of crosscutting alteration has been found. Many of the samples taken from core are so strongly altered that a protolith cannot be determined. Within the approximately 150 meter thick mineralized package the main alteration types, described in temporal order, are chlorite + quartz, magnesium chlorite +/- sericite, and tremolite (Figure 41).

Chlorite + quartz

Two types of chlorite alteration occur in the mineralized horizon. The first type is a relatively Fe-rich chlorite that is interpreted to contain more iron than chlorite seen elsewhere in the mineralized horizon (described below). This interpretation is based on the darker color in thin section of the Fe-rich chlorite where it occurs. Iron rich chlorite composes 20-40% of the rock, making it much less intense than magnesium chlorite alteration. The chlorite occurs as fine grained, elongated grains in the groundmass. Quartz is pervasive and fine grained, and is also present as < 1 mm wide stringers. This

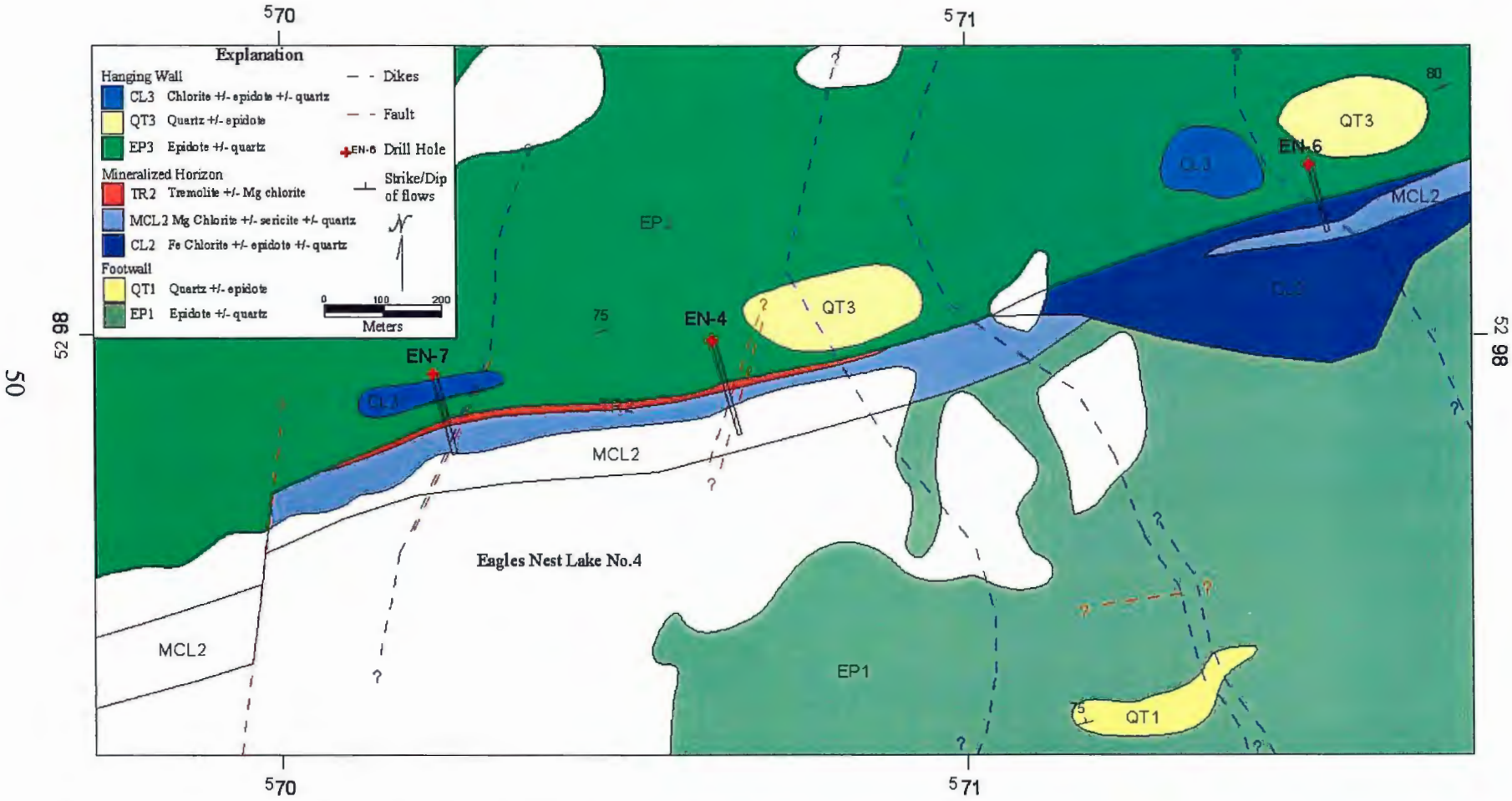

Figure 41: Alteration in the Mineralized Horizon at the Eagles Nest Prospect.

assemblage is most common in the eastern portion of the mineralized horizon. It is found in drill hole EN-6 and in outcrop stratigraphically below this hole.

Magnesium chlorite +/- sericite

Magnesium chlorite alteration is most common in the two western most drill holes, EN-4 and EN-7. In core it is pervasive, pale grey, very fine grained, foliated and composes 65-95% of the rock, with minor carbonate +/- quartz. In thin section the chlorite is composed of elongate, creamy white grains showing a weak foliation (Figure 42). The chlorite is interpreted to be Mg rich based on its white color under crossed polars of the microscope, and from chemical analysis of several samples of this alteration type. Minor quartz occurs as discrete bands or grains. Sericite may entirely pervade the rock or occur as blebs and stringers with magnesium chlorite (Figure 43). Chemical analysis of rocks with a significant percentage of sericite show strongly elevated Cr contents and slightly elevated V contents. This suggests that at least some of the sericite may be a green mica like fuchsite. Some samples of rocks with > 75% sericite are faintly translucent green in hand specimen. The magnesium chlorite +/- sericite alteration type is approximately 50 meters thick, very intense but localized, and composes 95% of the rock, obliterating all primary textures and minerals. It appears to lie parallel to stratigraphy. When less intense, it takes the form of blebs, disseminated euhedral mineral grains, and sericite replacement of plagioclase, making up 2-40% of the rock.

Tremolite

Tremolite alteration is not wide spread, but very intense. It occurs near the top of the last banded iron formation as a 3-4 meter thick stratiform unit. Tremolite grains are fibrous, subhedral, and randomly oriented, composing 50-95% of the rock (Figure 44). In banded iron formations, the tremolite is associated with chert layers and is not found in the magnetite bands. Where most intense, tremolite composes 95% of the rock and erases all primary characteristics of the protolith. It may have minor calcite and magnetite associated with it. In core it is pale grey, fine grained, and foliated.

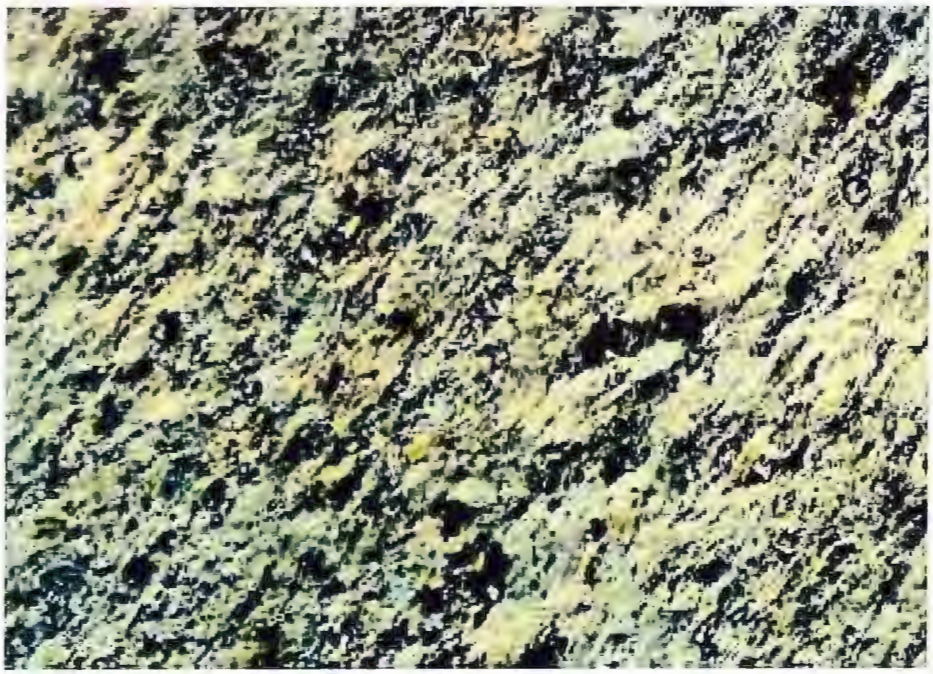

Figure 42: Photomicrograph of intense Magnesium chlorite alteration. Crossed polars, field of view 2.5 mm.

Figure 43: Photomicrograph of Magnesium chlorite with sericite alteration. Crossed polars, field of view = 2.5 mm.

Figure 44: Photomicrograph of tremolite alteration with calcite. Crossed polars, field of view = 2.5 mm.

Hanging Wall Alteration

The alteration assemblages observed in the hanging wall rocks are similar to those seen in the footwall rocks. The alteration occurs in andesitic and basaltic pillowed and massive lavas that have been metamorphosed to greenschist facies. Alteration styles are also similar, occurring along pillow rims, as veinlets, amygdules, and replacement blebs, and locally, as large, pervasively altered patches in the lavas. Sampling in the hanging wall was not extensive. Alteration mineral assemblages in the hanging wall, described in temporal order are epidote +/- quartz, quartz +/- epidote, actinolite + epidote +/- quartz, chlorite +/- quartz +/- epidote

Epidote +/- quartz

Epidote +/- quartz is the most common alteration type observed in the hanging wall rocks and occurs in two distinctive styles. One style forms as centimeter to meter scale, pale apple green patches of pervasively altered rock. The mineral assemblage of the patchy, pervasive alteration consists of 20-40%, 0.1 mm, subhedral epidote clots and 5-15%, 0.1 mm grains and 0.1 mm wide stringers of quartz. A second alteration style consists of epidote in amygdules and veinlets, or as 2-4 mm angular blebs in the rock, these are visible in outcrop.

Quartz +/- epidote

Quartz +/- epidote alteration is common in the hanging wall. It occurs in veinlets and amygdules that are easily observed in outcrop. Quartz veinlets are 1-2 mm wide and typically are continuous over only a few feet. Amygdules along pillow rims are frequently quartz filled. Pervasive quartz alteration of the rock is rare. The total percentage of quartz in the rock may be 5-10%.

Actinolite + epidote +/- quartz

Actinolite alteration occurs in groundmass of both andesite and basalt lavas or as discrete approximately 1-2 mm patches. Actinolite in the groundmass is composed of fibrous, randomly oriented grains that make up 35-70% of the rock. Actinolite is the

predominant constituent of pillow rims, making them soft, dark green, and foliated in outcrop. Disseminated 0.1 mm clots of fine grained, subhedral epidote are commonly observed in thin section. Minor quartz occurs in the fine grained groundmass and as 0.1 mm wide stringers.

Chlorite +/- epidote +/- quartz

The chlorite +/- epidote +/- quartz alteration assemblage occurs within the groundmass of the rock. Optically, this chlorite appears to have an intermediate Fe:Mg ratio and appears to be very similar compositionally to the chlorite seen in the rocks of the footwall and mineralized horizon. The alteration is of moderate intensity and composes 25-30% of the rock. Chlorite is fine-grained and elongated where pervasive in the groundmass. It is less common in veinlets and stringers, where it is associated with calcite and quartz. Epidote occurs as 0.1 mm clots and/or is disseminated throughout the groundmass in <0.2 mm grains.

Late Calcite Alteration

Calcite is associated with most of these assemblages, but is interpreted to be post mineralization. It occurs as blebs and veinlets beginning in the footwall at shallow depths below the mineralization and increases in intensity upwards into the hanging wall. It is patchy and may compose 5-70% of the rock. It is associated to some degree with all alteration types.

Comparison to Five Mile Lake

The proximity and similarity of the Five Mile Lake Prospect to Eagles Nest Prospect are the reason a brief comparison of the two sequences is given here. This may assist in understanding the larger-scale volcanic context in which the Eagles Nest system existed. The Five Mile Lake VMS Prospect lies four miles west of Eagles Nest (Figure 2). Geophysical surveys at Five Mile indicate the presence of a strong conductor underneath the lake (Peterson, in prep). Recent detailed mapping by George Hudak (pers com. 2000) and Dean Peterson (Peterson and Jirsa, 1999a) have defined a hydrothermal

system favorable to massive sulphide formation, and past exploratory diamond drilling has intersected high Cu and Zn values associated with exhalite horizons (Peterson and Jirsa, 1999). At this time, the Five Mile Lake sequence is believed to be stratigraphically equivalent to Eagles Nest (Peterson, in prep).

Lithology and Chemistry

The Five Mile Lake Prospect is composed of mafic pillow lavas with small scoriacous pyroclastic and/or debris flow deposits and a small, rhyolitic lava dome (Hudak, pers com 2000). The pillows contain up to 30-40% vesicles ranging in diameter up to > 1 cm. Pipe vesicles are well developed and may be several centimeters long and arranged around the circumference of pillows. All evidence points to subaqueous extrusion, but at very shallow water depths. Vesiculation in pillows of the Eagles Nest lower footwall are similar to that at Five Mile, but hanging wall vesiculation is substantially less.

Four least altered samples of mafic lavas from the Five Mile Lake Prospect are chemically similar to the mafic lavas of the Eagles Nest footwall when plotted on Jenson, Winchester and Floyd, and TAS diagrams (Figure 45, 46, & 47). These samples have experienced weak alteration, but appear to be mineralogically similar to least altered samples at Eagles Nest. The Winchester and Floyd and the TAS discrimination plots show these rocks to be andesites. The samples plot within the calc-alkaline trend on the Jenson plot and in the basaltic field. This discrepancy between the Jenson plot and the other two diagrams is consistent with that seen at Eagles Nest as discussed above. The mafic lavas of Eagles Nest and Five Mile Lake appear to be chemically equivalent.

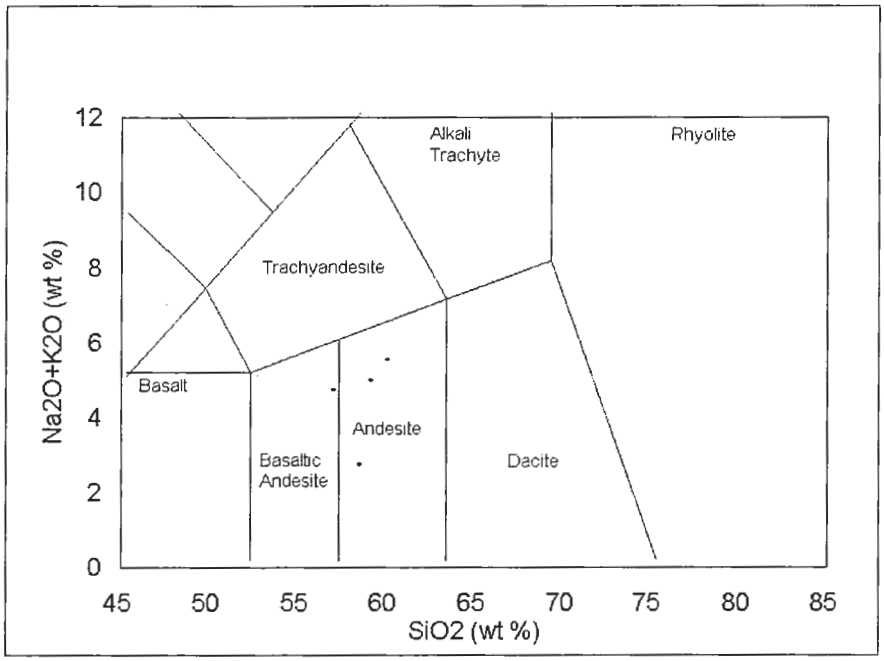

Figure 45: TAS diagram (LeMaitre, 1986) of least altered rocks from Five Mile Lake.

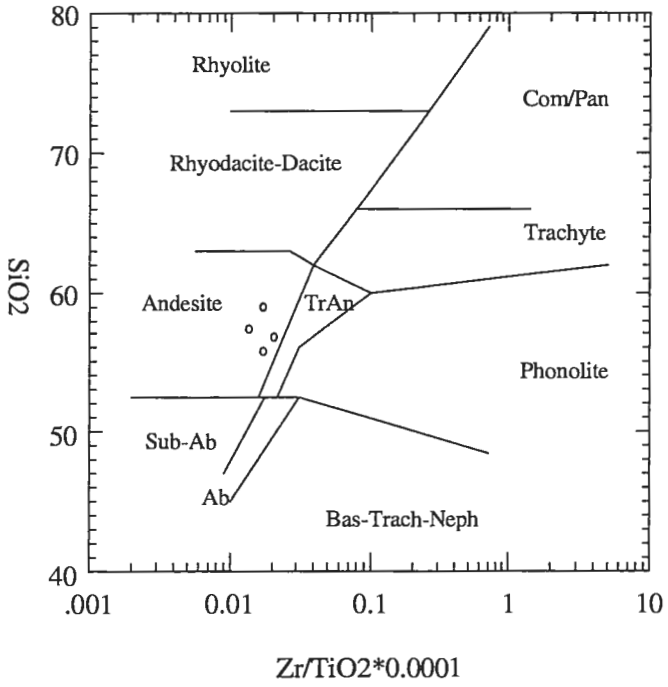

Figure 46: Winchester and Floyd diagram (1977) of least altered rocks from Five Mile Lake. Com = Comendite, Pan = Pantellerite, Neph = Nephalinite, Bas = Basalt, AB = Alkaline Basalt, Trach = Trachyte.

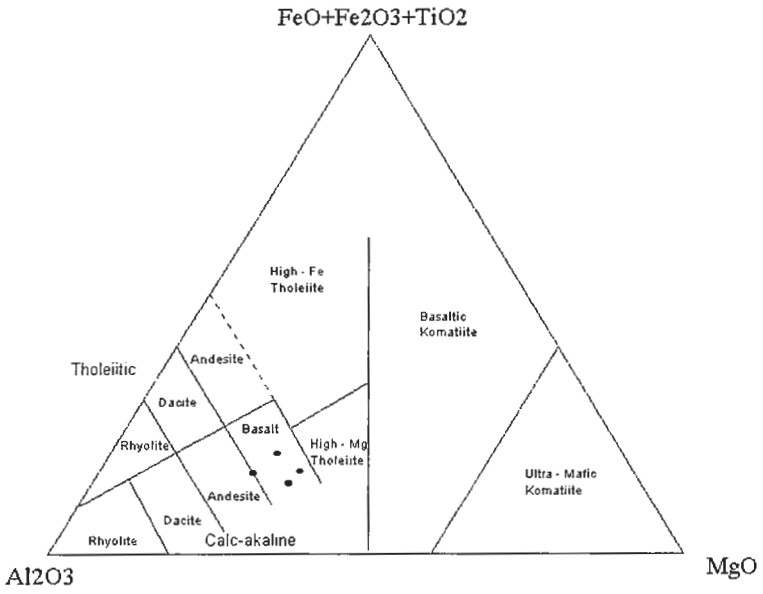

Figure 47: Jenson diagram (1976) of least altered rocks from Five Mile Lake.

Alteration

Alteration at Five Mile Lake differs in intensity, distribution, and mineral assemblage. Preliminary mapping by George Hudak shows that all of the pillowed lavas at Five Mile show strong quartz +/- epidote alteration (pers com 2000). Chlorite is locally predominant in pillow rims and as approximately 1 cm crosscutting veinlets. This contrasts with Eagles Nest where the footwall is only randomly altered by epidote +/- quartz, and actinolite is dominant over chlorite in pillow rims. All indications suggest that Eagles Nest alteration has been less intense or occurred at a lower temperature (Seyfried and Janecky, 1985).

CHAPTER 4

GEOCHEMISTRY

Fifty samples from outcrop and drill core at Eagles Nest have been analyzed for whole rock geochemistry (Appendix 1). The samples were analyzed using instrumental neutron activation (INAA), inductively coupled plasma (ICP), inductively coupled plasma mass spectroscopy (ICP-MS), and X-ray fluorescence spectroscopy (XRF). The analysis was used to test for ten major element oxides and 46 trace elements. This data is used for normative calculations (Appendix 2), rock discrimination plots, and isocon diagrams.

The Isocon Method

Grant's Isocon method (1986) was used to define changes in rock mass and the concentration of individual components as a result of hydrothermal alteration at Eagles Nest. The data under consideration are from chemical analysis of 50 samples from outcrop and drill core. The rock samples are taken from the rock and alteration units described in previous chapters.

The Isocon method defines mass change and element movement within altered rocks by plotting chemical data on an X-Y graph. It is based directly on Gresens' (1967)

	Gresens	Grant
Superscript of unaltered sample	A	O
Superscript for altered sample	B	A
Subscript for component	n	i
Specific gravity	g	ρ
Volume of sample	v	V
Volume factor	f_v	
Mass of sample		M
Mass of component i		M_i
Reference mass of original sample	a	M^O
Gain or loss of mass of component relative to the reference mass	x	ΔM_i
Concentration	C	C

Table 1: Abbreviations for Gresens' and Grant's equations (Grant, 1986).

equations for calculating volume and compositional changes of an altered rock from its chemical analysis. Gresens' basic equation is:

$$X_n = \left[f_v\left(g^B / g^A\right)C_n^B - C_n^A\right]a$$

(see Table 1 for variable definitions).

If using a chemical analysis summed to 100 wt % a in the equation will = 100g.

Grant has rearranged Gresen's equation to show ratios of constant mass. Grant's revised abbreviations are given in Table 1. From Grant's revised equation, the ratio of masses before (M^O) and after (M^A) an alteration event is:

$$\frac{M^A}{M^O} = \frac{V^A}{V^O} \bullet \frac{\rho^A}{\rho^O} = f_v(g^B / g^A) \qquad (1)$$

The mass of a given component after alteration (M^A) is found by adding the mass of the unaltered rock (M^O) to the change in mass of that component:

$$M_i^A = M_i^O + \Delta M_i$$

This may be expressed in terms of concentration units by dividing the above equation by M^O, the mass of the unaltered rock:

$$\frac{M_i^A}{M^O} = \frac{M_i^O}{M^O} + \frac{\Delta M_i}{M^O} \qquad (2)$$

The final concentration (M_i^A / M^A), may be obtained by multiplying equation (2) by (M^O / M^A):

$$\frac{M_i^A}{M^A} = \frac{M^O}{M^A} \bullet \frac{M_i^A}{M^O} = \frac{M^O}{M^A}\left(\frac{M_i^O}{M^O} + \frac{\Delta M_i}{M^O}\right).$$

This equation, represented in concentration units, is:

$$C_i^A = \frac{M^O}{M^A}\left(C_i^O + \Delta C_i\right). \qquad (3)$$

Which is Gresens' equation revised so that it can be represented as:

$$\Delta M_i = \left[\left(\frac{M^A}{M^O}\right)C_i^A - C_i^O\right]M^O$$

For each component within the rock, an equation of the form of equation (3) can be written, (M^O/M^A) is constant. To find this ratio it is necessary to identify immobile components where $\Delta C_i = 0$ and then solve simultaneous equations of the form:

$$C_i^A = (M^O / M^A) C_i^O$$

This is most easily accomplished by plotting the chemical data on an X-Y graph with C_i^O along the X-axis and C_i^A along the Y-axis. Immobile components will plot along a straight line through the origin with a slope of (M^O/M^A) which represents the ratio of constant mass before and after alteration. This line connects points of equal geochemical concentration ($\Delta C_i = 0$) and is referred to as an isocon. The equation for the isocon is:

$$C^A = (M^O / M^A) C^O . \qquad (5)$$

For example, the following three instances may be represented by an isocon. If the component alumina is assumed to be constant (immobile), equation (3) becomes:

$$(M^O / M^A) = (C^A_{Al2O3} / C^O_{Al2O3}),$$

and the isocon is:

$$C^A = (C^A_{Al2O3} / C^O_{Al2O3}) C^O .$$

The isocon representing constant mass is:

$$C^A = C^O .$$

The isocon representing constant volume is:

$$C^A = (\rho^O / \rho^A) C^O .$$

Once an isocon has been established the *relative* gains and losses of individual components are determined by the amount of offset a given component has from the isocon. To find the value of change of a component relative to its concentration before alteration it is necessary to divide equation (3) by C_i^O and rearrange to get:

$$(\Delta C_i / C_i^O) = (M^A / M^O)(C_i^A / C_i^O) - 1. \qquad (6)$$

(M^A/M^O) is taken from the best fit isocon. For constant alumina:

$$(\Delta C_i / C_i) = (C^O_{Al2O3} / C^A_{Al2O3})(C_i^A / C_i^O) - 1.$$

For constant mass:

$$(\Delta C_i / C_i) = (C_i^A / C_i^O) - 1.$$

For constant volume:

$$(\Delta C_i / C_i) = (\rho^A / \rho^O)(C_i^A / C_i^O) - 1.$$

Example from Eagles Nest

The first step in applying the isocon method to alteration assemblages observed at Eagles Nest is to define a least altered rock sample to compare the altered rocks against. Finding a least altered equivalent rock is essential because the isocon method requires that the two rocks being compared had the same chemical composition before one was altered. If no equivalent rock can be determined, the isocon method cannot be used. As a result of thin section and hand sample study, sample ENS699-100 (an andesite) was chosen to represent the least altered mineral assemblage within rocks of the footwall. It has experienced only greenschist grade metamorphism, and is composed of 70% very fine grained quartz/feldspar groundmass, 15-20% chlorite (0.1 - 0.2 mm grains and blebs), 8% epidote (0.1 - 0.2 mm blebs), 5% quartz (stringers, 0.1 - 0.2 mm blebs, and 0.1 mm grains), and 2% carbonate +/- quartz (veinlets) (Figure 14). This least altered sample is then compared to stratigraphically equivalent altered samples to determine what components of the rock have been affected by the alteration event. For this particular example, ENS699-100 is compared to a strongly altered sample from the footwall, ENS699-23, which has been intensely epidotized and is composed of 60% epidote, 20% actinolite, 10% quartz, 7% plagioclase, and 3% sericite.

Secondly, it was necessary to determine which elements had remained immobile within the rock during alteration. In order to obtain valid information from the isocon method, an element or group of elements that have been unaffected by hydrothermal fluid activity must first be found. These immobile elements can then be used to define an isocon to which all other elements are compared. The alumina reference isocon was used for this study. In previous alteration studies, alumina has been shown to be mostly unaffected by hydrothermal fluids (MacLean and Kranidiotis, 1987; Riverin and Hodgson, 1980; MacGeehan and MacLean, 1980, Roberts and Reardon, 1978; and

others). These studies have also shown Zr and Ti to be generally immobile, but more prone to movement than alumina (MacLean and Kranidiotis, 1987). Therefore, alumina can reasonably be assumed to have been immobile at Eagles Nest. In this case, after plotting several rock samples on isocon diagrams, Zr and Ti appear to have been affected by alteration and show some mobility. This conclusion is drawn because Zr and Ti did not plot along the alumina isocon, and typically did not define a distinct isocon of their own. Therefore, Zr and Ti are not relied on to assist in establishing the alumina isocon.

Figure 48 shows the isocon diagram plotting the least altered sample ENS699-100 against epidote altered sample ENS699-23. Major oxides plus Zr, Cu, and Zn are plotted as components. Some components have been scaled so that their values fall into the range from 0 to approximately35 units on the X and Y axes. Unit values are weight percent for oxides and parts per million for trace elements. The scaling is done by multiplying each individual component by some number so that its value is decreased or increased enough to fall into the above range. For instance, a sample with 60 wt % SiO_2 would be multiplied by 0.5 to give it a value of 30 wt % SiO_2 and a sample with 0.5 wt % TiO_2 would be multiplied by 20 to give a value of 10 wt % TiO_2. The scaling is necessary to make data points plot where they can be more easily read, and to magnify relationships between components of very low concentrations.

An isocon with a slope of 1 duplicates the constant mass isocon and indicates that no mass has been gained or lost during an alteration event. The constant alumina isocon in this example has a slope of $(M^O/M^A) = 1.3$, which implies that a mass change of $(M^A/M^O) = .77$, or - 23% occurred as a result of the alteration event. Any component that plots off the constant alumina isocon is assumed to have been affected by alteration. Components that plot above the isocon have been enriched during alteration and components that plot below the isocon have been depleted. The distance the component lies from the isocon gives a general idea of the magnitude of the movement. A better estimate of the gain or loss of a component is found by superimposing a percentage scale on the isocon diagram. This is done by drawing a vertical line from any point on the isocon downward to the X-axis. The total distance from the isocon to the X-axis represents 100 percent of a given component's concentration within the sample. This line

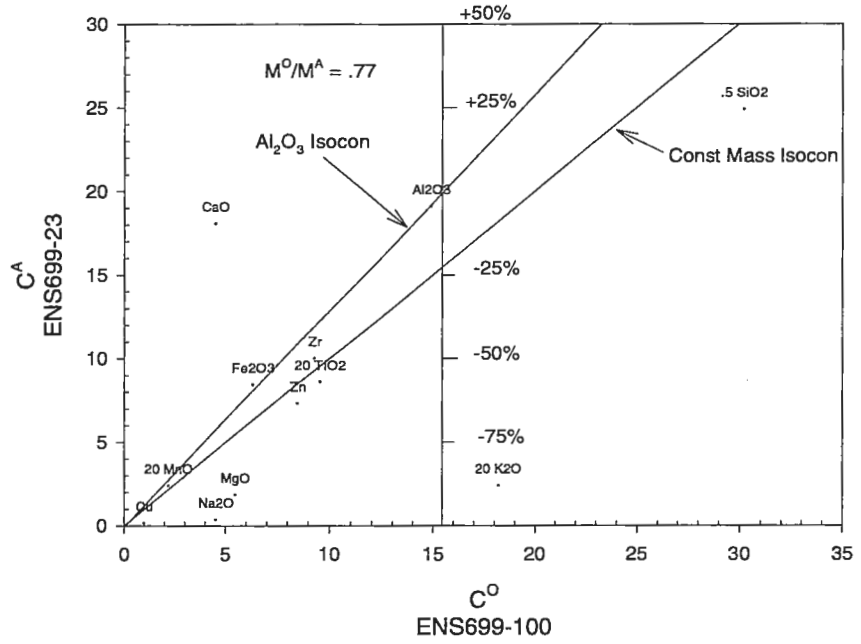

Figure 48: Isocon diagram comparing least altered andesite and epidote altered andesite. The straight line from the origin through Al_2O_3 is the isocon representing constant Al. The vertical line with scaling marks is used to determine percent gains or losses of a component by drawing a line from the origin through the component of interest and reading the gain or loss where the line crosses the scale. The vertical scale line may be extended above the graph as far as necessary to accommodate the component with the greatest gain. M^O/M^A is the change in mass of the rock during alteration. The constant mass isocon represents $M^O/M^A = 0$.

can be graduated so that one quarter of the length from the isocon to the X-axis represents a –25% concentration decrease, one half the length equals a –50% concentration decrease, and so on. If a component were to plot exactly on the X-axis itself, this would mean that all of that component had been removed from the rock. The same scale can be extended above the isocon with as many repetitions as needed to accommodate the component with the greatest concentration increase. To read the concentration change in any component, draw a line from the origin through the component's plot point and extend it until it crosses the scaling line. Measure the percentage gain or loss at this point.

The isocon diagram shows that during intense epidote alteration of the andesitic flows Ca is the only component added to the rock and it is increased by approximately

216% (Figure 48). Iron and Mn fall along the isocon and remain mostly immobile. Zirconium and Ti have been very slightly depleted. Major depletion was experience by Si (+/- -36%), Mg (+/- -73%), K (+/- -90%), and Na (+/- -93%). These elemental gains and losses are borne out by the observed mineral assemblages in the altered rock. Addition of Ca is taken up in the large increase of epidote and, to a lesser extent, in the increase of actinolite. Disappearance of chlorite and plagioclase from the altered sample account for depletion of Mg and Na, respectively. Destruction of alkali feldspar in the fine-grained groundmass, not distinguishable optically, is thought to explain potassium depletion. Though modal quartz increases in the altered sample, the isocon analysis shows that the actual concentration of SiO_2 has been significantly depleted.

Isocon Analysis Results

The isocon method was applied to all appropriate samples from Eagles Nest. To be useful, samples could not have experienced such intense alteration that a protolith could not be determined. It had to be possible to match a least altered, stratigraphically equivalent rock to the altered rock. There would be no value in comparing an altered sediment to a least altered andesite. Alteration in the mineralized zone has been so intense that protoliths could not be determined and therefore, no isocon analysis could be applied to these rocks. The alteration types in the mineralized zone that could not be analyzed for are Mg chlorite +/- sericite, chlorite + quartz, and tremolite. All samples used in the isocon study have thin sections that have allowed comparison of mineralogy to the rock's chemical characteristics. For thin section descriptions see Appendix 4. Table 2 presents the chemical analyses used for the isocon comparison.

Footwall Alteration

The rocks of the footwall are suitable for analysis by the isocon method. Samples of lavas from the epidote +/- quartz, quartz +/- epidote, actinolite +/- epidote, and chlorite +/- quartz +/- sericite alteration groups have been plotted against sample ENS699-100 a stratigraphically similar least altered andesite lava. Based on field work and isocon analysis of the footwall rocks, it appears that alteration in the footwall is probably related

SAMPLE	Rk Type	SiO2 %	TiO2 %	Al2O3 %	Fe2O3 %	MnO %	MgO %	CaO %	Na2O %	K2O %	Zr PPM	Zn PPM	Cu PPM
Footwall													
ENS699-08	and	56.85	0.67	13.93	9.08	0.12	3.19	10.57	1.68	0.52	122	74	358
ENS699-23	and	49.76	0.43	19.10	8.44	0.12	1.86	18.08	0.36	0.12	100	73	15
ENS699-19	and	65.20	0.54	10.59	7.26	0.10	6.44	3.76	0.54	0.74	115	98	15
ENS699-44	and	69.64	0.35	11.77	4.48	0.09	2.87	4.88	3.57	0.48	44	91	28
ENS699-10	and	53.49	0.56	16.56	9.95	0.14	6.99	5.39	3.95	0.28	119	121	34
ENS699-20	and	53.74	0.62	15.07	6.94	0.13	7.26	9.29	4.05	0.37	135	75	4
ENS699-57	and	49.86	0.66	17.27	9.57	0.14	8.68	5.22	1.79	1.01	108	119	14
ENS699-85	and	54.80	0.79	14.12	9.08	0.16	3.94	6.72	4.07	0.08	82	133	23
ENS699-100	ls alt and	60.40	0.48	14.90	6.34	0.11	5.49	4.51	4.54	0.91	93	85	10
Hanging Wall													
ENC699-07	and	59.78	0.49	11.60	8.54	0.11	6.04	3.66	0.26	1.82	100	137	107
ENC699-08	and	49.43	0.58	12.29	8.17	0.11	2.73	9.03	1.47	0.47	120	123	57
3260000162	bas	47.43	1.40	11.30	18.56	0.30	8.82	7.71	1.84	0.14	99	191	31
ENC699-06	bas	44.16	0.72	13.42	11.85	0.17	7.70	8.86	2.07	0.09	45	142	73
ENS699-134	ls alt bas	47.04	1.35	11.81	14.80	0.21	5.37	7.64	2.56	0.13	89	144	110
ENS699-141	ls alt and	57.26	0.59	14.96	7.32	0.12	6.46	4.32	4.84	0.37	77	115	4

Table 2: Chemical data used in isocon analysis. Rock type: and = andesite, bas = basalt, ls alt = least altered.

to the fluids that deposited the banded iron formation and massive sulphide in the mineralized horizon. The following alteration assemblages are described in temporal order.

Epidote +/- quartz

Two samples of the most intense epidote +/- quartz alteration from the footwall were compared to the least altered equivalent lava using isocon diagrams (Figure 49 & 50). It is expected that this type of lower semiconformable alteration will result in significant addition of Ca, whereas Na, Mg, Fe, Zn, and Cu may be depleted (Morton and Gibson, 1993). At Eagles Nest, the primary addition during epidote +/- quartz alteration is Ca, as expected by the large percentage of epidote seen in the altered rock (Table 3). Magnesium and Na have been consistently depleted in the rock and reflect the removal of primary pyroxene and/or amphibole, and plagioclase feldspar. Potassium has been strongly depleted and this may be explained by removal of alkali feldspar from the fine grained groundmass. No alkali feldspar is visible using optical techniques. Small amounts of Zn have been leached from both samples. The behavior of Cu is erratic, showing strong depletion in one samples and significant enrichment in the other. The Cu variation may be related to local differences in alteration intensity. Of the two samples considered, silica is immobile in one and depleted by 36% in the other. Mass change in the silica immobile rock is nearly zero whereas the silicadepleted rock has a mass decrease of 23%. This relationship between silica and mass has not been resolved. Titanium and Zr vary within 40% of the isocon showing that they have not remained immobile. The remaining components do not show consistent behavior between the two samples.

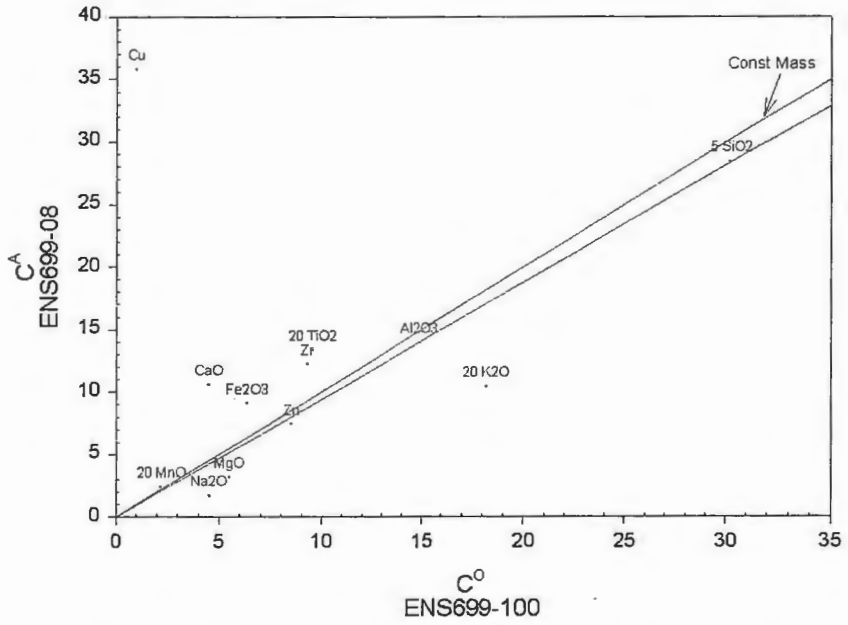

Figure 49: Isocon diagram comparing least altered footwall andesite with epidote altered andesite.

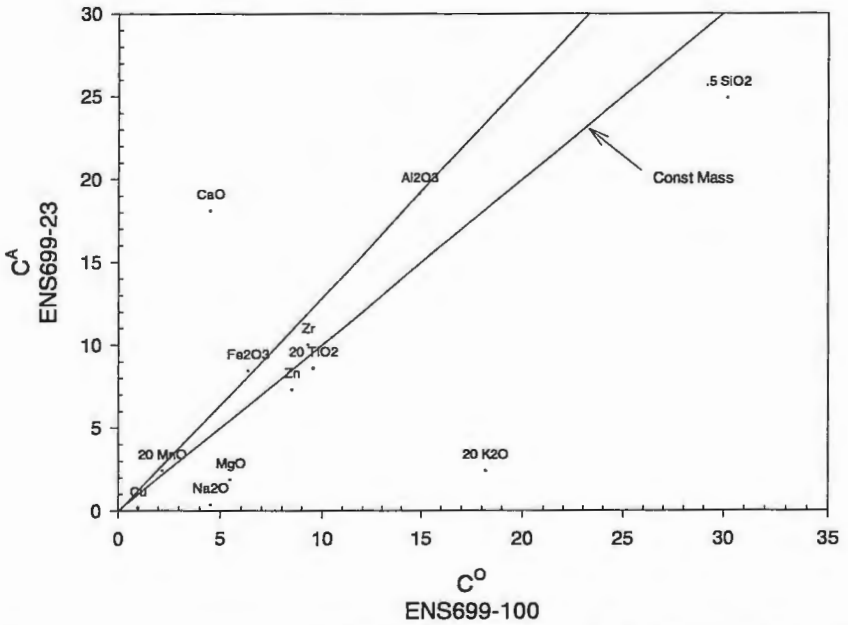

Figure 50: Isocon diagram comparing least altered footwall andesite with epidote altered andesite.

Component	ENS 08 (%)	ENS 23 (%)
SiO2	0	-36
TiO2	48	-27
Fe2O3	52	0
MnO	0	0
MgO	-32	-73
CaO	+150	+216
Na2O	-60	-93
K2O	-40	-90
Zr	38	-17
Zn	-10	-35
Cu	3000	-90
Mass	2	-23

Table 3: Gains and losses of significant components due to epidote +/- quartz alteration of footwall andesites. From isocon analysis.

Quartz +/- epidote

Two rock samples exhibiting quartz +/- epidote alteration have been compared by isocon analysis with the least altered equivalent andesite (Figure 51 & 52). In these samples, silica has increased by 40% to 50%, and quartz is prevalent in the rock as expected. Calcium is slightly increased in both samples, possibly due to a small increase in epidote within the rock. Sodium is strongly depleted and this is probably associated with feldspar destruction. Sodium's inconsistent behavior is likely due to the spatially variable intensity of the alteration. Movement in all other components is inconsistent and minor. Mass depletion is 23% and 43% in the two samples considered (Table 4).

Actinolite +/- epidote

Actinolite +/- epidote alteration is defined as the alteration type where there are veinlets and discrete blebs of actinolite throughout the rocks. This alteration is distinct from the pervasive actinolite that is believed to have resulted from regional metamorphism. This alteration is patchy and has not strongly affected the rock. Plotting actinolite alteration samples against the least altered andesite samples (Figure 53 & 54), shows that silica has been depleted by 20-30% and rock mass has decreased by 15-20%. Potassium has been strongly depleted possibly as a result of feldspar destruction. These are the only

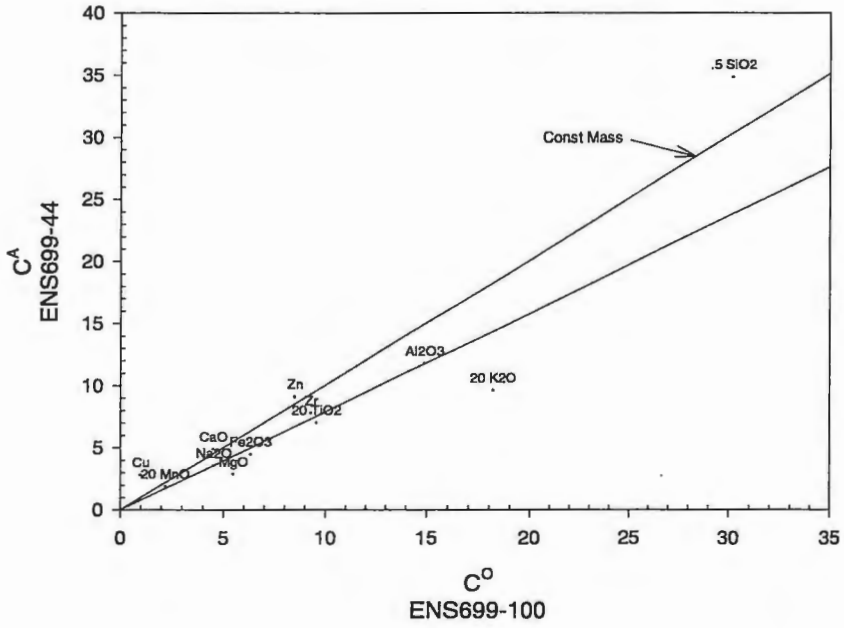

Figure 51: Isocon diagram comparing least altered footwall andesite with quartz altered andesite.

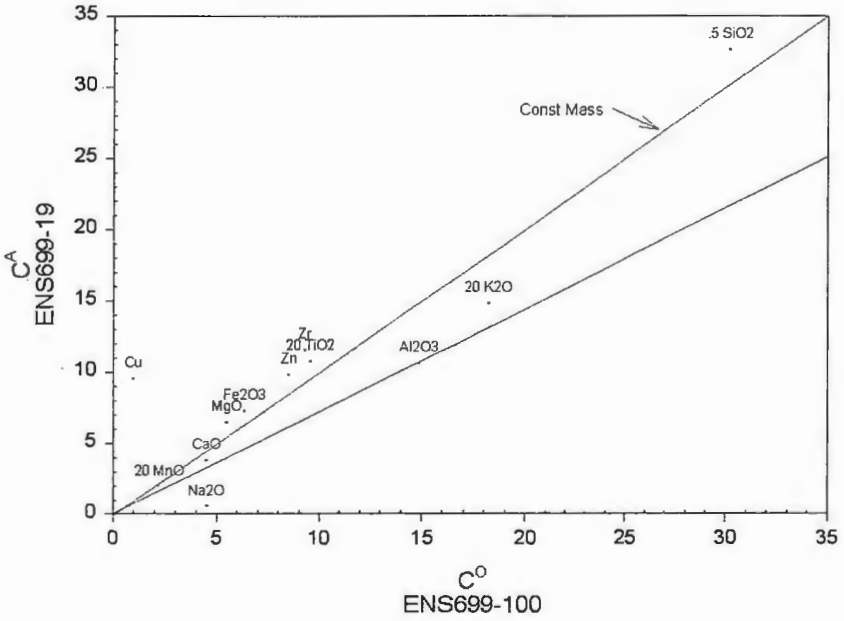

Figure 52: Isocon diagram comparing least altered footwall andesite with quartz altered andesite.

Component	ENS 44 (%)	ENS 19 (%)
SiO2	40	50
TiO2	-8	55
Fe2O3	-12	60
MnO	0	12
MgO	-34	65
CaO	34	15
Na2O	0	-80
K2O	-34	12
Zr	5	72
Zn	35	60
Cu	290	1000
Mass	23	43

Table 4: Gains and losses of significant components due to quartz +/- epidote alteration of footwall andesites. From isocon analysis.

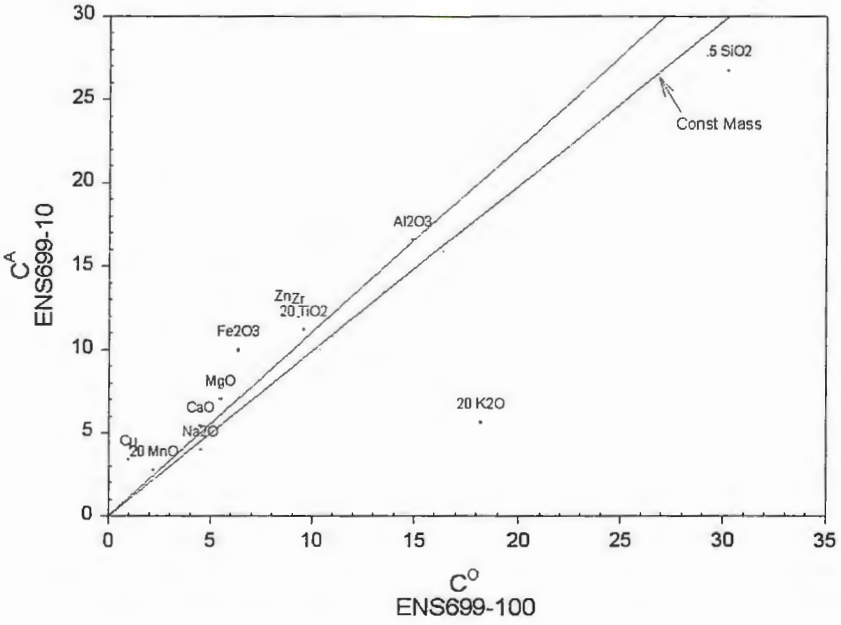

Figure 53: Isocon diagram comparing least altered footwall andesite to actinolite altered andesite.

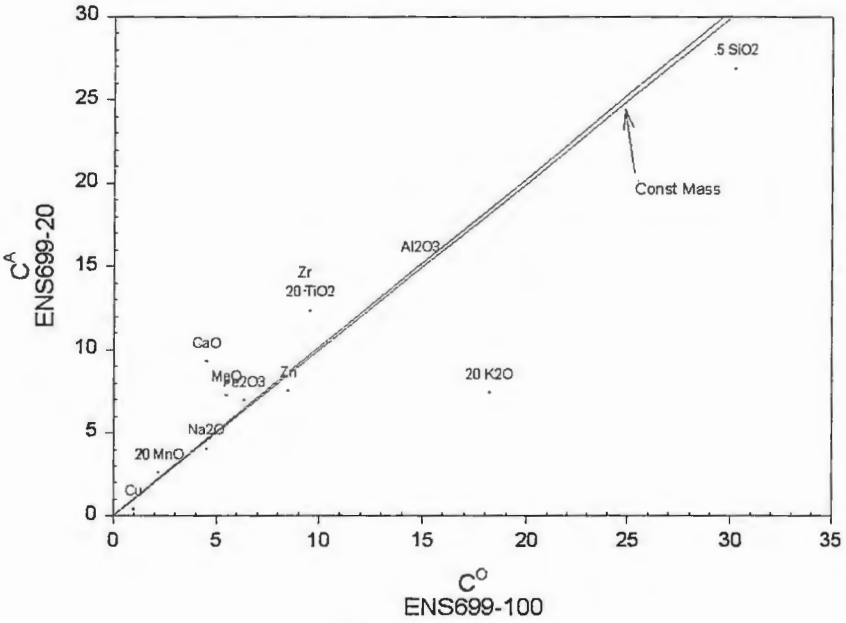

Figure 54: Isocon diagram comparing least altered footwall andesite to actinolite altered andesite.

Component	ENS 10 (%)	ENS 20 (%)
SiO2	-20	-12
TiO2	5	30
Fe2O3	40	10
MnO	10	12
MgO	17	35
CaO	10	105
Na2O	-21	-8
K2O	-71	-60
Zr	15	45
Zn	30	-15
Cu	210	-50
Mass	-10	-6

Table 5: Gains and losses of significant components due to actinolite +/- epidote alteration of footwall andesites. From isocon analysis.

components that show similar behavior in the two samples considered (Table 5). Sodium concentration has remained the same in one sample, but has decreased by 35% in the other. It is unclear whether sodium depletion is directly related to actinolite +/- epidote alteration. Copper has undergone nearly complete removal from ENS699-104, which may suggest that this alteration is responsible for the small percentage of chalcopyrite

seen in the stratigraphically higher mineralized horizon. Most components show minor changes, fluctuating within +/- 15% of the Al_2O_3 isocon, which probably reflects the patchy nature of this alteration type.

Chlorite +/- quartz +/- sericite

Two samples with chlorite +/- quartz +/- sericite alteration have been plotted against the least altered andesite sample (Figure 55 & 56) and gains and losses have been determined based on the Al_2O_3 isocon (Table 6). Iron and Mn have increased during this alteration. An increase in the abundance of chlorite of an intermediate to Fe-rich composition is observed in thin sections of the altered rocks. Calcium enrichment in ENS699-85 is associated with late calcite alteration. Sodium movement is variable likely as a result of alteration intensity differences. The strong Na and K depletion in ENS699-85 appears to be due to feldspar destruction is probably a result of the chlorite alteration event. Silica is slightly depleted. Mass change has been minor.

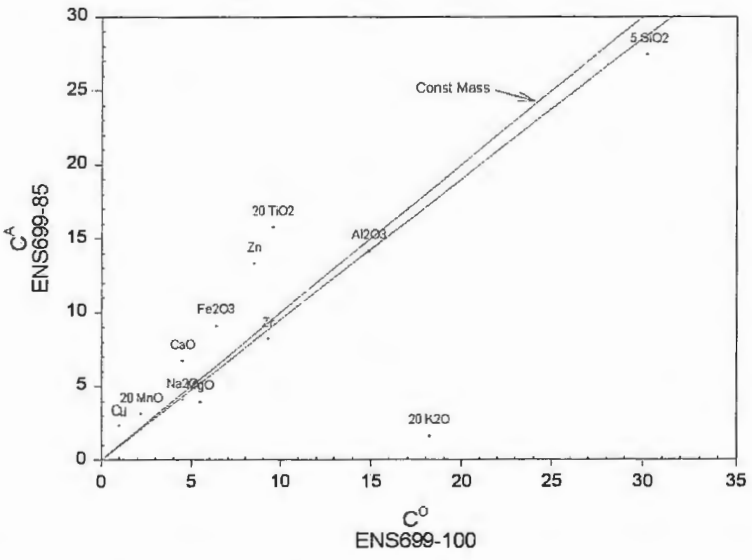

Figure 55: Isocon diagram comparing least altered footwall andesite with chlorite altered andesite.

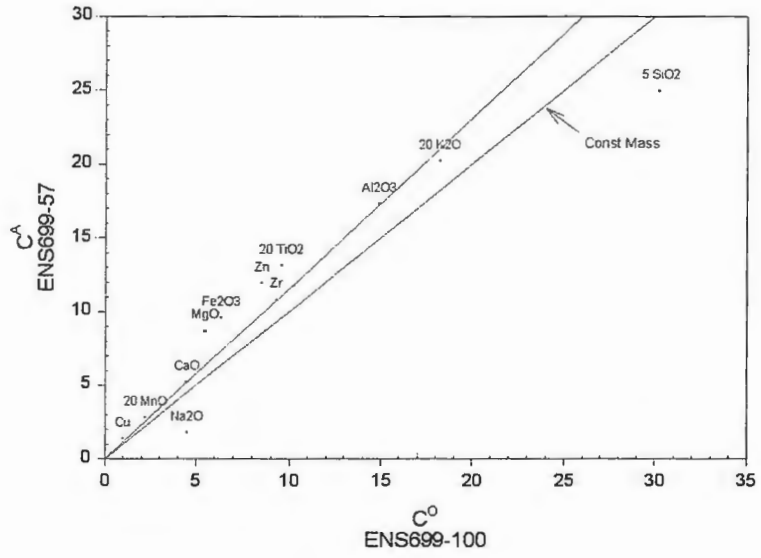

Figure 56: Isocon diagram comparing least altered footwall andesite with chlorite altered andesite.

Component	ENS 85 (%)	ENS 57 (%)
SiO2	-5	-26
TiO2	70	18
Fe2O3	50	30
MnO	50	10
MgO	-26	40
CaO	55	0
Na2O	0	-65
K2O	-91	-3
Zr	-8	0
Zn	70	20
Cu	160	12
Mass	4	-12

Table 6: Gains and losses of significant components due to chlorite +/- quartz +/- sericite alteration of footwall andesites. From isocon analysis.

Hanging Wall

Alteration in the hanging wall consists dominantly of patchy quartz and epidote assemblages which occur in pillows and massive lavas of both andesite and basalt flows. Late calcite alteration is common, but sporadic. The limited number of samples from the hanging wall makes it difficult to adequately establish alteration characteristics. Two

samples from the basalt unit were compared to ENS699- 134, the least altered basalt. Two samples from the andesites have been plotted against ENS699-141, their least altered equivalent. It should be noted that the least altered andesite comes from a flow above the basalt, whereas the altered andesites that it is being compared to are from drill hole EN-6 below the basalt unit, and are therefore, not truly stratigraphically equivalent. Hanging wall alteration is similar in character to that in the footwall.

Andesite

Samples ENC699-07 and 08 from drill hole EN-6 are compared to sample ENS699-141 that is located in andesite flows above the basaltic sequence (Figure 57 & 58). These are the only samples of andesite taken from the hanging wall, which is the reason non stratigraphic equivalents are being compared. The isocon analysis shows that both samples have experienced a 15-25% gain in mass (Table 7). Among the oxides the only additions of elements common to both samples are those of Fe and P. Iron has been increased by only 30-40% and might be accounted for in ENC699-08 by the weak

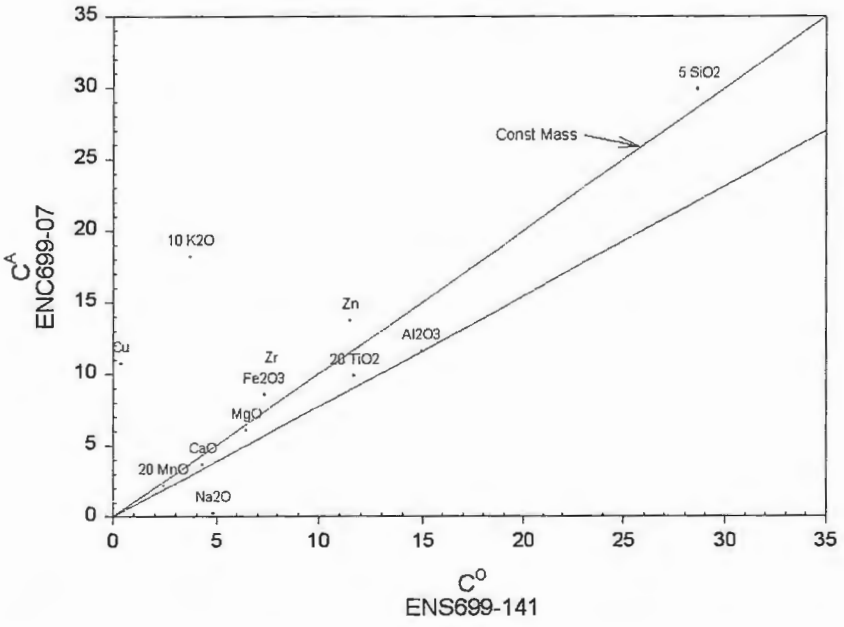

Figure 57: Isocon diagram comparing least altered hanging wall andesite with quartz + sericite altered andesite.

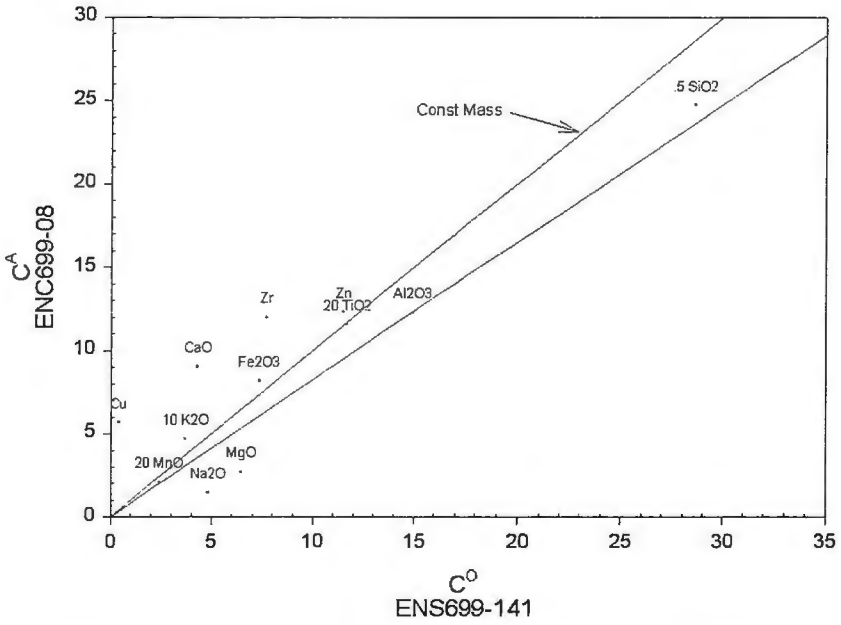

Figure 58: Isocon diagram comparing least altered hanging wall andesite with chlorite altered altered andesite

Component	ENC 07 (%)	ENC 08 (%)
SiO2	30	0
TiO2	0	12
Fe2O3	42	30
MnO	0	0
MgO	12	-50
CaO	0	150
Na2O	-90	-65
K2O	520	45
Zr	62	80
Zn	45	20
Cu	>1000	>1000
Mass	25	18

Table 7: Gains and losses of significant components after alteration of hanging wall andesites. From isocon analysis.

chlorite alteration it has experienced. However, it is not mineralogically apparent where the Fe was added in ENC699-07. Although calcite is the predominant mineral in both samples, Ca has only been added to ENC699-08 whereas its concentration has remained

unchanged in ENC699-07. Potassium addition between the two samples is significantly different. The increase of 520% in one rock appears to be due to a strong, local increase in sericite. Significant depletions of Na (65% & 90%) are seen in both samples. This is a reflection of the removal of plagioclase from the rock during alteration. The 30% Si added to ENC699-07 is likely as a result of minor quartz alteration in veinlets. Finally, Zr and Cu have been significantly increased during alteration of the rock.

Basalt

Comparing basaltic samples ENC699-06 and 3260000162 to least altered sample ENS699-134 only minor changes in element concentrations are observed (Figure 59 & 60). Mass change is small, ranging from –14% to +4% (Table 8). Weak chlorite alteration of the samples probably causes the minor increase in Fe and the somewhat larger increase in Mg. Minor depletion of Na in both samples may be explained by removal of the original feldspar from the rock. Sample ENC699-06 contains 45% calcite, but shows no concentration change in Ca. Overall, alteration of the two samples taken from the hanging wall basalt flows has not been extreme.

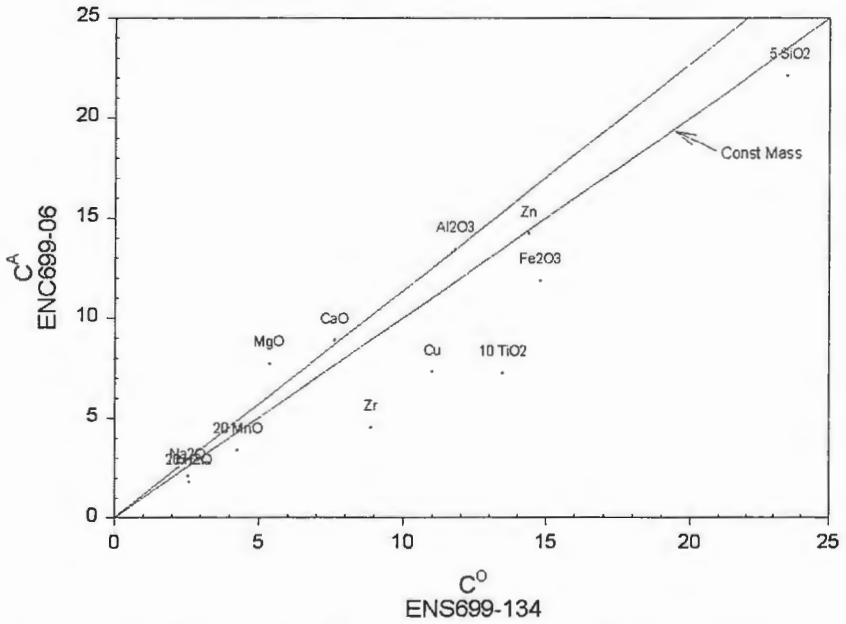

Figure 59: Isocon diagram comparing least altered hanging wall basalt with mildly chlorite altered basalt.

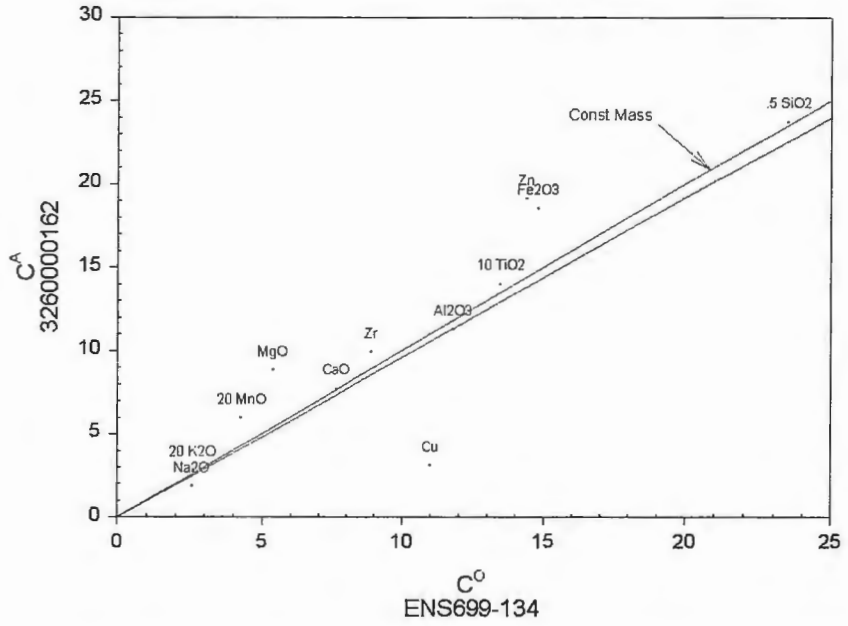

Figure 60: Isocon diagram comparing least altered hanging wall basalt with mildly chlorite altered basalt.

Component	ENC 06 (%)	326 162 (%)
SiO2	-18	5
TiO2	-52	10
Fe2O3	-30	30
MnO	-27	45
MgO	27	72
CaO	0	0
Na2O	-27	-15
K2O	-37	0
Zr	-55	15
Zn	-14	38
Cu	-43	-70
Mass	-14	4

Table 8: Gains and losses of significant components after alteration of hanging wall basalts. From isocon analysis.

Alteration Model

As stated earlier in this thesis, the heat source to the hydrothermal system responsible for the alteration at Eagles Nest may be the Purvis Lake Pluton. As mapped by Peterson (1999a), the pluton has its western most, and stratigraphically highest extent in the area immediately below the Eagles Nest mineralization. This may suggest that this system was located on the outer flanks of a subaqueous volcano at some distance from the primary center of volcanic activity. As the source of heat, the synvolcanic intrusion influences the location, and to some extent the style of alteration and mineralization above it. If hydrothermal fluids were derived primarily from local sea water, and did not experience a long residence time within the rock, there may not have been enough heat at the margin of the intrusion to raise the temperature of the fluid to levels needed to leach and mobilize significant volumes of metals from the surrounding andesitic lavas (Seyfried and Janecky, 1985).

Temperature has been demonstrated to be a significant factor in the ability of a hydrothermal fluid to leach metals from rock (Seyfried and Janecky, 1985). Laboratory experiments designed to simulate the characteristics of subseafloor circulation beneath a seafloor hot spring have shown that the concentration of Cu and Zn is greatest when the temperature of a hydrothermal fluid is 375-400° C (Figure 61) (Seyfried and Janecky, 1985). The same experiment shows that the concentration of Fe in solution increases exponentially with increasing temperature. At 350° C Fe concentration, though relatively low, is still significantly greater than that of Zn and Cu (Table 9). The temperature of the hydrothermal fluid at Eagles Nest may have never become hot enough to leach significant Cu and Zn from the rock. This is a plausible explanation for the predominance of iron formation in the Eagles Nest mineralization and the scarcity of Cu and Zn minerals.

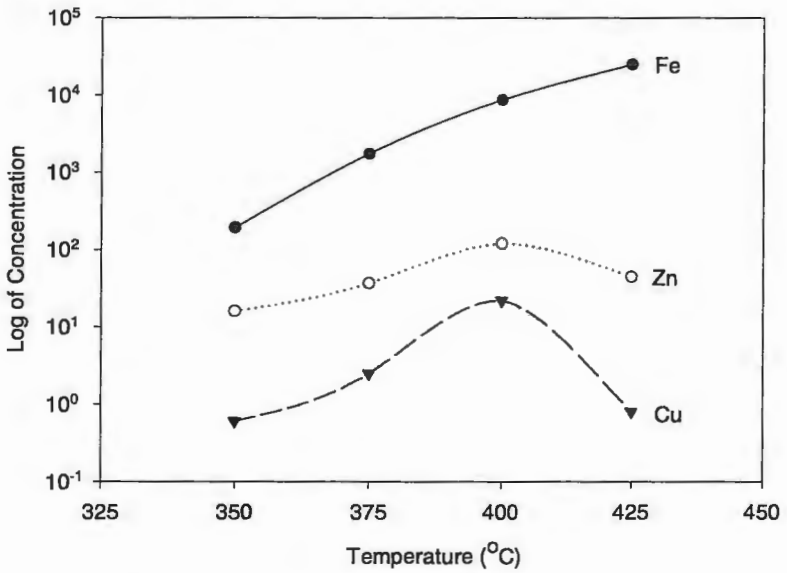

Figure 61: Graph showing the concentration of Cu, Zn, and Fe (in μmolal) in an experimental hydrothermal fluid at 400 bars, as temperature increases from 350° C to 425° C. Data from Seyfried and Janecky (1985).

Rock Type	T/P	pH	Fe	Zn	Cu
EPR-crystalline basalt	350/400	4.8	192	16	.6
EPR-crystalline basalt	375/400	3.8	1754	37	2.5
EPR-crystalline basalt	400/400	3.3	8684	121	22
EPR-crystalline basalt	425/400	2.8	25067	45	.8

Table 9: Concentration of metals in μmolal from 350° C to 425° C hydrothermal solution at 400 bars. EPR = East Pacific Rise. Experimental results from Seyfried and Janecky (1985).

The geochemistry of alteration in the footwall shows inconsistent depletions of Cu and Zn and only minor depletions of Fe. Enough iron could be leached from the rock to create an iron formation of the small scale at Eagles Nest without significantly reducing the overall iron content of the andesites. Another possible explanation for the source of metals at Eagles Nest is by the contribution of metals from a magmatic fluid expelled by the subvolcanic intrusion.

Epidote +/- quartz and quartz +/- epidote alteration follows the style of lower semiconformable alteration as outlined in genetic models for volcanogenic massive sulphide mineralization (Franklin, 1993). From extensive study of many large volcanogenic massive sulphide deposits it has been shown that the existence of semiconformable epidote-quartz alteration implies relatively high temperature hydrothermal activity related to a nearby cooling intrusion, and is a good indication that conditions were favorable for VMS deposition (Franklin, 1993; Morton and Gibson, 1993). The nature and size of this alteration coupled with its placement immediately above the Purvis Lake Pluton suggests that it may represent a reservoir zone at the bottom of a hydrothermal system. The patchy nature of the alteration results from relatively small-scale (meters) permeability contrasts in the andesite lavas that the fluid moved through, however, it also may suggest that alteration intensity was relatively weak. In addition, the crosscutting veinlets, small patches, and pillow rims of actinolite in the footwall are likely associated with the relatively low temperature fluids which lead to deposition of the iron formation, rather than massive sulphide (Morton, pers com). The surface expression of this hydrothermal system at Eagles Nest seems to be only iron formation with minor Fe, Zn, and Cu sulphides.

Based on limited drill hole control, Mg chlorite alteration appears to be stratiform in nature, and extends laterally throughout the iron formation and sediments. This intense alteration is syn- to post-mineralization in its timing and likely formed beneath the sea floor by addition of Mg during shallow draw down of sea water (Franklin, 1993). Magnesium in the seawater would have been available to form chlorite if the seafloor waters were a reducing environment as they may have been due to the oxygen depleted Archean atmosphere (Franklin, 1993). This allowed chlorite to form by inhibiting the

formation of sulphate which otherwise would have formed magnesium hydroxysulphate (Franklin, 1993). Sericite within the Mg chlorite +/- sericite alteration zone occurs as thin, intense bands (<1-2 meters), or is mixed with the Mg chlorite on a centimeter scale. The large, predominately sericite zones do not appear to be a distinct alteration unit, but may occur where dikes with chemical compositions different from the sediments and lavas crosscut the mineralized horizon. Due to intense replacement by sericite, the protolith in these zones can not be accurately determined. Immediately above the Mg chlorite alteration is a narrow zone of intense tremolite +/- Mg chlorite alteration that may represent a similar seafloor or shallow, sub seafloor alteration process.

Calcite alteration is a overprint from a later event. Evidence for this is found in the distribution of calcite in both the mineralized package and in the hanging wall where it spans the time gap that defines the contact between mineralization and hanging wall. This alteration is interpreted to be unrelated to the mineralization forming fluid and occurred after the Eagles Nest area had long since become covered by new lava flows.

CHAPTER 5

Summary

Based on field mapping, thin section study, and chemical analyses, the rocks at the Eagles Nest Volcanogenic Massive Sulphide Prospect can be described as having been metamorphosed to greenschist grade and containing relatively large percentages of actinolite, with lesser amounts of chlorite, epidote, and quartz. This assemblage of minerals overprints primary lithologies as well as earlier alteration mineral assemblages.

The general stratigraphy of the Eagles Nest map area is as follows:

The Purvis Lake Pluton is likely a synvolcanic intrusion with at least three different magmatic phases including diorite, tonalite and granodiorite. The pluton's western most margin is located in the southeast portion of the field area. The pluton shows D_2 cleavage and has little, if any, metamorphic aureole observed over its mapped extent. The top of the pluton is characterized by numerous inclusions of epidote altered andesite along with mafic, intermediate, and felsic intrusive clasts (Figure 9). One outcrop of similar xenolith filled diorite is found approximately 400 meters above the main body of the pluton.

The footwall to the mineralization is composed dominantly of andesitic pillowed lava flows which show variable amygdule content (2-35%) and variable pillow sizes (20 centimeters to +/- 1 meter in diameter). The percentage of amygdules in the rock is greatest in the flows just above the Purvis Lake Pluton, and generally decreases up stratigraphy to the mineralized horizon. Hyaloclastite is common in pillow rims. Massive flows occur, but are less common and not as strongly amygdaloidal. One large outcrop of lobe-hyaloclastite has been found. It consists of 15 centimeters to 0.5 meter diameter lava pods with quenched rims that occur in a matrix of hyaloclastite. All of the lavas strike generally east-west and dip 70-80° to the north. Many dikes of mafic to intermediate composition crosscut the footwall sequence and range in width from several centimeters to greater than 1 meter.

The mineralized horizon consists of 100-150 meters of mafic sediments, thin andesite lava flows, banded iron formations, and one thin felsic volcaniclastic unit. None of these rocks are exposed at the surface, and descriptions are based on core from three

diamond drill holes. The entire package is strongly altered and primary textures are frequently obliterated. The sedimentary units are fine-grained and identified as such by the presence of a small percentage of broken quartz grains. The units appear to be thin, and their first occurrence marks the transition from the footwall to the mineralized horizon. Banded iron formation is found in 1.5 to 20 meter thick units composed of alternating chert and magnetite bands. Interlayered with the iron formation units are thin andesite lava flows. This cycle from iron formation to lava flow occurs at least three times. Thin lenses of semi-massive and massive pyrite with minor chalcopyrite and sphalerite occur in the banded iron formation. A thin unit of very fine grained felsic volcaniclastics with < 1 mm quartz crystals is seen in one drill hole near the bottom of the sequence. Many dikes of compositions similar to those in the footwall crosscut the mineralized horizon.

The hanging wall to the mineralization is composed of andesitic and basaltic pillowed lava flows. The basalt unit is possibly as much as 100 meters thick and was identified from chemical analysis by high TiO_2, FeO, and MgO combined with low SiO_2 values. When compared to an andesite lava, basalt flows have a lower viscosity, and therefore exhibit a more "fluidal" looking, elongate pillow morphology. Pillow size ranges from 20 centimeters to greater than 1 meter in diameter. These basaltic pillows have a low height to width ratio, and have a flattened appearance in outcrop. Amygdules are slightly more numerous toward the top edge of the pillows, and are not as abundant as amygdules in the lower part of the footwall. The basalt flows appear to be the first lava flows on top of the mineralized horizon to the west, but an andesite flow lies between the mineralization and the basalts in the eastern most drill hole. Andesite lavas over lay the basalt unit. The andesites are also pillowed, but pillow morphology is not as “fluidal” in appearance as those in the basalts. The andesites have similar amygdule contents when compared to the basalts. Many mafic to intermediate dikes are seen in the hanging wall.

Hydrothermal alteration at Eagles Nest is wide spread, locally intense, and consists of two distinct styles:

Lower semi-conformable alteration: This alteration style is widespread in both the footwall and hanging wall rocks. However, the hanging wall alteration must have

occurred later in time than that in the footwall, as it is situated above the mineralized horizon. Alteration is composed of epidote, quartz, chlorite, and actinolite mineral assemblages. Epidote +/- quartz alteration turns the rock pale green and occurs with quartz. Where epidote alteration is most intense it composes 60-80% of the rock, but also fills amygdules, and occurs as veinlets and blebs where less intense. It occurs most commonly in pillow interiors. Geochemically, epidote alteration depletes the rock in Na, Mg, Fe, +/- Si, Cu, and Zn, while enriching it in Ca relative to an unaltered andesite.

Quartz +/- epidote alteration occurs in the rocks as fillings in amygdules and as veinlets. It is less common as a replacement of the original rock. As expected, quartz alteration has increased the Si content of the rock.

Chlorite +/- quartz alteration occurs as moderately strong, pervasive alteration and/or as blebs and veinlets. From optical study, the chlorite appears to be intermediate between Fe and Mg compositional end members. Chlorite alteration adds Fe and Mg to the rock, while removing Na, K, and minor Si.

Actinolite +/- epidote alteration occurs as strong pervasive mats of randomly oriented fibers, and as veinlets and small diameter (1-2 mm) patches. Pillow rims are very strongly altered to actinolite at Eagles Nest. Actinolite alteration causes gains of Mg, Ca, and Fe in the rocks, with loss of Na, K, and minor Si.

Pervasive stratiform alteration: The rocks of the mineralized horizon have been so intensely altered that many times it is impossible to determine a protolith. Because of this, component gains and losses could not be determined for this alteration. The most common alteration product is Mg chlorite which may compose up to 95% of the rock and sometimes has strong sericite alteration associated with it. Tremolite alteration occurs near the top of the sequence, is pervasive, and replaces up to 95% of the rock. These two alteration assemblages appear to be stratiform. Chlorite alteration similar to that seen in the footwall is present in the eastern portion of the mineralized horizon. It is not as intense and has a higher Fe content when compared to the Mg chlorite assemblage.

Conclusions

The Eagles Nest Prospect is situated in a sequence of calc alkaline andesite lava flows that were deposited on the ocean floor during island arc-type volcanism in the Late Archean. The Purvis Lake Pluton most likely represents the synvolcanic intrusion responsible for the volcanism. However, the pluton may not have been located at its present position when the Eagles Nest area was volcanically active. The presence of large, angular xenoliths at the top of the pluton suggests that magma continued to rise after volcanism at Eagles Nest ceased, stoping its way higher into the volcanic pile as volcanic activity continued higher in the stratigraphy. Many of the dikes that crosscut the Eagles Nest sequence are probably feeders from the Purvis Lake Pluton to volcanism above.

The known distribution of the Purvis Lake Pluton, coupled with the distribution of mafic and felsic volcanic deposits above it, suggests that the Eagles Nest area was located on the western flank of a larger volcanic system. Water depth in this area increased as the sequence of lava flows was built up, at least to the level of the mineralized horizon. This is inferred from the amygdule content of the lava flows in the footwall. The greatest percentage of amygdules in the rocks at Eagles Nest are found in the lava flows immediately above the Purvis Lake Pluton. Amygdule content of the lavas decreases from this point upward in the stratigraphy, indicating an increase in water depth, which would increase hydrostatic pressure and therefore restrict the formation of vesicles in a lava (Macpherson, 1984). There is no evidence of subaerial or subaqueous explosive eruptive activity in the footwall or hanging wall rocks. The thin unit of felsic volcaniclastic material seen in the mineralized horizon may have originated as a sediment or mass flow at some site significantly distant from Eagles Nest. The Eagles Nest area appears to have remained entirely subaqueous, and the distribution, size, and abundance of vesicles in these flows suggests that they were extruded in water depths of more than 500 meters. The mineralized horizon represents a clear stratigraphic break, when volcanism in the area slowed and hydrothermal fluids began venting on the seafloor.

Based on the experimental work of Seyfried and Janecky (1985), the mineral assemblages observed in the altered and mineralized rocks at Eagles Nest indicate that a

relatively low temperature (approximately 350° C) fluid circulated above the western margin of the Purvis Lake Pluton. This fluid leached small amounts of primarily Fe and Si from the footwall, carried them to the surface, and precipitated them on the ocean floor as banded iron formations. The low solubility of Cu and Zn in this fluid would mean that large amounts of Cu and Zn were not leached from the lavas, and therefore no significant massive sulphide mineralization is found at Eagles Nest. The minor occurrence of Cu and Zn sulphides in the iron oxide mineralization may have been due to a small and/or short lived, magmatic fluid contribution of Cu and Zn to the hydrothermal system. Another possible explanation for the Cu and Zn sulphides is short lived leaching of metals from the footwall rocks associated with a temporary increase in fluid temperature. At several times during deposition of the BIF on the seafloor, small andesitic lava flows covered the area and may have temporarily ended hydrothermal venting. Stratiform Mg chlorite and tremolite alteration resulted from shallow draw down of seawater into the subseafloor and is syn- to post-mineralization in timing. The common and wide spread epidote +/- quartz alteration in the footwall and hanging wall are so ubiquitous that it is not a reliable guide to exploring for previously unknown massive sulphide deposits in a given area. Calcite alteration occurred significantly later in time, and may have been the result of fluid movement along faults and shears.

REFERENCES

Blatt, H. and Tracy, R.J., 1996, Petrology: Igneous, Sedimentary, and Metamorphic, 2nd Edition, W.H. Freeman and Company, New York.

Boerboom, T.J., and Zartman, R.E., 1993, Geology, geochemistry, and geochronology of the central Giants Range batholith, Northeastern Minnesota: Canadian Journal of Earth Sciences v. 30, pp. 2510-2522.

Card, K.D., 1990, A review of the Superior Province of the Canadian Shield, a product of Archean accretion: Precambrian Research, v. 48, pp. 99-156.

Coryell C.G., Chase J.W. and Winchester J.W., 1963, A procedure for geochemical interpretation of terrestrial rare-earth abundance patterns, Journal of Geophysical Research, v. 68, pp. 559-566.

Franklin, J.M., 1993, Volcanic associated massive sulphide deposits: in Mineral Deposit Modeling, Kirkham, R.V., Sinclair, W.D., Thorpe, R.I, and Duke, Jim., eds., Geological Association of Canada Special Paper 40, pp. 315-344.

Gibson, Harold L., Morton, Ronald L., and Hudak, George J., 1999, Submarine volcanic processes, deposits, and environments favourable for the location of volcanic-associated massive sulfide deposits, in Volcanic Associative Massive Sulphide Deposits: Processes and Examples in Ancient and Modern Settings; Eds., Barrie, T. and Hennington, M. *in* Reviews in Economic Geology, pp. 13-51.

Gill, James B., 1981, Orogenic andesites and plate tectonics, Berlin; New York: Springer-Verlag.

Grant, James A., 1986, The isocon diagram- A simple solution to Gresens' equation for metasomatic alteration, Economic Geology, v. 81, pp. 1976-1982.

Hudak, G.J., 2000, Personal communication during field trip to Five Mile Lake map area on August, 4.

Irvine, T.N., and Baragar, W.R.A., 1971, A guide to the chemical classification of the common volcanic rocks., Canadian Journal of Earth Sciences, v. 8, pp. 523-548.

Jenson, L.S., 1976, A new cation plot for classifying subalkalic volcanic rocks, Ontario Division of Mines, Miscellaneous Paper 66.

Jirsa, M.A., D.L. Southwick, and T.J. Boerboom, 1992, Structural evolution of Archean rocks in the western Wawa subprovince, Minnesota: refolding and of precleavage nappes during D_2 transpression, Canadian Journal of Earth Science, v. 29, pp. 2146-2155.

Jones, J.G., 1969, Pillow lavas as depth indicators., American Journal of Science, v. 267, pp. 181-195.

Kokelaar, P., 1986, Magma-water interactions in subaqueous and emergent basaltic volcanism, Bulletin of Volcanology, v.48, pp. 275-289.

LeMaitre, R.W.,1984, A proposal by the IUGS Subcommission on the Systematics of Igneous Rocks for a chemical classification of volcanic rocks based on the total alkali silica (TAS) diagram. Australian Journal of Earth Sciences 31, v.2, pp 243-255.

MacGeehan, P.J., and MacLean, W.H., 1980, An Archean sub-seafloor geothermal system, "calc-alkaline" trends, and massive sulphide genesis., Nature, v. 286, pp. 767-771.

MacLean, W.H. and Kranidiotis, P., 1987, Immobile elements as monitors of mass transfer in hydrothermal alteration: Phelps Dodge Massive Sulphide Deposit, Matagami, Quebec., Economic Geology, v. 82, pp. 951-962.

Macpherson, G.J., 1984, A model for predicting the volume of vesicles in submarine basalts., Journal of Geology, v. 92, pp. 73-82.

Masuda, A., 1962, Regularities in variation of relative abundances of lanthanide elements and an attempt to analyse separation-index patterns of some minerals., Journal of Earth Science Nagoya University, v. 10, pp. 173-187.

Michard, A., 1989, Rare earth element systematics in hydrothermal fluids., Geochimica Cosmochimica Acta, v. 53, pp. 745-750.

Middlemost, E.A.K., 1980, A contribution to the nomenclature and classification of volcanic rocks., Geol. Mag. 117 (I), pp. 51-57.

Moore, J.G. and Schilling, J., 1973, Vesicles, water, and sulfur in Reykjanes Ridge basalts., Contributions to Mineralogy and Petrology, v. 41, pp. 105-118.

Morey, G.G., Green, J.C., Ojankangas, R.W., and Sims, P.K., 1970, Stratigraphy of the Lower Precambrian rocks in the Vermilion District, northeastern Minnesota., Minnesota Geological Survey, Report of Investigation 14, 33 p.

Morton, R.L., 2000, personal communication, University of Minnesota-Duluth.

Morton, R.L., and Gibson, H., 1993, from A short course on physical volcanology, hydrothermal alteration, and massive sulphides deposits. August 23-28.

Morton, R.L., and Franklin, J.M., 1987, Twofold classification of Archean volcanic-associated massive sulphides deposits: Economic Geology, v. 82, pp. 1057-1063.

Pearce, J.A., 1983, Role of the sub-continental lithosphere in magma genesis at active continental margins., in Hawkesworth C.J. and Norry M.J. (eds.), Continental basalts and mantle xenoliths. Shiva, Nantwich, pp. 230-249.

Peterson, D.M., and Jirsa, M.A., 1999, Lode gold and massive sulphides prospects in the Archean western Vermilion District of Northeastern Minnesota, Minnesota Exploration Conference 1999 Field Trip Guidebook.

Peterson, D.M. and Jirsa, M.A., 1999a, Bedrock geologic map and mineral exploration data, western Vermilion district, St. Louis and Lake Counties, northeastern Minnesota: MGS Miscellaneous Map M-98, scale 1:48,000.

Peterson, D.M., (in prep), Development of Archean lode gold and massive sulfide deposit exploration models using Geographic Information System applications: targeting mineral exploration in northeastern Minnesota from analysis of analog Canadian mining camps: University of Minnesota Ph.D thesis.

Peterson, D.M., 2000, personal communication, University of Minnesota-Duluth.

Philpotts, A.R., 1989, Petrography of Igneous and Metamorphic Rocks., Prentice Hall Inc, New Jersey, p. 110.

Riverin, G., and Hodgson, ClJ., 1980, Wall-rock alteration at the Millenbach Cu-Zn mine, Noranda, Quebec., Economic Geology, v. 75, pp. 424-444.

Roberts, R.G., and Reardon, E.J., 1978, Alteration and ore-forming processes at Mattagami Lake mine, Quebec., Canadian Journal of Earth Sciences, v. 15, pp. 1-21.

Rollinson, H.R., 1993, Using geochemical data: evaluation, presentation, interpretation., Longman Scientific and Technical, Essex, England, pp. 133-148.

Schultz, K.J., 1980, The magmatic evolution of the Vermilion greenstone belt, NE Minnesota, Precambrian Research, v. 11, pp. 215-245.

Seyfried Jr., W.E. and Janecky, D.R., 1985, Heavy metal and sulfur transport during subcritical and supercritical hydrothermal alteration of basalt: Influence of fluid pressure and basalt composition and crystallinity, Geochimica et Cosmochimica Acta, v. 49, pp 2545-2560.

Skirrow, R.G. , and Franklin, J.M., 1994, Silicification and metal leaching in semi-conformable alteration beneath the Chisel Lake massive sulfide deposit, Snow Lake, Manitoba, Economic Geology, v. 89, pp. 31-50.

Southwick, D.L., Boerboom, T.J., and Jirsa, M.A., 1998, Geologic setting and descriptive geochemistry of Archean supracrustal and hypabyssal rocks, Soudan-Bigfork area, Northern Minnesota: implications for metallic mineral exploration. Minnesota Geological Survey Report of Investigations 51, 69 p.

Williams, H.R., 1990, Subprovince accretion tectonics in the south-central Superior Province. Canadian Journal of Earth Science, v. 27, pp. 570-581.

Winchester, J.A., and Floyd, P.A., 1977, Geochemical discrimination of different magma series and the differentiation products using immobile elements, Chemical Geology, v. 20, pp. 325-343.

Appendix 1: **Footwall** Major Oxide and Trace Element Chemistry

Negative values indicate concentrations below detection limits

SAMPLE	Rk Type	SiO2 %	TiO2 %	Al2O3 %	Fe2O3 %	MnO %	MgO %	CaO %	Na2O %	K2O %	P2O5 %	LOI %	TOTAL %
ENS699-08	and	56.85	0.67	13.93	9.08	0.12	3.19	10.57	1.68	0.52	0.15	1.76	98.52
ENS699-10	and	53.49	0.56	16.56	9.95	0.14	6.99	5.39	3.95	0.28	0.15	2.80	100.24
ENS699-19	and	65.20	0.54	10.59	7.26	0.10	6.44	3.76	0.54	0.74	0.12	3.24	98.54
ENS699-20	and	53.74	0.62	15.07	6.94	0.13	7.26	9.29	4.05	0.37	0.14	1.04	98.63
ENS699-23	and	49.76	0.43	19.10	8.44	0.12	1.86	18.08	0.36	0.12	0.10	1.83	100.19
ENS699-28	dk	42.00	0.65	9.77	12.70	0.20	21.84	6.29	0.09	-0.01	0.07	6.18	99.80
ENS699-39	and	57.75	0.44	13.13	8.04	0.12	5.46	9.33	2.29	0.88	0.12	1.32	98.87
ENS699-44	and	69.64	0.35	11.77	4.48	0.09	2.87	4.88	3.57	0.48	0.11	0.74	99.00
ENS699-53	and	58.24	0.56	15.62	6.67	0.10	5.95	3.09	3.91	0.92	0.14	3.79	99.00
ENS699-57	and	49.86	0.66	17.27	9.57	0.14	8.68	5.22	1.79	1.01	0.13	4.49	98.81
ENS699-62	and	56.73	0.52	17.28	6.53	0.18	4.89	6.06	5.35	1.11	0.21	1.35	100.19
ENS699-65	and	59.40	0.53	15.81	6.63	0.10	5.21	3.52	4.47	0.69	0.10	3.78	100.24
ENS699-85	and	54.80	0.79	14.12	9.08	0.16	3.94	6.72	4.07	0.08	0.11	6.34	100.21
ENS699-89	and	60.06	0.51	15.39	5.77	0.10	4.46	4.87	5.73	0.59	0.13	1.69	99.31
ENS699-95	dio	52.62	0.47	19.12	5.71	0.13	4.68	9.26	3.95	0.96	0.09	1.62	98.60
ENS699-100	and	60.40	0.48	14.90	6.34	0.11	5.49	4.51	4.54	0.91	0.11	1.73	99.52
ENS699-104	and	51.87	0.64	18.18	7.81	0.13	7.03	6.55	3.50	1.13	0.16	2.67	99.66
ENS699-149	and	58.30	0.52	15.60	6.26	0.13	5.72	4.61	4.68	0.49	0.14	2.31	98.76
98-059*	grd	65.66	0.28	16.42	3.28	0.03	1.33	3.44	5.15	1.55	0.10	2.33	99.60

Rk Type Key:

and= andesite, bas= basalt, dk= dike, dio= diorite, bif= banded iron formation, sed= sedimentary rock, vlc= volcanoclastic rock, alt= 100% alteration

* Purvis Lake Pluton sample from Peterson (in prep). Grd = granodiorite. All data shown.

Appendix 1: **Footwall** Major Oxide and Trace Element Chemistry

Negative values indicate concentrations below detection limits

Element	Rk Type	BA	SR	Y	ZR	BE	V	AU	AS	BR	CO	CR	CS
Units		PPB	PPM	PPM	PPM	PPM	PPM	PPB	PPM	PPM	PPM	PPM	PPM
Detec Lim								5	2	1	1	1	0.5
ENS699-08	and	140	249	16	122	1	125	10	343	-1	45	198	-0.5
ENS699-10	and	100	170	17	119	-1	125	50	18	-1	45	175	-0.5
ENS699-19	and	238	63	15	115	-1	103	-5	7	-1	45	137	-0.5
ENS699-20	and	129	198	15	135	1	116	-5	11	-1	13	195	-0.5
ENS699-23	and	33	84	13	100	-1	158	-5	8	-1	14	154	-0.5
ENS699-28	dk	6	6	10	49	-1	114	-5	2	-1	100	2490	-0.5
ENS699-39	and	265	194	17	91	1	121	-5	-2	-1	26	155	-0.5
ENS699-44	and	106	109	16	78	-1	59	-5	7	-1	18	132	-0.5
ENS699-53	and	475	333	20	138	1	127	-5	2	-1	22	201	-0.5
ENS699-57	and	230	149	17	108	1	147	-5	-2	-1	40	159	-0.5
ENS699-62	and	312	271	14	114	-1	113	-5	2	-1	22	123	-0.5
ENS699-65	and	231	167	12	80	-1	113	-5	-2	-1	30	129	-0.5
ENS699-85	and	42	74	15	82	-1	149	-5	3	-1	30	6	-0.5
ENS699-89	and	164	117	15	96	-1	84	-5	3	-1	25	151	-0.5
ENS699-95	dio	162	249	16	74	-1	106	-5	-2	-1	21	80	3.0
ENS699-100	and	282	134	15	93	-1	100	-5	2	-1	28	242	-0.5
ENS699-104	and	265	159	19	144	2	123	-5	-2	-1	27	168	1.8
ENS699-149	and	230	184	17	120	-1	96	-5	-2	-1	23	207	-0.5
98-059*	grd							-5					

Rk Type Key:

and= andesite, bas= basalt, dk= dike, dio= diorite, bif= banded iron formation, sed= sedimentary rock, vlc= volcanoclastic rock, alt= 100% alteration

* Purvis Lake Pluton sample from Peterson (in prep). Grd = granodiorite. All data shown.

Appendix 1: **Footwall** Major Oxide and Trace Element Chemistry

Negative values indicate concentrations below detection limits

Element	Rk Type	HF	IR	MO	RB	SB	SC	SE	TA	TH	U	W	LA
Units		PPM	PPB	PPM	PPM	PPM	PPM	PPM	PPM	PPM	PPM	PPM	PPM
Detec Lim		0.5	5	5	20	0.2	0.1	3	1	0.5	0.5	3	0.5
ENS699-08	and	3.0	-5	-5	-20	2.6	19.6	-3	-1	2.6	0.9	-3	13.9
ENS699-10	and	3.0	-5	-5	-20	0.4	18.9	-3	-1	2.8	-0.5	-3	16.9
ENS699-19	and	3.0	-5	-5	41	-0.2	17.4	-3	-1	2.6	1.0	-3	15.2
ENS699-20	and	3.7	-5	-5	-20	-0.2	19.7	-3	-1	2.9	-0.5	-3	13.4
ENS699-23	and	2.3	-5	-5	-20	0.3	13.7	-3	-1	2.2	0.9	-3	13.7
ENS699-28	dk	1.0	-5	-5	-20	-0.2	19.7	-3	-1	0.6	-0.5	-3	2.6
ENS699-39	and	2.3	-5	-5	43	-0.2	15.0	-3	-1	2.2	1.1	-3	18.2
ENS699-44	and	2.4	-5	-5	-20	0.3	8.8	-3	-1	1.8	0.7	-3	6.1
ENS699-53	and	3.5	-5	-5	-20	0.2	18.2	-3	-1	3.1	1.3	-3	22.2
ENS699-57	and	2.3	-5	-5	-20	-0.2	25.8	-3	-1	1.6	-0.5	-3	9.9
ENS699-62	and	3.2	-5	-5	90	-0.2	17.1	-3	-1	2.3	0.8	-3	15.7
ENS699-65	and	-0.5	-5	-5	-20	0.2	19.7	-3	1	1.6	-0.5	-3	7.5
ENS699-85	and	2.6	-5	-5	-20	-0.2	23.8	-3	-1	0.9	-0.5	-3	8.3
ENS699-89	and	2.7	-5	-5	-20	-0.2	16.7	-3	-1	1.3	-0.5	-3	9.5
ENS699-95	dio	1.8	-5	-5	30	-0.2	19.4	-3	-1	0.9	-0.5	-3	7.2
ENS699-100	and	2.4	-5	-5	61	-0.2	17.6	-3	-1	1.4	-0.5	-3	8.8
ENS699-104	and	3.1	-5	-5	-20	-0.2	17.4	-3	-1	3.0	0.6	-3	16.6
ENS699-149	and	3.0	-5	-5	-20	-0.2	16.4	-3	-1	3.2	0.7	-3	15.8

Rk Type Key:

and= andesite, bas= basalt, dk= dike, dio= diorite, bif= banded iron formation, sed= sedimentary rock, vlc= volcanoclastic rock, alt= 100% alteration

Appendix 1: **Footwall** Major Oxide and Trace Element Chemistry

Negative values indicate concentrations below detection limits

Element	Rk Type	CE	ND	SM	EU	TB	YB	LU	CU	PB	ZN	AG	NI
Units		PPM	PPM	PPM	PPM	PPM	PPM	PPM	PPM	PPM	PPM	PPM	PPM
Detec Lim		3	5	0.1	0.1	0.5	0.1	0.05	1	5	1	0.4	1
ENS699-08	and	28	10	2.8	1.0	-0.5	1.5	0.23	358	77	74	-0.4	99
ENS699-10	and	31	15	3.2	1.0	-0.5	1.5	0.23	34	6	121	-0.4	143
ENS699-19	and	28	13	2.6	0.6	-0.5	1.5	0.23	95	-5	98	-0.4	118
ENS699-20	and	22	13	2.8	0.7	-0.5	1.4	0.21	4	-5	75	-0.4	112
ENS699-23	and	25	10	2.4	0.6	-0.5	1.3	0.20	15	-5	73	-0.4	53
ENS699-28	dk	8	-5	1.5	0.7	-0.5	1.0	0.15	4	-5	135	-0.4	1258
ENS699-39	and	34	16	3.1	1.4	-0.5	1.5	0.23	47	-5	107	-0.4	167
ENS699-44	and	12	7	1.9	0.6	-0.5	1.2	0.18	28	-5	91	-0.4	123
ENS699-53	and	38	17	3.7	1.1	-0.5	1.5	0.23	63	-5	61	-0.4	150
ENS699-57	and	20	7	2.3	0.6	-0.5	1.3	0.18	14	-5	119	-0.4	129
ENS699-62	and	28	11	2.7	0.5	-0.5	1.2	0.18	11	-5	114	-0.4	119
ENS699-65	and	14	7	1.6	0.5	-0.5	1.1	0.16	124	-5	87	-0.4	94
ENS699-85	and	20	7	2.5	0.8	-0.5	1.5	0.23	23	-5	133	-0.4	65
ENS699-89	and	19	9	2.4	0.6	-0.5	1.3	0.21	8	-5	88	-0.4	113
ENS699-95	dio	15	7	2.2	0.6	-0.5	1.2	0.18	2	-5	85	-0.4	44
ENS699-100	and	21	7	2.2	0.4	-0.5	1.1	0.16	10	-5	85	-0.4	152
ENS699-104	and	31	12	2.7	0.8	-0.5	1.7	0.25	1	-5	91	-0.4	146
ENS699-149	and	31	14	2.9	0.8	-0.5	1.5	0.23	28	-5	65	-0.4	144
98-059*	grd								51		20		

Rk Type Key:

and= andesite, bas= basalt, dk= dike, dio= diorite, bif= banded iron formation, sed= sedimentary rock, vlc= volcanoclastic rock, alt= 100% alteration

* Purvis Lake Pluton sample from Peterson (in prep). Grd = granodiorite. All data shown.

Appendix 1: **Footwall** Major Oxide and Trace Element Chemistry

Negative values indicate concentrations below detection limits

Element	Rk Type	CD	Bl
Units		PPM	PPM
Detec Lim		0.5	5
ENS699-08	and	1.3	-5
ENS699-10	and	0.8	-5
ENS699-19	and	0.5	-5
ENS699-20	and	-0.5	-5
ENS699-23	and	-0.5	-5
ENS699-28	dk	0.6	-5
ENS699-39	and	-0.5	-5
ENS699-44	and	-0.5	-5
ENS699-53	and	-0.5	-5
ENS699-57	and	0.5	-5
ENS699-62	and	-0.5	-5
ENS699-65	and	0.5	-5
ENS699-85	and	0.6	-5
ENS699-89	and	-0.5	-5
ENS699-95	dio	-0.5	-5
ENS699-100	and	0.5	-5
ENS699-104	and	-0.5	-5
ENS699-149	and	-0.5	-5

Rk Type Key:

and= andesite, bas= basalt, dk= dike, dio= diorite, bif= banded iron formation, sed= sedimentary rock, vlc= volcanoclastic rock, alt= 100% alteration

Appendix 1: **Mineralized Horizon** Major Oxide and Trace Element Chemistry

Negative values indicate concentrations below detection limits

SAMPLE	Rk Type	SiO2	TiO2	Al2O3	Fe2O3	MnO	MgO	CaO	Na2O	K2O	P2O5	LOI	TOTAL
		%	%	%	%	%	%	%	%	%	%	%	%
3260000174	bif	28.02	0.03	0.40	38.98	1.01	8.56	13.38	0.06	0.02	0.15	8.28	98.88
3260000182	alt	45.27	0.91	35.97	1.86	0.03	0.46	0.36	0.79	8.90	0.02	4.67	99.24
3260000184	alt	30.65	1.07	27.05	9.22	0.06	18.68	0.09	0.31	1.97	0.02	9.98	99.10
3260000190	alt	42.15	0.78	12.37	18.82	0.05	13.47	0.26	0.05	0.17	0.09	12.45	100.65
3260000196	bif	4.44	0.03	0.58	18.77	0.81	12.93	24.34	0.01	-0.01	0.06	34.93	96.90
3260000199	alt	37.14	0.51	10.69	10.18	0.10	18.97	4.72	0.12	0.02	0.11	16.32	98.89
3260000200	alt	14.18	0.02	0.82	9.06	0.64	7.60	30.97	0.15	0.06	0.03	34.42	97.93
3260000203	and	57.03	0.44	16.29	4.55	0.06	3.45	5.94	5.05	0.48	0.19	5.66	99.13
3260000204	and	49.81	0.67	15.82	6.74	0.09	5.82	5.58	4.92	0.43	0.08	8.69	98.67
3260000220	alt	40.96	0.04	0.61	11.36	0.80	12.12	22.55	0.08	0.06	0.02	9.10	97.68
3260000223	bif	22.54	0.15	3.77	43.19	0.30	5.30	1.17	0.01	0.04	0.37	22.05	98.91
3260000228	sed	84.47	0.23	7.45	2.14	0.01	2.31	0.14	0.33	1.28	-0.01	2.12	100.46
3260000230	alt	27.83	0.93	23.10	9.45	0.09	25.27	0.04	0.23	0.14	0.01	11.53	98.64
3260000231	alt	32.46	0.93	21.16	6.15	0.06	26.21	0.06	0.25	0.06	0.01	11.34	98.71
3260000232	alt	36.77	1.45	31.62	3.60	0.02	13.09	0.05	0.74	4.84	0.02	7.94	100.14
3260000234	alt	31.31	1.04	23.52	5.42	0.04	27.08	0.05	0.19	0.26	0.05	11.52	100.46
3260000236	alt	31.53	1.46	21.33	5.61	0.04	28.22	0.03	0.16	0.05	0.02	11.70	100.15
3260000240	alt	63.96	0.81	10.09	8.51	0.04	10.55	0.39	0.16	0.06	0.35	5.24	100.15
ENC699-16	dk	45.61	0.50	11.68	7.76	0.15	7.73	9.72	1.85	0.75	0.26	12.67	98.68
ENC699-17	sed	46.81	0.72	16.84	9.36	0.10	8.50	5.57	3.54	0.21	0.11	8.68	100.43
ENC699-18	sed	42.94	0.49	16.13	8.95	0.11	10.53	6.76	2.35	0.22	0.09	10.58	99.14
ENC699-19	vlc	47.57	0.49	14.73	8.01	0.15	6.23	7.95	3.24	0.55	0.13	11.06	100.12
ENC699-21	sed	48.89	0.38	14.67	5.93	0.13	4.61	10.61	3.23	1.09	0.07	10.88	100.48

Rk Type Key:

and= andesite, bas= basalt, dk= dike, dio= diorite, bif= banded iron formation, sed= sedimentary rock, vlc= volcanoclastic rock, alt= 100% alteration

Appendix 1: **Mineralized Horizon** Major Oxide and Trace Element Chemistry

Negative values indicate concentrations below detection limits

Element	Rk Type	BA	SR	Y	ZR	BE	V	AU	AS	BR	CO	CR	CS
Units		PPB	PPM	PPM	PPM	PPM	PPM	PPB	PPM	PPM	PPM	PPM	PPM
Detec Lim								5	2	1	1	1	0.5
3260000174	bif	6	24	8	12	-1	9	-5	-2	-1	8	14	-0.5
3260000182	alt	2663	218	29	69	1	310	-5	3	-1	2	630	2.1
3260000184	alt	508	55	28	163	-1	302	6	-2	-1	65	188	2.1
3260000190	alt	48	8	23	76	-1	187	31	4	-1	79	159	-0.5
3260000196	bif	5	25	4	9	-1	10	17	4	-1	5	8	-0.5
3260000199	alt	5	29	19	142	-1	86	-5	2	-1	15	41	1.2
3260000200	alt	3	53	8	20	-1	-5	20	4	-1	9	4	-0.5
3260000203	and	333	375	10	101	1	69	-5	3	-1	18	91	-0.5
3260000204	and	73	265	14	66	-1	139	-5	2	-1	31	192	-0.5
3260000220	alt	11	28	5	17	-1	28	9	2	-1	4	11	-0.5
3260000223	bif	9	7	28	42	-1	155	134	16	-1	227	25	-0.5
3260000228	sed	84	12	6	88	-1	75	6	-2	-1	4	50	-0.5
3260000230	alt	47	3	24	148	-1	303	-5	2	-1	17	135	-0.5
3260000231	alt	9	7	24	130	-1	237	-5	-2	-1	25	175	-0.5
3260000232	alt	1601	109	22	205	-1	464	-5	-2	-1	17	204	1.5
3260000234	alt	90	10	87	71	-1	420	-5	-2	-1	49	370	0.7
3260000236	alt	7	3	5	71	-1	467	-5	-2	-1	8	661	-0.5
3260000240	alt	18	54	16	78	1	171	5	2	-1	50	877	-0.5
ENC699-16	dk	354	168	13	77	2	142	-5	-2	-1	42	768	-0.5
ENC699-17	sed	58	121	14	74	-1	155	7	2	-1	49	235	-0.5
ENC699-18	sed	40	92	9	45	-1	110	-5	-2	-1	52	325	-0.5
ENC699-19	vlc	155	133	12	66	-1	122	5	-2	-1	31	180	3.2
ENC699-21	sed	371	175	9	69	-1	96	-5	-2	-1	33	171	-0.5

Rk Type Key:

and= andesite, bas= basalt, dk= dike, dio= diorite, bif= banded iron formation, sed= sedimentary rock, vlc= volcanoclastic rock, alt= 100% alteration

Appendix 1: **Mineralized Horizon** Major Oxide and Trace Element Chemistry

Negative values indicate concentrations below detection limits

Element	Rk Type	HF	IR	MO	RB	SB	SC	SE	TA	TH	U	W	LA
Units		PPM	PPB	PPM	PPM	PPM	PPM	PPM	PPM	PPM	PPM	PPM	PPM
Detec Lim		0.5	5	5	20	0.2	0.1	3	1	0.5	0.5	3	0.5
3260000174	bif	-0.5	-5	-5	-20	0.3	1.1	-3	-1	-0.5	-0.5	-3	1.8
3260000182	alt	2.4	-5	-5	201	0.3	20.5	-3	-1	0.6	0.7	-3	0.4
3260000184	alt	4.4	-5	-5	51	-0.2	41.5	-3	-1	3.3	-0.5	-3	9.9
3260000190	alt	1.9	-5	7	25	-0.2	24.4	24	-1	0.8	0.7	9	11.4
3260000196	bif	-0.5	-5	-5	-20	-0.2	1.1	-3	-1	-0.5	-0.5	-3	2.6
3260000199	alt	3.3	-5	-5	-20	-0.2	13.3	-3	-1	2.7	-0.5	-3	17.2
3260000200	alt	-0.5	-5	-5	-20	-0.2	1.9	3	-1	-0.5	-0.5	-3	3.3
3260000203	and	2.8	-5	-5	-20	0.4	7.9	-3	-1	2.8	0.8	-3	21.2
3260000204	and	1.6	-5	-5	-20	-0.2	22.9	-3	-1	1.0	-0.5	-3	6.4
3260000220	alt	-0.5	-5	-5	-20	0.2	5.4	-3	-1	-0.5	-0.5	-3	1.2
3260000223	bif	1.2	-5	-5	-20	0.5	61.5	226	-1	-0.5	-0.5	7	5.7
3260000228	sed	2.1	-5	-5	21	-0.2	10.7	-3	-1	1.4	-0.5	-3	7.1
3260000230	alt	4.0	-5	-5	-20	-0.2	38.2	-3	-1	1.6	-0.5	-3	2.8
3260000231	alt	3.6	-5	-5	-20	0.3	35.9	-3	-1	2.3	1.0	-3	14.6
3260000232	alt	5.2	-5	-5	95	-0.2	58.0	-3	-1	3.1	-0.5	-3	19.0
3260000234	alt	2.8	-5	-5	-20	-0.2	73.7	-3	-1	3.9	-0.5	-3	1.8
3260000236	alt	-0.5	-5	-5	28	0.4	203.0	-3	-1	2.6	-0.5	4	0.4
3260000240	alt	2.2	-5	-5	-20	0.2	22.5	-3	-1	2.3	1.0	-3	19.4
ENC699-16	dk	2.3	-5	-5	-20	-0.2	26.7	-3	-1	2.8	1.0	-3	14.6
ENC699-17	sed	1.7	-5	-5	-20	-0.2	26.0	-3	-1	1.1	-0.5	-3	7.7
ENC699-18	sed	1.4	-5	-5	-20	-0.2	20.7	-3	-1	0.5	-0.5	-3	5.8
ENC699-19	vlc	1.7	-5	-5	-20	0.2	17.8	-3	-1	1.0	-0.5	3	8.2
ENC699-21	sed	1.5	-5	-5	-20	0.2	16.4	-3	-1	1.5	1.2	-3	6.5

Rk Type Key:

and= andesite, bas= basalt, dk= dike, dio= diorite, bif= banded iron formation, sed= sedimentary rock, vlc= volcanoclastic rock, alt= 100% alteration

Appendix 1: **Mineralized Horizon** Major Oxide and Trace Element Chemistry

Negative values indicate concentrations below detection limits

Element	Rk Type	CE	ND	SM	EU	TB	YB	LU	CU	PB	ZN	AG	NI
Units		PPM	PPM	PPM	PPM	PPM	PPM	PPM	PPM	PPM	PPM	PPM	PPM
Detec Lim		3	5	0.1	0.1	0.5	0.1	0.05	1	5	1	0.4	1
3260000174	bif	4	-5	0.8	0.8	-0.5	0.6	0.10	86	-5	228	-0.4	1
3260000182	alt	3	-5	0.5	0.7	0.6	2.6	0.39	4	13	14	-0.4	5
3260000184	alt	21	10	2.4	0.8	-0.5	3.1	0.46	2	7	217	-0.4	193
3260000190	alt	25	13	3.6	1.1	0.5	2.7	0.41	1058	-5	155	-0.4	98
3260000196	bif	6	-5	0.6	0.7	-0.5	0.5	0.08	70	-5	83	-0.4	5
3260000199	alt	40	17	3.4	0.7	-0.5	2.0	0.32	8	-5	204	-0.4	31
3260000200	alt	8	-5	1.0	0.6	-0.5	0.5	0.08	7	-5	80	-0.4	10
3260000203	and	45	22	4.2	1.0	-0.5	0.6	0.11	6	6	75	-0.4	65
3260000204	and	13	-5	1.8	0.6	-0.5	1.4	0.22	102	5	109	-0.4	90
3260000220	alt	-3	-5	0.6	0.3	-0.5	0.4	0.06	5	-5	259	-0.4	62
3260000223	bif	16	9	5.1	2.4	1.0	2.5	0.40	104	-5	160	0.4	576
3260000228	sed	15	11	2.1	0.5	-0.5	0.7	0.11	3	-5	65	-0.4	9
3260000230	alt	8	-5	1.0	0.5	-0.5	2.8	0.56	6	-5	132	-0.4	242
3260000231	alt	32	12	2.5	0.9	0.5	2.8	0.56	1	-5	70	-0.4	174
3260000232	alt	42	20	4.3	1.1	-0.5	3.1	0.46	-1	7	130	-0.4	106
3260000234	alt	10	-5	2.2	1.5	-0.5	8.5	1.33	201	-5	241	-0.4	362
3260000236	alt	-3	-5	-0.1	-0.1	-0.5	1.0	0.15	6	-5	207	-0.4	177
3260000240	alt	47	24	5.4	1.6	-0.5	1.4	0.21	2	-5	100	-0.4	352
ENC699-16	dk	29	18	3.7	0.9	-0.5	1.2	0.18	73	-5	114	-0.4	108
ENC699-17	sed	17	9	2.2	0.7	-0.5	1.7	0.25	60	-5	88	-0.4	168
ENC699-18	sed	10	-5	1.5	0.5	-0.5	1.1	0.16	9	-5	90	-0.4	321
ENC699-19	vlc	16	9	2.0	0.6	-0.5	1.2	0.18	3	6	113	-0.4	126
ENC699-21	sed	11	5	1.3	0.5	-0.5	1.0	0.15	13	-5	89	-0.4	104

Rk Type Key:

and= andesite, bas= basalt, dk= dike, dio= diorite, bif= banded iron formation, sed= sedimentary rock, vlc= volcanoclastic rock, alt= 100% alteration

Appendix 1: **Mineralized Horizon** Major Oxide and Trace Element Chemistry

Negative values indicate concentrations below detection limits

Element	Rk Type	CD	Bl
Units		PPM	PPM
Detection Lim		0.5	5
3260000174	bif	0.5	-5
3260000182	alt	-0.5	-5
3260000184	alt	0.5	-5
3260000190	alt	0.5	-5
3260000196	bif	0.7	-5
3260000199	alt	-0.5	-5
3260000200	alt	0.7	-5
3260000203	and	-0.5	-5
3260000204	and	-0.5	-5
3260000220	alt	0.7	-5
3260000223	bif	0.5	-5
3260000228	sed	-0.5	-5
3260000230	alt	-0.5	-5
3260000231	alt	-0.5	-5
3260000232	alt	-0.5	-5
3260000234	alt	-0.5	-5
3260000236	alt	-0.5	-5
3260000240	alt	0.6	-5
ENC699-16	dk	0.6	-5
ENC699-17	sed	0.6	-5
ENC699-18	sed	0.7	-5
ENC699-19	vlc	0.5	-5
ENC699-21	sed	-0.5	-5

Rk Type Key:

and= andesite, bas= basalt, dk= dike, dio= diorite, bif= banded iron formation, sed= sedimentary rock, vlc= volcanoclastic rock, alt= 100% alteration

Appendix 1: **Hanging Wall** Major Oxide and Trace Element Chemistry

Negative values indicate concentrations below detection limits

SAMPLE	Rk Type	SiO2	TiO2	Al2O3	Fe2O3	MnO	MgO	CaO	Na2O	K2O	P2O5	LOI	TOTAL
		%	%	%	%	%	%	%	%	%	%	%	%
ENS699-121	and	49.59	0.80	14.68	11.40	0.20	6.97	11.52	1.83	0.49	0.06	2.00	99.53
ENS699-131	bas	49.09	1.39	13.02	16.14	0.22	6.30	7.88	2.13	0.21	0.14	2.57	99.08
ENS699-134	bas	47.04	1.35	11.81	14.80	0.21	5.37	7.64	2.56	0.13	0.12	8.08	99.12
ENS699-141	and	57.26	0.59	14.96	7.32	0.12	6.46	4.32	4.84	0.37	0.08	2.37	98.70
3260000162	bas	47.43	1.40	11.30	18.56	0.30	8.82	7.71	1.84	0.14	0.13	2.45	100.09
3260000215	and	53.34	0.98	17.29	8.85	0.20	2.95	10.01	0.98	1.58	0.13	2.48	98.77
ENC699-06	bas	44.16	0.72	13.42	11.85	0.17	7.70	8.86	2.07	0.09	0.08	10.09	99.21
ENC699-07	and	59.78	0.49	11.60	8.54	0.11	6.04	3.66	0.26	1.82	0.15	7.88	100.33
ENC699-08	and	49.43	0.58	12.29	8.17	0.11	2.73	9.03	1.47	0.47	0.14	14.85	99.26

Element	Rk Type	BA	SR	Y	ZR	BE	V	AU	AS	BR	CO	CR	CS
Units		PPB	PPM	PPM	PPM	PPM	PPM	PPB	PPM	PPM	PPM	PPM	PPM
Detec Lim								5	2	1	1	1	0.5
ENS699-121	and	84	113	21	49	-1	242	-5	-2	-1	46	235	-0.5
ENS699-131	bas	50	127	39	101	-1	346	-5	2	-1	42	72	-0.5
ENS699-134	bas	42	98	33	89	-1	313	32	-2	-1	49	78	-0.5
ENS699-141	and	97	93	12	77	-1	126	-5	4	-1	31	176	-0.5
3260000162	bas	21	42	37	99	-1	377	-5	-2	-1	44	62	-0.5
3260000215	and	387	101	19	90	-1	249	19	-2	-1	36	231	-0.5
ENC699-06	bas	14	91	16	45	-1	235	-5	-2	-1	45	241	-0.5
ENC699-07	and	351	42	16	100	-1	96	-5	-2	-1	29	132	-0.5
ENC699-08	and	125	217	13	120	-1	110	-5	-2	-1	42	182	-0.5

Rk Type Key:

and= andesite, bas= basalt, dk= dike, dio= diorite, bif= banded iron formation, sed= sedimentary rock, vlc= volcanoclastic rock, alt= 100% alteration

Appendix 1: **Hanging Wall** Major Oxide and Trace Element Chemistry

Negative values indicate concentrations below detection limits

Element	Rk Type	HF	IR	MO	RB	SB	SC	SE	TA	TH	U	W	LA
Units		PPM	PPB	PPM	PPM	PPM	PPM	PPM	PPM	PPM	PPM	PPM	PPM
Detec Lim		0.5	5	5	20	0.2	0.1	3	1	0.5	0.5	3	0.5
ENS699-121	and	1.6	-5	-5	-20	-0.2	39.9	-3	-1	-0.5	-0.5	-3	2.6
ENS699-131	bas	3.1	-5	-5	-20	-0.2	41.3	-3	-1	0.8	-0.5	-3	6.8
ENS699-134	bas	2.3	-5	-5	-20	0.3	38.4	-3	-1	0.7	-0.5	-3	6.4
ENS699-141	and	1.8	-5	-5	-20	-0.2	22.0	-3	-1	1.3	-0.5	-3	7.0
3260000162	bas	3.0	-5	-5	-20	-0.2	41.7	-3	-1	0.8	-0.5	-3	5.6
3260000215	and	2.4	-5	-5	43	-0.2	33.8	-3	1	1.3	-0.5	-3	7.9
ENC699-06	bas	1.1	-5	-5	-20	0.3	34.8	-3	-1	-0.5	-0.5	-3	2.6
ENC699-07	and	2.8	-5	-5	42	-0.2	16.3	-3	-1	2.3	-0.5	-3	15.5
ENC699-08	and	1.8	-5	-5	39	-0.2	30.4	-3	-1	0.5	-0.5	-3	4.5

Element	Rk Type	CE	ND	SM	EU	TB	YB	LU	CU	PB	ZN	AG	NI
Units		PPM	PPM	PPM	PPM	PPM	PPM	PPM	PPM	PPM	PPM	PPM	PPM
Detec Lim		3	5	0.1	0.1	0.5	0.1	0.05	1	5	1	0.4	1
ENS699-121	and	9	5	1.9	0.6	-0.5	2.0	0.30	63	-5	140	-0.4	134
ENS699-131	bas	18	11	4.2	1.4	1.1	4.0	0.60	127	-5	164	-0.4	46
ENS699-134	bas	17	6	3.7	1.0	0.9	3.5	0.54	110	-5	144	-0.4	46
ENS699-141	and	16	5	2.2	0.6	-0.5	1.4	0.22	4	-5	115	-0.4	150
3260000162	bas	15	5	4.0	0.9	0.8	4.2	0.63	31	-5	191	-0.4	44
3260000215	and	21	9	2.8	0.8	0.5	2.2	0.32	9	-5	212	-0.4	117
ENC699-06	bas	8	-5	1.7	0.5	-0.5	2.1	0.31	73	-5	142	-0.4	135
ENC699-07	and	33	12	2.9	0.7	-0.5	1.7	0.27	107	-5	137	-0.4	127
ENC699-08	and	12	7	2.6	1.0	-0.5	2.8	0.41	57	-5	123	-0.4	118

Rk Type Key:

and= andesite, bas= basalt, dk= dike, dio= diorite, bif= banded iron formation, sed= sedimentary rock, vlc= volcanoclastic rock, alt= 100% alteration

Appendix 1: **Hanging Wall** Major Oxide and Trace Element Chemistry

Negative values indicate concentrations below detection limits

Element	Rk Type	CD	BI
Units		PPM	PPM
Detec Lim		0.5	5
ENS699-121	and	0.7	-5
ENS699-131	bas	0.8	-5
ENS699-134	bas	0.9	-5
ENS699-141	and	-0.5	-5
3260000162	bas	0.8	-5
3260000215	and	0.5	-5
ENC699-06	bas	1.0	-5
ENC699-07	and	0.6	-5
ENC699-08	and	1.0	-5

Rk Type Key:

and= andesite, bas= basalt, dk= dike, dio= diorite, bif= banded iron formation, sed= sedimentary rock, vlc= volcanoclastic rock, alt= 100% alteration

Appendix 2: Normative calculations of selected samples.

List of mineral name abbreviations used in the CIPW Norm (from Philpotts, 1989).

Abbreviation	**Mineral**
Q	Quartz
or	Orthoclase
ab	Albite
an	Anorthite
lc	Leucite
ne	Nepheline
C	Corundum
ac	Acmite
ns	Na metasilcate
Di wo	Diopside wollastonite
Di en	Diopside enstatite
Di fs	Diopside ferrosilite
Hy en	Hyperstene enstatite
Hy fs	Hyperstene ferrosilite
Ol fo	Olivine forsterite
Ol fa	Olivine fayalite
mt	Magnetite
he	Hematite
il	Ilmenite
ap	Apatite

%Fe2O3 and %FeO calculated from %Fe2O3* (total Fe) by:

$$\%Fe_2O_3 = \%TiO_2 + 1.5$$
(Irvine and Baragar, 1971)

$$\%FeO = (\%Fe_2O_3^* - TiO_2 - 1.5) \times 0.8998$$
(Jenson, 1976)

Appendix 2: Normative calculations of selected samples.

Sample	Average Andesite 1 (Gill, 1981)		
Oxides	wt%	Normative Minerals	Weight %
SiO2	60.30	Q	14.73
TiO2	0.78	or	12.42
Al2O3	17.50	ab	30.42
Fe2O3	3.40	an	25.34
FeO	3.20	lc	0.00
MnO	0.18	ne	0.00
MgO	2.80	C	0.00
CaO	5.90	ac	0.00
Na2O	3.60	ns	0.00
K2O	2.10	Di wo	1.01
P2O5	0.26	Di en	0.71
		Di fs	0.21
		Hy en	6.29
		Hy fs	1.90
		Ol fo	0.00
		Ol fa	0.00
		mt	4.93
		he	0.00
		il	1.48
		ap	0.57
		Total	100.00

Sample	Average Andesite 2 (Gill, 1981)		
Oxides	wt%	Normative Minerals	Weight %
SiO2	57.60	Q	12.47
TiO2	0.77	or	8.97
Al2O3	17.30	ab	27.34
Fe2O3	3.10	an	28.67
FeO	4.30	lc	0.00
MnO	0.15	ne	0.00
MgO	3.60	C	0.00
CaO	7.20	ac	0.00
Na2O	3.20	ns	0.00
K2O	1.50	Di wo	2.59
P2O5	0.21	Di en	1.64
		Di fs	0.79
		Hy en	7.46
		Hy fs	3.59
		Ol fo	0.00
		Ol fa	0.00
		mt	4.54
		he	0.00
		il	1.48
		ap	0.46
		Total	100.00

Appendix 2: Normative calculations of selected samples.

Sample	High Al Basalt (Philpotts, 1989)		
Oxides	wt%	Normative Minerals	Weight %
SiO2	49.10	Q	0.00
TiO2	1.50	or	4.18
Al2O3	17.70	ab	24.73
Fe2O3	2.80	an	33.47
FeO	7.20	lc	0.00
MnO	0.10	ne	0.00
MgO	6.90	C	0.00
CaO	9.90	ac	0.00
Na2O	2.90	ns	0.00
K2O	0.70	Di wo	5.99
P2O5	0.30	Di en	3.75
		Di fs	1.87
		Hy en	8.62
		Hy fs	4.30
		Ol fo	3.53
		Ol fa	1.94
		mt	4.10
		he	0.00
		il	2.88
		ap	0.66
		Total	100.00

Sample	ENS699-100	Least altered Andesite	
Oxides	wt%	Normative Minerals	Weight %
SiO2	60.40	Q	11.89
TiO2	0.48	or	5.53
Al2O3	14.90	ab	39.41
Fe2O3	1.98	an	18.04
FeO	3.92	lc	0.00
MnO	0.11	ne	0.00
MgO	5.49	C	0.00
CaO	4.51	ac	0.00
Na2O	4.54	ns	0.00
K2O	0.91	Di wo	1.79
P2O5	0.11	Di en	1.21
		Di fs	0.44
		Hy en	12.89
		Hy fs	4.66
		Ol fo	0.00
		Ol fa	0.00
		mt	2.95
		he	0.00
		il	0.94
		ap	0.25
		Total	100.00

Appendix 2: Normative calculations of selected samples.

Sample	ENS699-95	Purvis Lake Pluton - Diorite	
Oxides	wt%	Normative Minerals	Weight %
SiO2	52.62	Q	0.57
TiO2	0.47	or	5.88
Al2O3	19.12	ab	34.56
Fe2O3	1.97	an	32.67
FeO	3.36	lc	0.00
MnO	0.13	ne	0.00
MgO	4.68	C	0.00
CaO	9.26	ac	0.00
Na2O	3.95	ns	0.00
K2O	0.96	Di wo	5.99
P2O5	0.09	Di en	4.10
		Di fs	1.40
		Hy en	8.01
		Hy fs	2.74
		Ol fo	0.00
		Ol fa	0.00
		mt	2.96
		he	0.00
		il	0.92
		ap	0.20
		Total	100.00

Sample	98-059	Purvis Lake Pluton - Granodiorite	
Oxides	wt%	Normative Minerals	Weight %
SiO2	65.66	Q	21.05
TiO2	0.28	or	9.44
Al2O3	16.42	ab	44.83
Fe2O3	1.78	an	16.98
FeO	1.35	lc	0.00
MnO	0.03	ne	0.00
MgO	1.33	C	0.22
CaO	3.44	ac	0.00
Na2O	5.15	ns	0.00
K2O	1.55	Di wo	0.00
P2O5	0.10	Di en	0.00
		Di fs	0.00
		Hy en	3.42
		Hy fs	0.62
		Ol fo	0.00
		Ol fa	0.00
		mt	2.66
		he	0.00
		il	0.55
		ap	0.22
		Total	100.00

Appendix 2: Normative calculations of selected samples.

Sample	ENS699-131	Hanging Wall Basalt	
Oxides	wt%	Normative Minerals	Weight %
SiO2	49.09	Q	7.73
TiO2	1.39	or	1.34
Al2O3	14.68	ab	19.47
Fe2O3	2.89	an	32.28
FeO	7.66	lc	0.00
MnO	0.22	ne	0.00
MgO	6.30	C	0.00
CaO	7.88	ac	0.00
Na2O	2.13	ns	0.00
K2O	0.21	Di wo	4.19
P2O5	0.00	Di en	2.46
		Di fs	1.52
		Hy en	14.58
		Hy fs	9.05
		Ol fo	0.00
		Ol fa	0.00
		mt	4.53
		he	0.00
		il	2.86
		ap	0.00
		Total	100.00

Sample	ENS699-134	Hanging Wall Basalt	
Oxides	wt%	Normative Minerals	Weight %
SiO2	47.04	Q	4.45
TiO2	1.35	or	0.86
Al2O3	11.81	ab	24.12
Fe2O3	2.85	an	22.66
FeO	10.75	lc	0.00
MnO	0.21	ne	0.00
MgO	5.37	C	0.00
CaO	7.64	ac	0.00
Na2O	2.56	ns	0.00
K2O	0.13	Di wo	8.19
P2O5	0.00	Di en	3.76
		Di fs	4.35
		Hy en	11.20
		Hy fs	12.95
		Ol fo	0.00
		Ol fa	0.00
		mt	4.61
		he	0.00
		il	2.86
		ap	0.00
		Total	100.00

Appendix 2: Normative calculations of selected samples.

Sample	ENS699-141	Hanging Wall Andesite	
Oxides	wt%	Normative Minerals	Weight %
SiO2	57.26	Q	10.01
TiO2	0.59	or	2.27
Al2O3	14.96	ab	42.47
Fe2O3	7.32	an	18.66
FeO	0.00	lc	0.00
MnO	0.12	ne	0.00
MgO	6.46	C	0.00
CaO	4.32	ac	0.00
Na2O	4.84	ns	0.00
K2O	0.37	Di wo	1.30
P2O5	0.08	Di en	1.12
		Di fs	0.00
		Hy en	15.65
		Hy fs	0.00
		Ol fo	0.00
		Ol fa	0.00
		mt	0.41
		he	7.32
		il	0.00
		ap	0.18
		Total	99.39

Appendix 3: Results of XRD analysis of selected samples

Sample	Mineralogy	Rock Type
3260000174	chlorite, tremolite, talc, magnetite, calcite	BIF
3260000184	chlorite, quartz, magnetite, pyrite, Sericite	all alteration
3260000205	quartz, chlorite, calcite, biotite	dike
3260000228	quartz, sericite, chlorite	sediment
3260000231	quartz, chlorite, magnetite	all alteration
3260000234	chlorite, quartz, epidote	all alteration
3260000240	chlorite, quartz	all alteration
ENS699-05	quartz, feldspar, actinolite, epidote	lava
ENS699-115	actinolite, quartz, epidote, feldspar, calcite, chlorite	lava
ENS699-121	tremolite, chlorite, sericite, epidote, quartz, feldspar	lava
ENS699-19	quartz, feldspar, actinolite, epidote, chlorite	hyaloclastite
ENS699-20	quartz, chlorite, actinolite, epidote	lava
ENS699-28	chlorite, quartz, tremolite, epidote	dike
ENS699-31	quartz, chlorite, actinolite, feldspar, epidote	lava
ENS699-66	quartz, actinolite, feldspar, chlorite, epidote, pyrite	lava

Appendix 4: Thin section descriptions. * indicates accompanying chemical analysis.

ENS699-05 70% quartz/feldspar, 25% actinolite, 2% biotite, 2% epidote, 2% chlorite, trace opaques. Silicified lava with very fine grained (0.05-0.2mm), granular, quartz/feldspar groundmass. Fine grained actinolite, blocky when associated with quartz; actinolite percentage triples and grains become elongate from one side of slide to other. Subhedral 0.2-0.3 mm clots of epidote. One 2 mm triangular quartz "fragment" with plagioclase in interior.

ENS699-10* 50% actinolite, 25% epidote, 5-8% quartz/felspar, 15% chlorite, 3-4% plagioclase, 4% amygdules. Very fine grained (< 0.05 mm) amygdaloidal lava composed of elongate actinolite, chlorite, and quartz/feldspar with epidote clots; rounded, 0.2-2 mm quartz + epidote +/- chlorite amygdules; very fine grained halos of more concentrated plagioclase + epidote + quartz/feldspar surrounding amygdules; minor 0.2 mm chlorite blebs.

ENS699-12 60% actinolite, 25% chlorite, 8-10% epidote, 5-8% quartz, 1% amygdules. Very fine grained ($\leq$ 0.05 mm) amygdaloidal lava. Deformed, 0.1-0.4 mm quartz + epidote amygdules. 3-10 mm wide compositional banding between quartz + actinolite alteration and epidote + chlorite+/-quartz alteration. Actinolite is elongate and very fine grained. Mg chlorite grains 0.02-0.1 mm. Light-brown limonite alteration in irregular cracks << 0.02 mm wide.

ENS699-15 70% actinolite, 25% Mg chlorite, 3-4% quartz, 1% calcite, trace opaques. Fine grained (0.1-0.5 mm) porphyritic dike. 10% 0.5-2 mm elongate to equidimensional phenocrysts (some glomerocrysts) completely replaced by chlorite + actinolite +/- calcite. Some showing 60°-120° habit may have been amphiboles. Actinolite grains are elongate or diamond shaped, no preferred orientation, some twinned, some with 60°-120° cleavage;

Appendix 4: Thin section descriptions. * indicates accompanying chemical analysis.

minor disseminated .1 mm quartz. Chlorite grains 0.2-0.4 mm in groundmass. Few phenocrysts have light brown limonite in cracks.

ENS699-16 45% plagioclase, 38% actinolite, 8% epidote, 2% quartz, .5% chlorite, trace opaques. Fine grained (0.1-0.5mm), porhyritic, amygdaloidal lava. 0.2-0.5 mm euhedral, twinned plagioclase phenocrysts with 0.1 -0.2 mm radiating masses of actinolite and actinolite interstitial to plagioclase. Epidote disseminated or as granular patches. Very fine grained interstitial chlorite. Minor quartz. One 0.5 mm epidote amygdule.

ENS699-17 35% quartz/feldspar groundmass, 25% plagioclase, 10-15% sericite, 10% epidote, 4-5% chlorite, 3-4% calcite, 3% quartz, trace opaques. Fine grained quartz-feldspar dike. One millimeter phenocrysts of plagioclase in very fine grained quartz/feldspar groundmass; plagioclase partially altered to sericite; chlorite as thin stringers that wrap around plagioclase phenocrysts; minor <.5 mm quartz grains; disseminated, subhedral 0.2 mm epidote grains and 0.1 mm clots. 0.1 mm calcite blebs in groundmass.

ENS699-24 50% plagioclase, 15-20% clinopyroxene, 15% actinolite, 5% magnetite, 3% calcite, 0.5% sericite. Fine grained (< 0.5 mm) mafic dike. Euhedral to subhedral, twinned 0.8-1.5 mm plagioclase partly altering to sericite; 0.5-2 mm patches of fibrous actinolite +/- calcite; minor 0.1-0.2 mm quartz grains; subhedral 0.5 mm disseminated magnetite grains.

ENS699-28* 85% tremolite, 10-15% chlorite. Fine grained (<.1 mm) strongly foliated, strongly altered ultra mafic dike. Fibrous, foliated actinolite +/- chlorite; flattened, 0.5 mm blebs of fibrous actinolite grains oriented 90° to primary foliation of rock; irregular << 0.1 mm cracks filled with dark

Appendix 4: Thin section descriptions. * indicates accompanying chemical analysis.

brown limonite.

ENS699-30 25% plagioclase, 15-20% clinopyroxene, 10-15% quartz/feldspar, 10-15% actinolite, 10% chlorite, 10% sericite, 2-3% epidote. Fine grained (< 0.5 mm) granular intrusive of the Purvis Lake Pluton. Pyroxene grains 0.5-1 mm, euhedral to subhedral, sometimes twinned, and partially altered to actinolite. Euhedral sericite replacing 0.2-0.5 mm plagioclase. Euhedral to subhedral, disseminated .4 mm epidote grains. Very fine grained, interstitial quartz/feldspar.

ENS699-31 40% actinolite, 20% chlorite, 10-15% epidote, 12% quartz/feldspar, 8% quartz, 3% biotite. Very fine grained (0.05-0.1 mm) massive lava. Actinolite + quartz + chlorite + biotite cross cut by irregular veinlets of quartz + epidote +/- chlorite. Largest grains are disseminated, 0.1 mm epidote grains. Minor altered plagioclase in veinlets. Alteration in veinlets and as replacements.

ENS699-33 55% actinolite, 20% chlorite, 10-12% calcite, 10% quartz, 2-3% biotite, 1-2% epidote. Fine grained (0.5-1 mm) dike. Actinolite (needles) + quartz + chlorite with interstitial 0.5 mm calcite; quartz grains to 0.2 mm; 0.5-2 mm biotite grains partially altering to chlorite; 0.5-1.5 mm chlorite +/- actinolite +/- calcite +/- quartz replacing phenocrysts; one 6 mm diameter alteration bleb. One percent irregular cracks filled with light brown limonite.

ENS699-35 50% epidote, 40% actinolite, 10-12% quartz/feldspar, trace opaques, 3% amygdules. Amygdaloidal lava. Very fine grained (< 0.3 mm) epidote + actinolite with 0.5-1 mm quartz + epidote + actinolite amygdules. One 0.1 mm quartz veinlet.

Appendix 4: Thin section descriptions. * indicates accompanying chemical analysis.

ENS699-36 45% actinolite, 30% plagioclase, 12% epidote, 8-10% quartz, 3-4% sericite, 2-3% chlorite. Fine grained (0.5 mm), mafic dike. Subhedral, 0.3-0.5 mm plagioclase altering to sericite; subhedral 0.3-0.5 mm actinolite with poor cleavage. Disseminated 0.3 mm quartz grains and 0.4 mm quartz patches.

ENS699-39* 40% actinolite, 30% epidote, 10% quartz, 10% plagioclase, 5% sericite, 60% amygdules. Fine grained (0.2-0.4 mm) amygdaloidal lava. Strong actinolite + quartz alteration; 0.2-3 mm quartz +/- epidote +/- sericite +/- actinolite subrounded amygdules (sericite may be replacing anhedral plagioclase) in groundmass of massive, patchy actinolite interspersed with 0.5 mm long, slender, interlocking actinolite grains with interstitial quartz +/- anhedral feldspar. Texture appears graphic.

ENS699-42 66% plagioclase, 30% quartz, 3% sericite, 1% epidote. Medium grained (3 mm) plagioclase – quartz intrusive. Euhedral to subhedral twinned plagioclase altering to sericite. Quartz interstitial to plagioclase.

ENS699-44* 35% quartz, 25% actinolite, 10% epidote, 30% quartz/feldspar, 5% amygdules. Fine grained (< 0.1 mm) silicified amygdaloidal lava. Groundmass is fine grained quartz +/- fibrous actinolite; disseminated, 0.05 mm epidote clots; minor actinolite patches and 0.5 mm veinlets. 0.2-1 mm quartz amygdules; 3 mm quartz veinlet; irregular, 1 mm quartz patches.

ENS699-45 45% actinolite, 35% plagioclase, 15% quartz, 5% sericite, 1% epidote, trace chlorite. Fine grained (0.2-1.5 mm) actinolite – plagioclase dike. One millimeter actinolite grains, some twinned, some diamond shaped; 0.2-0.3 mm plagioclase altering to sericite; interstitial, ≤ 0.2 mm quartz.

Appendix 4: Thin section descriptions. * indicates accompanying chemical analysis.

ENS699-49 50% actinolite, 25% epidote, 15% Mg chlorite, 10-12% quartz, 1% sericite. Very fine grained (0.2 mm) massive lava. Very fine grained (<<.1 mm) actinolite groundmass with disseminated 0.1-0.2 mm Mg chlorite and quartz grains. Epidote uniformly disseminated in 0.1 - 0.2 mm granular blebs. One 2 mm veinlet of altered feldspar + sericite +/- calcite; calcite in interior of veinlet.

ENS699-53* 30% quartz, 30% quartz/feldspar, 10% plagioclase, 10% epidote, 10% Fe chlorite, 3% calcite. Fine grained (0.1 mm) porphyritic, amygdaloidal lava. Quartz/fspar +/- chlorite +/- epidote groundmass with 5% 0.5-1 mm irregular, quartz +/- calcite amygdules and 5-8%, 0.2-0.5 mm, subhedral, twinned plagioclase phenocrysts; minor quartz +/- calcite veinlets and stringers; minor 0.2 mm chlorite blebs. Abrupt change to massive fine grained (0.05-0.1 mm) lava (?) composed of chlorite + epidote + quartz/feldspar; epidote is disseminated and subhedral; chlorite as elongate blebs. Contact is sharp with limonite filled, irregular cracks.

ENS699-55 40% actinolite, 30% quartz, 10% plagioclase, 8% chlorite, 5% calcite, 3-5% biotite, 1% epidote, trace sphalerite. Fine grained (0.2-0.5mm) intermediate dike. Uniform texture of elongate actinolite + biotite; quartz + plagioclase + calcite compose remainder.

ENS699-57* 25% actinolite, 25% chlorite, 20% epidote, 15-20% sericite, 3-5% quartz/feldspar, 1-2% quartz. Fine grained (< 0.1 mm) strongly altered massive lava. Very fine grained actinolite + chlorite groundmass with .1 mm irregular sericite blebs and 0.05-0.1 mm subhedral epidote alteration patches. Most sericite blebs are irregular, but some are pseudomorphs after plagioclase. Fine cracks filled with limonite.

Appendix 4: Thin section descriptions. * indicates accompanying chemical analysis.

ENS699-58 40% plagioclase, 30% amphibole, 15% quartz, 8-10% sericite, 5% chlorite, 2-3% epidote. Fine grained (1-1.5 mm) plagioclase – amphibole dike. Subhedral, equant plagioclase grains strongly altered to sericite + clay + epidote. Subhedral to anhedral, elongate green amphibole with some twins and faint 60°-120° cleavage. Chlorite and quartz are interstitial. Epidote in veinlets and minor disseminations.

ENS699-61 45% quartz/feldspar + chlorite + actinolite groundmass, 35% quartz, 10% epidote, 5% chlorite, 5% actinolite, 1% calcite, trace opaques. Very fine grained (< 0.02 mm) hyaloclastite. Angular, 1–10 mm hyaloclastite fragments composed of groundmass with epidote blebs and 1% quartz + epidote amygdules. Fractures filled with 95% quartz and actinolite +/- epidote. One percent epidote, quartz, and calcite veinlets.

ENS699-62* 25% actinolite, 10% chlorite, 15% epidote, 3% quartz, 30% quarz/feldspar, 15% plagioclase. Fine grained (< 0.1 mm) strongly altered massive lava. Least altered rock is very fine grained (< 0.05 mm) actinolite + quartz/feldspar + epidote with 2% subhedral, .1 mm plagioclase grains; disseminated, subhedral, .1 mm epidote. Altered rock is .2 mm actinolite + epidote +/- quartz concentrated along outside of irregular fractures. Alteration follows < 0.01 mm fractures and alters rock within 1-2 mm of the fracure.

ENS699-64 45% actinolite, 15-20% epidote, 12% chlorite, 8% quartz, 5% plagioclase, 3% sericite, trace opaques, 3% amygdules. Very fine grained (0.05 mm) amygdaloidal lava. 1-2% 0.5-1 mm plagioclase phenocrysts completely replaced by sericite. Groundmass is very fine grained epidote + chlorite + quartz/feldspar + actinolite with .1 mm euhedral, twinned plagioclase grains. Epidote +/- quartz amygdules.

Appendix 4: Thin section descriptions. * indicates accompanying chemical analysis.

ENS699-65* 15% quartz, 20% chlorite, 10% calcite, 5-10% epidote, 5-8% plagioclase, 1% pyrite, 25% amygdules. Fine grained (0.1 mm) porphyritic, amygdaloidal lava. Anhedral quartz/feldspar + chlorite groundmass with 0.2-0.5 mm calcite blebs and veinlets; 0.4-0.8 mm, round quartz amygdules and 3-4% subhedral, twinned plagioclase phenocrysts partly altering to sericite; .1 mm disseminated epidote; minor 0.5 mm pyrite; one 1 mm quartz + epidote + pyrite + calcite stringer.

ENS699-66 55% actinolite, 15-20% epidote, 15% quartz/feldspar, 10% Fe chlorite, <1% opaques, 30% amygdules. Very fine grained (≤ 0.05 mm) scoriacious lava. Blebs of 1-3 mm actinolite +/- chlorite in groundmass of very fine grained actinolite and quartz/feldspar. Euhedral, ≤ 0.3 mm disseminated epidote grains. Stretched, flattened, touching 0.5-1.5 mm amygdules of actinolite +quartz +/- chlorite +/-epidote.

ENS699-68 Contact between lava and dike.

Lava: 60% actinolite, 15% quartz/feldspar, 8-10% chlorite, 5% plagioclase, <5% epidote, 2-3% sericite. Granular, equant, subhedral, .05mm actinolite in quartz/feldspar groundmass; disseminated 0.08-1 mm epidote clots and euhedral chlorite grains; 3% phenocrysts of 0.5-1 mm euhedral plagioclase grains altering to sericite; 1% subhedral, 0.5 mm chlorite phenocrysts. One < 0.1 mm wide calcite veinlet.

Dike: 70% plagioclase, 15% quartz, 10% amphibole, 2-3% epidote, <5% sericite. Fine grained (1 mm) granular plagioclase – quartz dike. Subhedral, zoned, twinned, 1 mm plagioclase grains altering to sericite. Subhedral to anhedral, 0.5-0.8 mm, sometimes twinned amphibole. Interstitial 0.1-0.3 mm quartz. Disseminated epidote.

Appendix 4: Thin section descriptions. * indicates accompanying chemical analysis.

ENS699-69 50% quartz/feldspar + actinolite groundmass, 20% quartz, 15% epidote, 10% actinolite, 5% plagioclase, <1% chlorite, 15-20% amygdules. Very fine grained (0.05 mm) amygdaloidal lava. 2-3% subhedral plagioclase phenocrysts, some twinned, altering to sericite + clay. Subhedral to anhedral, disseminated 0.25 mm actinolite blebs and ≤ 0.3 mm epidote clots. Epidote in 0.1 mm stringers. Quartz as stringers and irregular replacement bands. Quartz +/- epidote 0.5-0.75 mm well rounded amygdules.

ENS699-71 Contact between lava and dike.
Lava: 48% actinolite, 40% epidote, 5% quartz, <5% chlorite, 3% sericite. Massive, fine grained (0.2mm) lava. Uniform grain size throughout. Two 0.2 mm quartz stringers. Sharp contact.
Dike: 55% plagioclase, 20% quartz, 10% amphibole, 5% epidote, 3% sericite, 1% chlorite, < 1% calcite. Fine grained (0.5-1 mm). Subhedral plagioclase strongly altering to sericite; anhedral amphibole; interstitial quartz; disseminated epidote and chlorite.

ENS699-84 45% quartz/feldspar groundmass, 35% chlorite, 10-15% sericite, 5% epidote, 3% calcite, 2% amygdules. Very fine grained (0.1 mm), weakly foliated amygdaloidal lava. Groundmass is quartz/feldspar + chlorite + epidote; ≤ 0.5 mm tabular blebs of sericite may be completely replaced plagioclase; chlorite is very fine grained in groundmass and shows foliation; minor disseminated calcite blebs. Stretched 4 mm calcite +/- chlorite +/- sericite +/- quartz amygdules.

ENS699-85* 50% plagioclase, 25% Fe chlorite, 3-4% quartz, 15% calcite, 5% epidote, 1% sericite. Fine grained (0.1-0.3 mm) massive lava. Euhedral, twinned, fresh, .1 mm plagioclase in finer quartz/feldspar + chlorite groundmass;

Appendix 4: Thin section descriptions. * indicates accompanying chemical analysis.

	disseminated, subhedral, 0.1 mm epidote; 3-4 mm alteration band of quartz + epidote + calcite with some empty space and a gradational contact with fresh rock; minor 0.1 mm sericite blebs.
ENS699-86	65% plagioclase, 30% chlorite, 3% quartz, 3% calcite, trace opaques. Fine grained (0.1-0.4 mm) massive lava. Euhedral to subhedral, twinned plagioclase with fine grained interstitial chlorite; minor interstitial quartz; minor disseminated calcite; irregular disseminated opaque clots.
ENS699-89*	50% plagioclase, 25% actinolite, 10% chlorite, 10% epidote, 10% quartz, 3% calcite. Fine grained 0.1-0.2 mm amygdaloidal, porphyritic lava. 3% 0.5-1 mm euhedral, twinned, fresh plagioclase phenocrysts and glomerocrysts in groundmass of euhedral 0.1 mm plagioclase, subhedral actinolite, subhedral epidote, and quartz/feldspar; actinolite is radiating; <1% 0.5-1 mm round quartz +/- epidote amygdules; minor disseminated calcite blebs. Some of the fine grained plagioclase grains show a quenched texture and some appear to be silicified.
ENS699-95* Purvis Lake Pluton	50% plagioclase, 40% amphibole, 5% quartz, 3-4% epidote. Fine grained (1-1.5 mm) diorite. 1-2 mm, twinned, subhedral green amphibole in 0.8-1 mm twinned, zoned, subhedral, moderately altered plagioclase with minor interstitial quartz; disseminated 1 mm epidote patches.
ENS699-99	40% amphibole, 35% plagioclase, 25% quartz, trace sericite. Fine grained (1 mm) dike. Subhedral amphibole with some twinning; subhedral, rarely twinned plagioclase weakly altering to sericite; interstitial quartz.
ENS699-100*	70% quartz/feldspar groundmass, 15-20% chlorite, 5-8% epidote, 5%

Appendix 4: Thin section descriptions. * indicates accompanying chemical analysis.

quartz, 2% calcite. Fine grained (0.05-0.1 mm) massive lava. Quartz/feldspar groundmass with 0.1 - 0.2 mm blebs of chlorite chlorite, 0.2 mm disseminated epidote clots, and 0.1-0.2 mm quartz stringers, blebs, and grains; minor, < 0.1 mm subhedral plagioclase grains. 2% calcite +/- quartz 0.5-1 mm veinlets;

ENS699-101 50% quartz/feldspar, 25% chlorite, 20% epidote, 5% quartz, 1% calcite. Very fine grained (<0.05 mm) massive lava. Quartz/feldspar + chlorite + epidote groundmass with 5% disseminated 0.5 mm patches of sericite, chlorite, and quartz. Quartz, calcite, and chlorite 0.05-0.1 mm stringers. Epidote becomes slightly more coarse than groundmass across slide.

ENS699-103 70% actinolite, 20% plagioclase, 10% chorite, 1% epidote, 1% quartz. Very fine grained (< 0.05) massive lava. Groundmass is actinolite + plagioclase + chlorite. Subhedral, 0.05 mm plagioclase. Lava becomes fractured into irregular 2-3 mm, subrounded, fragments, not angular like hyaloclastite. Open spaced filled with fibrous, radiating, 0.2 mm actinolite grains.

ENS699-104* 30% actinolite, 30% plagioclase, 10-15% Fe chlorite, 10% epidote, 5% quartz, 5-8% sericite, trace opaques. Fine grained (0.05-0.1 mm) massive lava. Sericite completely replacing 0.4-1 mm relict plagioclase phenocrysts and glomerocrysts with fibrous actinolite patches in groundmass of 0.05-0.1 mm euhedral, fresh plagioclase with chlorite + epidote +/- quartz/feldspar; 1% quartz, actinolite, and chlorite 0.5 mm, faint amygdules. Minor quenched plagioclase grains.

ENS699-105 60% quartz/feldspar, 15% chlorite, 10-15% epidote, 8% quartz, 3% actinolite. Very fine grained (< 0.05 mm), weakly foliated, strongly

Appendix 4: Thin section descriptions. * indicates accompanying chemical analysis.

altered lava. Groundmass is quartz/feldspar + chlorite +/- actinolite. Large patches of 0.2 mm quartz phenocrysts; 2-3 mm patches of massive chlorite along irregular chlorite and glass stringers; 2-3 mm patches of disseminated quartz + groundmass +/- actinolite; ≤ 0.2 mm disseminated epidote grains.

ENS699-106 70% actinolite, 12% epidote, 8% quartz, 5% plagioclase, 3% chlorite, 1-2% sericite, 1% amygdules. Fine grained (< .1 mm) amygdaloidal lava. Groundmass is very fine grained actinolite +/- quartz/feldspar with 0.05-0.1 mm euhedral to subhedral disseminated epidote and 0.15 mm disseminated quartz; minor 0.1 mm euhedral, disseminated plagioclase grains. Quartz +/- actinolite +/- epidote, ≤ 1 mm amygdules with one 4 mm amygdule.

ENS699-107 35% actinolite, 25% quartz/feldspar, 20% plagioclase, 15% quartz, 1-2% epidote, 1-2% chlorite, 1-2% sericite, trace calcite. Fine grained (0.1 mm) porphyritc lava. Groundmass is quartz/felspar + actinolite; subhedral, 0.4-1 mm plagioclase phenocrysts moderately altered to sericite; granular quartz +/- epidote in 0.1 mm bands and 3-4 mm irregular blebs; fibrous actinolite in faint 0.2 mm bands within groundmass.

ENS699-109 40% epidote, 35% actinolite, 15% chlorite, 8-10% quartz, trace opaques. Fine grained (< 0.1 mm) massive lava. Uniform epidote + actinolite + chlorite groundmass with disseminated 0.15 mm quartz grains and 3-4% 2-3 mm patches of massive epidote alteration; minor quartz veinlets.

ENS699-111 60% plagioclase 25% Fe chlorite, 10% epidote, 5-8% quartz. Fine grained (0.3 mm) massive lava. Fresh, euhedral to subhedral, twinned, 0.3-0.4 mm plagioclase grains with interstitial Fe chlorite; disseminated

Appendix 4: Thin section descriptions. * indicates accompanying chemical analysis.

0.4-0.5 mm quartz grains; disseminated 0.1-0.2 mm calcite blebs; disseminated 0.1 mm epidote clots.

ENS699-115 80% actinolite, 15% epidote, 5% Fe chlorite, 1% quartz, <1% plagioclase. Very fine grained (0.1 mm) lava. Groundmass is massive actinolite with granular epidote, minor disseminated euhedral 0.05 mm plagioclase grains, minor disseminated quartz grains, and minor, 0.05 mm Fe chlorite grains; epidote + chlorite in 1-3 mm replacement blebs and as 1-2 mm veinlets; one < 0.1 mm quartz veinlet offsetting epidote veinlets. Actinolite groundmass has 0.2 mm round structures outlined by extremely fine grained (<< 0.001 mm) granular epidote (?) with actinolite filling interstitial spaces. Almost looks like an overprint.

ENS699-118 55% calcite, 30% Fe chlorite,15% plagioclase, trace epidote, trace opaques, trace quartz. Strongly altered, very fine grained (0.05 mm) lava (?). Very fine grained calcite blebs with interstitial Fe chlorite; some larger 0.1-0.2 mm calcite blebs; 2-3 mm veinlets of coarser (1 mm) calcite + chlorite +/- quartz +/- calcite.

ENS699-121* 40% tremolite, 35% epidote, 10% chlorite, 8% sericite, 2-3% quartz, 1% plagioclase, trace opaques. Fine grained (0.05-0.1 mm) massive lava. Uniform texture of actinolite + chlorite + epidote with 0.05 mm euhedral plagioclase grains completely replaced by sericite; zones of strong epidote alteration with euhedral 0.2 mm grains. Minor quenched plagioclase grains.

ENS699-122 30% quartz/feldspar, 25% chlorite, 20% epidote, 20% calcite, 1-2% magnetite, <1% pyrite. Fine grained (0.2 mm), weakly foliated, massive lava. Quartz/feldspar + chlorite groundmass with 0.2-0.5 mm calcite and

epidote as disseminations and as patches. Uniformly disseminated 0.2 mm magnetite grains; minor 1-2 mm pyrite grains; 2% 1 mm veinlets of calcite + epidote +/- quartz.

ENS699-125 30% actinolite, 20% chlorite, 15-20% epidote, 15% plagioclase, 5% quartz, 3% magnetite, trace pyrite. Fine grained (0.1-0.4 mm) massive lava. Actinolite is subhedral, some twinned, and slightly coarser than background; subhedral to anhedral, twinned, fresh plagioclase; Uniformly disseminated 0.1-0.2 mm magnetite; one 3-4 mm clot of pyrite surrounded by quartz may be irregular amygdule.

ENS699-131* 65% actinolite, 15-20% epidote, 8-10% quartz, 5% Fe chlorite, 1% pyrite, trace opaques, 1% amygdules. Fine grained (0.1 mm) amygdaloidal lava. Uniform subhedral actionolite + chlorite + epidote with disseminated 0.1 mm quartz grains; disseminated, .1 mm, granular epidote clots; minor 0.3-0.5 mm quartz + chlorite + epidote amygdules; one patch of strong epidote alteration; minor fine cracks filled with limonite.

ENS699-133 70% actinolite, 15% quartz/feldspar, 8% chlorite, 5% epidote, 1% calcite, 1% magnetite. Fine grained (0.1 mm) massive lava with 2 mm blebs of epidote + quartz. Groundmass is actinolite + chlorite + quartz/feldspar; disseminated .1 mm epidote; uniformly disseminated 0.05-0.1 mm magnetite. < 0.01 mm irregular cracks filled with light brown limonite; 1 mm veinlets and 1-3 mm blebs of epidote + quartz +/- actinolite alteration.

ENS699-134* 45% quartz/feldspar, 25% Fe chlorite, 15% calcite, <5% quartz, 5% plagioclase, 1-2% pyrite or magnetite. Fine grained (0.1-0.2 mm) massive lava. 25% 0.6-1 mm calcite grains in groundmass of very fine

Appendix 4: Thin section descriptions. * indicates accompanying chemical analysis.

grained quartz/feldspar + fine grained chlorite; minor subhedral plagioclase grains; poorly defined quartz + calcite +/- chlorite alteration stringers.

ENS699-135 65% actinolite, 25% plagioclase, 8% epidote, 2% chlorite, 1% magnetite. Fine grained (0.2-0.4 mm) porphyritic lava. Minor, 0.7-1 mm plagioclase phenocrysts. Subhedral actinolite with euhedral to subhedral twinned plagioclase grains; finer grained (0.1 mm) disseminated epidote in clots; uniformly disseminated 0.1-0.2 mm magnetite; 2-3 mm faint, irregular alteration (?) patches of finer grained feldspar + epidote + actinolite.

ENS699-137 55% actinolite, 25% plagioclase, 8-10% chlorite, 5% epidote, 3% quartz, trace calcite. Fine grained (0.1-0.2 mm) massive lava with epidote alteration blebs. Actinolite with finer, subhedral, 0.05 mm, twinned plagioclase grains; chlorite in groundmass; epidote in 2-4 mm blebs (3%) and disseminated 0.1 mm grains.

ENS699-139 70% actinolite, 12-15% epidote, 10% Fe chlorite, 3% quartz, 3-4% amygdules. Fine grained (0.05-0.1 mm) amygdaloidal lava. Actinolite + chlorite groundmass with disseminated, subhedral 0.1 mm epidote and trace quartz; irregular, stretched, 2-3 mm quartz +/- epidote +/- chlorite amygdules.

ENS699-140 45% actinolite, 35% plagioclase, 5-8% chlorite, 5% quartz, 5% epidote, 3-5% sericite, trace calcite. Fine grained (0.1-0.2 mm) massive lava with bands of strong actinolite alteration. Relatively unaltered rock composed of euhedral, 0.2 mm plagioclase grains with finer, fibrous actinolite. Alteration bands of extremely fine grained actinolite with irregular, 0.4-2 mm fragments (?) of fine grained (0.1-0.4 mm) quartz + sericite +

Appendix 4: Thin section descriptions. * indicates accompanying chemical analysis.

feldspar +/- actinolite +/- opaques.

ENS699-141* 55% plagioclase, 5% Fe chlorite, 25% actinolite, 3-4% epidote, 4-5% quartz, 1% sericite. Fine grained (0.05-0.1 mm) massive lava. Euhedral, twinned, 0.1 mm fresh, randomly oriented plagioclase grains with subhedral actinolite, anhedral quartz/feldspar, and chlorite; disseminated 0.05 mm epidote; minor 0.4-1 mm plagioclase phenocrysts altering to sericite; one 3 mm patch of quartz alteration; minor fine cracks filled with limonite. Actinolite alteration patches. Minor quenched plagioclase grains.

ENS699-144 45% actinolite, 30% epidote, 15% Fe chlorite, 5% quartz, trace opaques. Massive, fine grained (0.1-0.2 mm) lava. Groundmass is radiating actinolite grains with granular epidote and chlorite; minor 0.1 mm quartz grains; 3-4% 2-4 mm epidote alteration blebs and minor 0.1 mm quartz veinlets; one 2 mm bleb of pyrite + quartz.

ENS699-145 50% actinolite, 45% plagioclase, 2% epidote, 1% Fe chlorite, 1% quartz, 1% magnetite. Fine grained (1–1.2 mm) dike. Euhedral to subhedral, twinned, randomly oriented, 1–1.5 mm plagioclase with subhedral, twinned, 1 mm actinolite; minor interstitial chlorite + quartz; uniformly disseminated magnetite; 1-2 mm patches of very fine grained (< 0.05 mm) actinolite + epidote + feldspar.

ENS699-149* 50% plagioclase, 25% actinolite, 10% quartz, 10% chlorite, 5% epidote, <1% sericite, <1% calcite, trace opaques. Fine grained (0.1-0.3 mm) porphyritic lava. Subhedral plagioclase partly altering to sericite with actinolite; disseminated .1 mm epidote; 0.05 mm quartz grains; phenocrysts of 1 mm, subhedral plagioclase; 1-1.5 mm alteration patches

Appendix 4: Thin section descriptions. * indicates accompanying chemical analysis.

of coarser actinolite +/- quartz +/- epidote; minor disseminated calcite blebs; zone of weak quartz alteration.

ENS699-154 40% quartz/feldspar/sericite groundmass, 35% epidote, 25% actinolite, 1-2% chlorite, trace opaques. Fine grained (0.2 mm) massive lava, possibly brecciated. Very fine grained (< 0.01 mm) sericite + quartz/feldspar groundmass surrounding 0.1 mm granular epidote clots and irregular actinolite grains; coarser actinolite +/- quartz +/- euhedral epidote filling space between fragments; breccia fragments are centimeter scale and subangular (possible hyaloclastite).

3260000159 45% actinolite, 20% plagioclase, 15% epidote, 5-8% Fe chlorite. Fine grained (1mm) granular lava with .5mm actinolite grains and euhedral, twinned, fresh 0.25-2 mm plagioclase; one 3mm glomerocryst of plagioclase and one 5mm phenocryst partly altered to amphibole and epidote. Two percent irregular chlorite blebs may be amygdules.

3260000162* 70% actinolite, 10% Fe chlorite, 8-10% quartz, 5% epidote, trace plagioclase. Fine grained (0.2 mm) amygdaloidal lava. Weakly radiating actinolite groundmass with minor quartz. 1-2 mm amygdules of 60% chlorite, 30% quartz + actinolite + epidote slightly stretched; epidote is extremely fine-grained (< 0.25mm). Three quartz veinlets, two at 90° to the other.

3260000167 Groundmass (70%)—65% quartz + feldspar, 15% chlorite, 10% calcite, 5% epidote. Phenocrysts (25-30%)—60% plagioclase, 40% quartz. Quartz- feldspar porphyry dike. Plagioclase phenocrysts are 2-4mm, euhedral, twinned, altering to sericite; 1-6 mm rounded quartz grains in very fine grained (0.1 mm) groundmass.

Appendix 4: Thin section descriptions. * indicates accompanying chemical analysis.

3260000174* 55% tremolite and talc, 40% magnetite, 3-4% quartz, 2-3% calcite, trace Mg chlorite. Fine grained (0.1-0.5 mm) banded iron formation. 2-10 mm beds of magnetite interbedded with one 3 mm chert + tremolite band; tremolite bands are fibrous, radiating with disseminated magnetite; cross cutting quartz and calcite veinlets.

3260000182* 96% sericite, 3% Mg chlorite, 1% epidote. Very fine grained (0.02-0.1 mm) moderately foliated sericite with 1 mm blebs of coarser grained sericite. Extremely fine grained, granular epidote clots, disseminated and partially outlining blebs.

3260000184* 70% Mg chlorite, 28% sericite, 2-3% pyrite. Fine grained (< 0.2 mm) strong alteration. Moderately foliated chlorite with 25% 1-2 mm rounded, elongate, partially disseminated blebs of sericite; sericite may be replacing phenocrysts; some are round, possible amygdules; 0.5 mm equant pyrite grains have chlorite and sericite partial or complete rims.

3260000189 85% quartz, 10% Mg chlorite, 5% pyrite. Massive chert exhalite. Fine grained (0.1-0.3 mm) quartz with bands of disseminated pyrite. Some quartz in coarse clots with pyrite.

3260000190* 60% Mg chlorite, 25% quartz, 8-10% pyrite. Fine grained (0.1-0.2 mm) alternating bands of chlorite, quartz, and pyrite. Chlorite bands are fine grained, foliated and wrap around disseminated quartz grains and stringers. Quartz bands alternate between quartz with minor pyrite and pyrite with minor quartz; local 0.5mm offsets of bands.

3260000191 30% chlorite, 30% quartz/feldspar groundmass, 25% calcite, 5% magnetite + pyrite. Fine grained (0.3-0.4 mm) epiclastic (?). Moderately

Appendix 4: Thin section descriptions. * indicates accompanying chemical analysis.

foliated chlorite + calcite + quartz in very fine grained quartz/feldspar groundmass with epidote as <.3 mm granular blebs; disseminated 0.1-0.5 mm magnetite + pyrite.

3260000196* 90% calcite, 1-2% Mg chlorite, 5% pyrite and magnetite, 1% quartz veinlets. Fine grained (0.02-0.05) banded calcite and oxide facies iron formation. Banded magnetite (0.05-0.4 mm) in groundmass of calcite. Large euhedral pyrite grains. Minor chlorite stringers crosscut calcite veinlets. 2 mm veinlet of quartz + calcite + feldspar.

3260000198 40% sericite, 25% quartz, 25% calcite, 1-2% pyrite. Fine grained epiclastics with 0.3 mm subrounded, disseminated quartz phenocrysts in fine grained sericite with patchy 3-4 mm calcite alteration blebs.

3260000199* 68% Mg chlorite, 20% calcite, 12% quartz, trace pyrite. Fine grained (0.5 mm) intense alteration. 40% very fine grained (< 0.05 mm) chlorite groundmass with 2-4 mm Fe calcite blebs and 0.5-1 mm irregular quartz grains.

3260000200* 65% calcite, 35% quartz, 1% opaques. Fine grained (0.1-0.6 mm) exhalite. Alternating bands of calcite and chert. Chert bands discontinuous; calcite is euhedral with grains to 1 mm. Cross cutting quartz veinlets. Extremely fine grained (< 0.1mm) veinlets of disseminated opaques with quartz, indistinguishable from chert except for opaques. Grain size of calcite varies from band to band.

3260000203* 55% quartz/feldspar groundmass, 15% chlorite, 15% sericite, 10% calcite, 3-4% quartz, 3% epidote. Fine grained (0.4-0.6 mm) lava. Very fine grained quartz/feldspar matrix with irregular, 0.4-0.8 mm fragments and

Appendix 4: Thin section descriptions. * indicates accompanying chemical analysis.

plagioclase grains(?) replaced by chlorite and sericite; rare 0.2-0.5 mm, euhedral, twinned plagioclase grains partially altered to sericite. 0.2 mm disseminated epidote clots. One 2 mm wide calcite veinlet.

3260000204* 55% plagioclase, 20% sericite, 15% calcite, 10% chlorite, 3-5% quartz. Fine grained (.1 mm) lava contacting fine grained (0.05-0.1mm), massive lava or may be a large fragment within the flow. Lava is 40-50% 0.5 mm, irregular calcite blebs and 0.5-0.8 mm sericite +/- calcite groundmass. Irregular contact with massive lava (fragment?) composed of euhedral 0.1 mm plagioclase grains in quartz/feldspar + chlorite groundmass; 20% disseminated, 0.05 mm calcite blebs; possible 0.2 mm quartz amygdule.

3260000205 35% biotite, 30% calcite, 20% Mg chlorite, 15% quartz, 1% epidote, <1% opaques. Fine grained (≤ .1 mm) dike. Biotite + chlorite + quartz groundmass; chlorite +/- fine grained calcite in 0.5-1 mm, irregular, rounded blebs; some biotite altering to chlorite.

3260000213 30% actinolite, 20% calcite, 25% Fe chlorite, 10-15% quartz/feldspar groundmass, 10% epidote, 2% opaques. Fine grained (0.75-1.25mm) epiclastic. Actinolite grains with disseminated 0.5mm irregular blebs of calcite; interstitial chlorite and very fine grained quartz/feldspar; epidote clots up to 0.5 mm. One 2 mm, irregular, crosscutting veinlet with chlorite on walls and calcite in interior.

3260000215* 40% epidote, 30% quartz, 15% chlorite, 1% sericite, trace calcite in veinlets. Fine grained (.1 mm), strongly epidote altered lava. Very fine grained quartz groundmass with 0.05-0.5mm granular clots and euhedral grains of epidote; 0.5 mm disseminated blebs of chlorite. Poorly defined, 1-3 mm, irregular, rounded zones of epidote + chlorite + quartz alteration.

Appendix 4: Thin section descriptions. * indicates accompanying chemical analysis.

One 2 mm veinlet of calcite + chlorite.

3260000220* 90% tremolite, 8-10% calcite, <1% epidote. Fine grained (.1-.2 mm), fibrous, randomly oriented, tremolite with 0.2 mm, disseminated, euhedral calcite blebs; extremely fine grained (< 0.1mm) granular clots of epidote; 0.1 mm calcite + tremolite veinlets.

3260000223* 35-40% pyrite, 25% quartz, 20% chlorite, 15% calcite, trace sericite. Fine grained (0.2-0.3 mm) sulphide facies banded iron formation. Weakly banded, massive and disseminated pyrite with interstitial, 0.2 mm quartz + chlorite + calcite; very fine grained quartz/feldspar groundmass altering to sericite; fine grained, elongated chlorite. Several 5-6mm irregular holes in slide.

3260000228* 92% quartz, 8% sericite, trace opaques. Fine grained (0.05 mm) epiclastic. Granular fine grained quartz with 5%, 1 mm disseminated broken quartz grains; very fine grained disseminated fibrous sericite, sometimes as elongated clots; extremely fine grained (< 0.1mm) granular clots of epidote.

3260000230* 98% Mg chlorite, 2% quartz-pyrite veinlet, trace sericite, trace opaques, trace epidote. Fine grained (0.1 mm), foliated white chlorite with elongated 1 mm blebs (<5%) replaced with chlorite oriented perpendicular to foliation direction, some with opaque grains within; 0.1 mm veinlets of finer grained chlorite; disseminated, subhedral sericite. Extremely fine grained (< 0.05 mm) granular clots of epidote.

3260000231* 99% Mg chlorite, <1% epidote. Fine grained (0.05-0.1 mm), foliated white chlorite containing minor "fragments" replaced by chlorite oriented

	perpendicular to foliation. 0.8-1.2 mm holes in slide, some shaped like pyrite grains, others are interior of "fragments". Small amount of quartz present according to XRD analysis.
3260000232*	65% sericite, 35% Mg chlorite, <1% pyrite. Fine grained (0.05-0.1 mm), moderately foliated, intense alteration. Sericite replacing 1 mm, elongate blebs with fine grained chlorite filling in around them; chlorite in elongated, discontinuous bands, locally grain size coarsens to ≈ 0.2 mm Extremely fine grained (< 0.05 mm) granular and prismatic epidote clots.
3260000234*	97% Mg chlorite, 2% quartz, .5% epidote, 1% pyrite. Fine grained (0.1 mm) intense alteration, moderately foliated chlorite groundmass with 4-5 mm blebs of 0.3 mm quartz + sulphide + chlorite replacing "fragments" (??). 1-2 mm stringers of coarser (0.2 mm) chlorite and faint, 1 mm chlorite-replaced "fragments" within matrix. Extremely fine-grained (< 0.1mm) epidote granular and prismatic clots.
3260000235	60% sericite, 30% chlorite, 5-8% opaques. All alteration. Fine to medium grained, weakly foliated chlorite amid interconnected blebs of sericite. 0.5-1 mm disseminated grains of opaques; some fractured with chlorite and sericite filling joints.
3260000236*	93% Mg chlorite, 1% quartz, 1% pyrite and magnetite, 1-2% unknown 3% holes in slide. Fine grained (0.05-0.1 mm) intense alteration. Chlorite matrix with 1 mm grains of pyrite and magnetite; 2 mm coarser chlorite patches. Extremely fine grained (< 0.1 mm) granular and prismatic clots of epidote. 1.5 mm holes in slide appear to be from weathered out pyrite.
3260000240*	78% Mg-Fe chlorite, 22% quartz, <1% epidote, 4-5% holes in slide. Fine

Appendix 4: Thin section descriptions. * indicates accompanying chemical analysis.

grained (0.05-0.1 mm) intense alteration. Quartz/feldspar groundmass with fine grained (0.1-0.2 mm) chlorite. 4-5% 0.1-0.2 mm irregular quartz grains; extremely fine grained, granular and prismatic clots of epidote.

ENC699-02 20% quartz, 25% calcite, 20% Fe chlorite, 20% plagioclase, 3% epidote, 1-2% magnetite. Fine grained (1 mm) massive lava. Chlorite (2 mm) and quartz (1mm) with finer calcite and quartz in groundmass. Euhedral, fresh, twinned, 1 mm plagioclase grains. 98% of calcite is fine grained and fills in around chlorite and quartz; minor 0.2-0.4 mm calcite grains. Two 3 mm wide veinlets of calcite + chlorite +/- quartz; magnetite disseminated as irregular 0.2 mm grains.

ENC699-04 45% epidote, 20% quartz, 15-20% chlorite, 15% calcite, 5-8% opaques (magnetite, sphalerite, pyrite). Fine grained (0.2-0.4 mm) strongly quartz + epidote altered lava. Disseminated grains and masses of 0.2-0.4 mm epidote predominate; disseminated, irregular quartz grains (1 mm) mixed with chlorite and opaques. Opaques occur as disseminated, euhedral to subhedral grains. Sphalerite is dark brown in both plane and polarized light. Cross cutting, bifurcating, sometimes offset veinlets of calcite + quartz +/- epidote +/- chlorite +/- opaques.

ENC699-06* 45% calcite, 40% chlorite, 2-3% quartz, 5-8% plagioclase in groundmass, 1% pyrite. Fine grained (0.2 mm) weakly foliated, strongly altered lava. .2 mm, elongate chlorite; 0.05-0.1 mm, euhedral and anhedral calcite with disseminated fine grained quartz and pyrite. One quartz/calcite veinlet.

ENC699-07* 60% calcite, 20% sericite, 8-10% quartz, 5% plagioclase, 5% chlorite, trace epidote, 2% amygdules. Fine grained (0.2 mm) amygdaloidal lava.

Appendix 4: Thin section descriptions. * indicates accompanying chemical analysis.

Strong calcite alteration in irregular patches; quartz alteration in fine grained (< 0.05 mm), 1 mm stringers; faint perlitic cracks with light brown limonite in anhedral plagioclase grains. Quartz +/- calcite +/- sericite, round to egg shaped amygdules showing two stages of mineral precipitation.

ENC699-08* 60% calcite, 25% Fe chlorite, 5% sericite, 4-5% plagioclase, 2-3% quartz. Fine grained (0.1-0.2 mm), massive, strongly calcite altered lava. Chlorite and quartz fill around 0.1-0.2 mm calcite blebs; < 0.5mm, euhedral, twinned plagioclase grains altering to sericite; quartz predominantly fine grained with rare 0.1 mm grains.

ENC699-09 55% quartz, 30% calcite, 5% Mg chlorite, 5% pyrite + magnetite. Banded iron formation. Disseminated opaque bands of pyrite and magnetite overprinting 1-5mm wide alternating bands of chert and calcite + chlorite; calcite as 0.5 mm blebs.

ENC699-10 Fault: Side A- 45% chlorite, 40% quartz, 10% calcite, <5% opaques. Side B- 45% calcite, 35% chlorite, 20% quartz/feldspar, <5% opaques. Knife edge fault delineated by change in foliation direction. Fine grained (0.1-0.5 mm) foliated epiclastics. Very fine grained (< 0.1 mm) quartz/feldspar groundmass. Chlorite composition strongly variable across slide. Side B- fine grained (≤ 1.5mm) chlorite + calcite with very fine grained quartz/feldspar groundmass. Side A- similar composition but finer grained. Calcite + chlorite in discreet blebs within quartz/feldspar groundmass.

ENC699-13 45% magnetite and pyrite, 35% calcite, 10% quartz, 5% chlorite, 5% tremolite or talc. Banded iron formation. Bands of magnetite +/- pyrite

with quartz and trace calcite alternating with calcite layers containing no quartz. Calcite bands of 0.2-0.4 mm, subhedral, calcite grains contain minor, very fine grained, fibrous, radiating talc blebs; Mg chlorite present as < 1mm discontinuous bands. 0.25 mm magnetite grains in contact with quartz or calcite. Few larger (3-4 mm) magnetite grains appear to be fractured.

ENC699-16* 35% calcite, 25-30% chlorite, 25% quartz, 5% plagioclase, 5% sericite, trace pyrite. Fine grained (0.4 mm) dike. Equigranular chlorite + quartz +/- plagioclase over printed by 0.4 mm calcite blebs. Plagioclase beginning to alter to sericite. Angular quartz grains some with ≈90° corners. Three 1-2 mm chlorite clots.

ENC699-17* 45% chlorite, 25-30% calcite, 10% plagioclase, 2-3% sericite, <5% quartz, <1% epidote. Fine grained (0.1-0.2 mm) epiclastic. .4 mm calcite blebs in quartz + chlorite +/- plagioclase matrix. Subhedral, twinned, fresh plagioclase. 3 mm wide veinlet of quartz in coarse calcite. Epidote present in extremely fine grained (<< 0.1mm) granular clots.

ENC699-18* 40% chlorite, 25% plagioclase, 25% calcite, 5-8% quartz, 2-3% sericite, trace epidote. Fine grained (0.1 mm) epiclastic. 0.05 mm chlorite + quartz groundmass with 0.1-0.2 mm disseminated, subhedral calcite grains; disseminated 0.05-0.1 mm sericite blebs; extremely fine-grained granular epidote clots (<<1mm). Very fine-grained material unidentifiable optically is black in polarized light and light green in plane light.

ENC699-19* 50% quartz-plagioclase groundmass, 30% calcite, 10-15% Mg chlorite, 5% sericite, 3-5% quartz, trace epidote. Fine grained (0.05-0.15 mm)

Appendix 4: Thin section descriptions. * indicates accompanying chemical analysis.

	moderately foliated felsic ash tuff. Fine grained quartz/feldspar + chlorite groundmass with subhedral, 0.2 mm calcite blebs and 0.1-0.2 mm euhedral sericite grains; Two 2mm wide zones of elongated, euhedral, aligned 0.2 mm sericite grains. Extremely fine-grained granular clots of epidote. Three 0.2 mm, rounded, granular quartz crystals. Foliation wraps around quartz crystals and some calcite grains.
ENC699-21*	40% quartz/feldspar groundmass, 25-30% calcite, 10-15% chlorite, 10% sericite, 5-8% quartz, 2% plagioclase, trace epidote. Fine grained (0.05-0.1 mm) epiclastic. < 0.05 mm quartz/feldspar +chlorite + sericite groundmass with 0.2-0.6 mm calcite blebs, 0.1-0.6 mm quartz grains, and 0.1-0.5 mm, twinned, partially altered to sericite, broken plagioclase grains. Quartz grains are subrounded and not optically continuous. Extremely fine-grained granular clots of epidote (<< 0.1mm). 2 mm wide calcite alteration stringers.